ENDOCYTOSIS IN ELONGATING ROOT TIP CELLS OF *LOBELIA ERINUS*

By

ANNE LACEY SAMUELS

B.Sc., McGill University, 1984

A THESIS SUBMITTED IN PARTIAL FULFILLMENT OF

THE REQUIREMENTS FOR THE DEGREE OF

DOCTOR OF PHILOSOPHY

in

THE FACULTY OF GRADUATE STUDIES

Department of Botany

We accept this thesis as conforming

to the required standard

THE UNIVERSITY OF BRITISH COLUMBIA

May 1989

In presenting this thesis in partial fulfilment of the requirements for an advanced degree at the University of British Columbia, I agree that the Library shall make it freely available for reference and study. I further agree that permission for extensive copying of this thesis for scholarly purposes may be granted by the head of my department or by his or her representatives. It is understood that copying or publication of this thesis for financial gain shall not be allowed without my written permission.

Department of Botany

The University of British Columbia
Vancouver, Canada

Date July 23, 1989

DE-6 (2/88)

ABSTRACT

Endocytosis was measured along the axis of differentiation of epidermal and cortical root cells of Lobelia erinus from meristematic to fully expanded vacuolate cells. Both lanthanum and lead were tested as markers of endocytosis; lanthanum proved to be more effective. Lanthanum treatment produced electron dense deposits in the apoplast of the root, as well as coated pits, coated vesicles, smooth vesicles and multivesicular bodies within the cells. X-ray microanalysis was used to confirm the lanthanide nature of the deposits.

In both secretory (meristematic and elongating cells actively depositing new cell wall material) and non secretory (mature vacuolate) cells the amount of endocytosis occurring was measured by counting the number of lanthanum labelled vesicles/um^2/cell. The amount of endocytosis correlated very well with the cell wall secretory activity. The highest amount of endocytosis was found in the elongating cells, with meristematic having an intermediate value. Mature, vacuolate cells had the least endocytosis. The relationship between endocytosis and secretory activity suggests that endocytosis may be acting to remove excess

membrane material added during exocytosis of secretory vesicles.

Cytochemical tests for polysaccharides were performed on both conventional transmission electron microscopy preparations and ultrarapidly frozen, freeze substituted preparations. The ultrastructural preservation was superior using the cryotechnique. The organelles involved in secretion of cell wall components were compared with the organelles associated with endocytosis in chapter 1. The Golgi showed distinct dictyosome polarity, small peripheral vesicles and an elaborate trans Golgi network. Vesicles in the cytoplasm displayed diverse staining properties. One population of larger, densely staining vesicles located on the trans Golgi and in the cortical cytoplasm was interpreted to be secretory vesicles.

Microtubules were disrupted with colchicine to test the importance of these cytoskeletal elements in endocytosis. Immunofluorescence was used to determine the concentration of colchicine which disrupted cortical microtubules in these cells. After colchicine treatment, there were fewer endocytotic vesicles and less lanthanum label in the multivesicular body, suggesting microtubules are involved in endocytosis during elongation.

Cell wall pore size was tested using electron dense apoplast markers. Partial enzyme digestions were used to find which components of the cell wall determine porosity. Pectin was found to be the most important component, while cellulose and protein did not seem to effect porosity in these primary roots. The porosity of the wall was interpreted in terms of the intact wall ultrastructure.

Ultrarapid freezing, freeze substitution were used to reexamine endocytosis in elongating cells. Using lanthanum as a marker for endocytosis, the results of the earlier, conventional TEM study were supported and extended. In addition to coated and smooth vesicles, multivesicular bodies were labelled. The instantaneous preservation of the endomembrane system allowed the localization of label in the partially coated reticulum and in vesicles associated with the Golgi as well. The partially coated reticulum and multivesicular body are proposed to represent plant endosomes. When interpreted in conjunction with the secretion study, it can be suggested that the heterogenous populations of vesicles occur in the cytoplasm of the elongating Lobelia erinus root cells.

TABLE OF CONTENTS

TABLE OF CONTENTS (continued)

LIST OF TABLES

LIST OF FIGURES

LIST OF FIGURES (continued)

LIST OF FIGURES (continued)

ACKNOWLEDGEMENTS

This thesis is dedicated to my supervisor Dr. Thana Bisalputra, on the occasion of his retirement, December 31, 1988, for his inspiration and timely advice.

The technical and moral support of Michael Weis is gratefully acknowledged. The expert computer help of Donald Wong is appreciated. Thanks to all the past and present grad students and brothers in arms for stimulating discussions. My gratitude also goes to Rob DeWreede and Brian Nichol for their calming influences. Finally, thanks to Brian Samuels for infinite patience.

GENERAL INTRODUCTION

The question addressed in this thesis is whether endocytosis occurs in the root cells of a germinating higher plant, Lobelia erinus. Endocytosis has been defined by deDuve (1963) as "invagination of plasmalemma, giving rise to an independent, cytoplasmic vesicle". The resulting cytoplasmic vesicle carries into the cell part of the extracellular environment. In higher plant cells, the porosity barrier of the cell wall prevents large particles from interacting with the surface membrane of healthy plant cells. Phagocytosis, defined as uptake of particles >0.5 um, is generally ruled out, although it may still occur in cases of specialized cell-cell interactions, such as Rhizobium-legume nodulation (Djordjevic et al. 1987).

Pinocytosis can be defined as uptake of solution, proteins (called ligands), and/ or viruses. Pinocytosis of molecules that are smaller than the pore size of the cell wall could occur in higher plant cells. For the purpose of this study, the more general term endocytosis will be used to describe this process. This term has become more widely used in the literature as endocytosis has been recognized as a mechanism for plasma membrane

turnover and homeostasis in a wide variety of animal cells (Besterman 1985). The specific binding of ligands by receptors on the cell surface and internalization of receptor-ligand complexes by coated vesicles is now called receptor mediated endocytosis (RME) (Goldstein et al. 1985). The prelysosomal organelles that receive membrane from the plasma membrane following endocytosis are called endosomes (Helenius et al. 1983, Schmid et al. 1988).

Endocytosis in higher plants has been postulated since the first transmission electron microscope (TEM) observations of vesicles near the higher plant plasma membrane (Buvat 1963, Mahlberg et al. 1971, Roland and Vian 1971). The difficulty of interpreting these images of vesicles is that "[the] direction of movement of this vesiculation is not apparent from electron microscope studies" (Baker and Hall 1973).

The existence of vesicles near the plasma membrane has been interpreted as strictly endocytosis (Nassery and Jones 1976, Nishizawa and Mori 1977, 1978, 1984) or as strictly exocytosis (Robinson 1985, Steer 1985). These interpretations are both speculative in the absence of markers for

endocytosis. One of the goals of the present study is to compare the pathways of endocytosis and exocytosis in a cell wall secreting cell. While the exocytosis of material from the Golgi to the plasma membrane has been well documented, endocytosis has remained a controversial subject in plant cell biology.

In the 1970's endocytosis was suggested as a mechanism of ion uptake (Baker and Hall 1973). Models were generated in which ions, bound to the extracellular surface of the plasma membrane, were internalized and carried to the central vacuole (MacRobbie 1970). This theory has been discounted on theoretical grounds (Cram 1980) and on further characterization of ion transporters (MacRobbie 1982). However, there are some specialized cell types where endocytosis may be a mechanism for ion or sucrose uptake (Rozema et al. 1977, Brossard-Chriqui and Iskander 1982, Auriac and Tort 1985).

Endocytosis was suggested to be the mechanism of protein uptake into roots (Nishizawa and Mori 1977, 1978). It must be considered that the proteins may have been partially degraded, or taken up into the apoplast or dead cells (Ulrich and MacLaren 1965, Drew et al. 1970). The morphological

evidence for protein uptake (Nishizawa and Mori 1977, 1978) was the presence of larger (about 0.5 um) vesicles forming from the plasma membrane, which resembled the intramembrane particle (IMP) free bleb artifacts induced by glutaraldehyde fixation (Hasty and Hays 1978).

The uptake of proteins or ions by endocytosis is probably not significant in the higher plant cell, but endocytosis could still play an important role in the turnover of plasma membrane components. One example of endocytosis as a mechanism for membrane homeostasis is the internalization of excess plasma membrane added during exocyosis. The result of an exocytotic vesicle fusing with the plasma membrane is a net increase in the cell surface area; an endocytotic vesicle budding from the plasma membrane would produce a net decrease in the cell surface area.

The study of endocytosis in higher plants has been slow as it is difficult to assay for endocytosis in the intact plant system. In light microscope studies of Pisum sativum liquid endosperm cells, the cytoplasm showed extensive vesiculation that resembled pinocytosis over a short time course. However, this vesiculation

was shown to be an artifact of sample preparation (Bradfute et al. 1964). Endocytotic vesicles are smaller than the limit of resolution of the light microscope; tracers for endocytosis must be small to fit through the cell wall. For these reasons electron microscopy has been used to study endocytosis in higher plant cells.

There are reports of endocytosis in intact higher plants using uranyl acetate as an electron dense marker. This marker severely damaged exterior root cap cells, while interior root cap cells showed evidence of endocytosis (Wheeler et al. 1972). Results obtained using this toxic marker must be viewed with caution, since uranyl acetate has been shown to induce vesiculation of both liposomes and plasma membranes of intact cells (Romanenko et al. 1986). In the presence of uranyl acetate, there were 15-20 times more membrane invaginations and vesicles formed. In contrast, incubation of vesicles with lanthanum nitrate produced the same effect as incubation in sodium chloride: little vesiculation was induced in the presence of calcium and no vesiculation in the absence of calcium. Therefore, lanthanum nitrate seems to be a more reliable marker for endocytosis

than uranyl acetate. Both lanthanum and lead have been used to show endocytosis in root cap cells of maize (Hubner et al. 1985). This is the single report of endocytosis in an intact tissue using a relatively reliable marker.

When higher plant cells have their cell walls enzymatically removed (protoplasts), electron dense markers for endocytosis can interact freely with the plasma membrane. Protoplasts can engulf polystyrene beads or bacterial spheroplasts (Mayo and Cocking 1969, Harding and Cocking 1986, Suzuki et al. 1977). Adsorptive pinocytosis, uptake of molecules bound to the plasma membrane, has been demonstrated using cationized ferritin and colloidal gold-lectin (Joachim and Robinson 1984, Tanchak et al. 1984, Hillmer et al. 1986). Protoplast studies have revealed the intracellular locations of membrane taken up by endocytosis. This includes coated and smooth cortical vesicles, multivesicular bodies, partially coated reticulum. Therefore, the protoplast studies show that the organelles necessary for endocytosis are present in the higher plant cell. Whether this process occurs in the intact cell where cells are under turgor is not addressed.

In this study, the process of endocytosis in intact elongating epidermal and cortical root cells is examined using lanthanum nitrate as a marker of the extracellular medium. The hypothesis that vesicular membrane recycling occurs in secretory cells is tested by comparing endocytosis in secretory cells (elongating wall secreting cells) and non-secretory cells (mature, vacuolate cells). The process of secretion is examined using cytochemistry for polysaccharides on conventional TEM preparations compared with ultra rapidly frozen/ freeze substituted material. The porosity of the primary cell wall surrounded these elongating root cells is measured using image analysis of colloidal gold particles. Finally, endocytosis is reexamined using cryo techniques to instantaneously immobilize the endomembranes.

Chapter 1:

ENDOCYTOSIS IN ELONGATING ROOT TIP CELLS OF *LOBELIA ERINUS*

Endocytosis has been demonstrated in higher plant protoplasts (Joachim and Robinson 1984, Tanchak et al. 1984, Tanchak et al. 1988, Hillmer et al. 1986, Record and Griffing 1988), and in walled root cap cells (Hubner et al. 1985). In this process, coated or smooth vesicles bud off from the plasma membrane, internalizing plasma membrane material as well as an aliquot of extracellular medium. The endocytotic vesicles are believed to carry membrane material to other organelles such as the multivesicular body (also known as multivesicular endosome, Tanchak and Fowke 1987), partially coated reticulum, the Golgi and the central vacuole (Record and Griffing 1988).

It is generally agreed that endocytosis and exocytosis (granulocrine secretion) are opposing activities of the overall intracellular transport system in most eukaryotic cells (see reviews by Farquhar 1985, Besterman 1985, Steinman et al. 1983). This has been established by the demonstration of endocytosis following secretory vesicle discharge in a wide variety of animal cells (Farquhar 1981). It appears that endocytosis represents a mechanism for membrane retrieval during the period of active secretion.

Although such a functional role for endocytosis has not been elucidated in plant cells, it has often been suggested that endocytosis is a factor in membrane recycling (Joachim and Robinson 1984, Hubner et al. 1985, Steer 1985). The most abundant secretory product of plants is polysaccharides, unlike most animal cells which secrete primarily proteins (Robinson 1984). During the development of each plant cell, polysaccharide cell wall components must be secreted to maintain wall thickness as the cell grows (Dauwalder and Whaley 1982, Fincher and Stone 1981, Dixon and Northcote 1985); it is generally agreed that the wall does not "thin" or stretch over the cell surface during cell wall growth (McNeil et al. 1984 Varner and Liang-Shiou 1989).

The primary cell wall consists of about 20 % cellulose and 80 % matrix material (McNeil et al. 1984). There are several lines of evidence that suggest that new cell wall matrix is added by the exocytosis of Golgi derived vesicles. Morphological studies show vesicle aggregation during cell plate formation (Hepler and Newcomb 1967, Whaley and Mollenhauer 1966).

Autoradiography of radioactive monosaccharides trace the route of polysaccharide synthesis from Golgi cisternae to vesicles and to the plasma membrane and cell wall (Pickett-Heaps 1966). Cell fractionation and isolation of endomembrane components have been used to show that the polysaccharides located in the Golgi have the same composition as those of the cell wall and that the enzymes of glycosylation are localized in the Golgi (Bowles and Northcote 1976). The kinetics of labelled polysaccharide transport through the fractionated organelles suggest an important role for the dictyosome in cell wall synthesis (Robinson et al. 1976).

By measuring the cell length and cell wall width before and after elongation, it is possible to calculate the surface area of plasma membrane material that must be added onto the cell surface by the exocytosis of Golgi derived vesicles (see Appendix 1). For example, in the primary root of Lobelia erinus seedlings, the cells increase in size from 20 um to 80 um in length. During elongation, most of the change in cell shape is due to increased cell length along the axis of the root. The sides of the expanding cells change from squares (meristem) to rectangles (vacuolate).

The volume of cell wall material secreted during the elongation of the root cell can be calculated from the observed thickness of the final cell wall minus the volume of the original cell wall. When this volume is divided by the volume of secretory vesicle the total number of vesicles needed to secrete the observed cell wall thickness can be found. The surface area of this number of vesicles can be compared to the final cell surface area. When these calculations are performed for this tissue, we find that about eight times the final cell surface area is required to secrete the cell wall observed.

This calculation agrees with similar computations (Raven 1987, Steer 1985) and suggests that membrane recycling should occur in secretory plant cells. The mechanism of membrane retrieval in plants is not well understood. By analogy with the animal systems, endocytosis is one possible mechanism.

In this study, the differentiating primary root cells of Lobelia erinus were used to compare the amount of endocytosis along the axis of differentiation of the root cells as they go from meristematic through differentiation to the mature,

vacuolate state. Endocytosis was demonstrated using heavy metal salts as a marker for the extracellular medium (procedure of Hubner et al. 1985). The amounts of endocytosis occurring in each cell type were then measured. This is the first time quantitative methods have been used to compare endocytosis in different cell types and directly address the question of whether vesicular membrane recycling occurs in actively secreting higher plant cells.

Lobelia erinus roots were used for this study because the elongation phase along a file of cells is as few as three to four cells, allowing easy comparision between actively secreting cells (elongating) and nonsecreting cells (vacuolate). For this reason, Lobelia erinus provides an ideal material for studying elongation by transmission electron microscopy with accompanying image analysis.

METHODS AND MATERIALS

electron microscopy

Lobelia erinus seeds were donated by Buckerfield's Seed Co., Vancouver, B.C. The seeds were germinated on filter paper moistened with deionized distilled water for 7 days.

The seedlings were incubated in heavy metal salt solutions following a modification of the procedure of Hubner *et al*. (1985). The solutions used were aqueous 5 mM $La(NO_3)_3$ (JBS #104, supplied by JBEM, Dorval, P.Q.), with pH adjusted to 7.6 using 1 N NaOH or aqueous 5 mM $Pb(NO_3)_2$ (Allied Chemicals, #1838), pH 5.6. The roots were immersed in either of the solutions or distilled water (control) for 1 hour at room temperature. They were then fixed without rinsing in a dilute Karnovsky's fixative: 1.5% formaldehyde, 1% glutaraldehyde, buffered in 50 mM PIPES pH 7.4, for 1 hour. After rinsing in buffer for 15 minutes, twice, the roots were postfixed in 1% OsO_4, buffered as above, for 2 hours at room temperature or overnight at 4^{o}. Dehydration was performed using a graded series of methanol solutions; propylene oxide was the solvent for the subsequent Epon resin (JEMBED 812) infiltration and embedding.

Light microscope sections (0.5 um) were cut with glass knives and stained with 1 % toluidine blue in 1 % sodium borate for 45 seconds. Silver sections (60-90 nm) were obtained using a Reichert OMU3 ultramicrotome and mounted on copper grids. The sections were poststained in saturated uranyl acetate in 70% methanol for 25 minutes. The sections were examined using a Zeiss EM10C.

X-ray microanalysis

For x-ray microanalysis, samples were prepared as above. Unstained sections of 250 nm in thickness were mounted on formvar coated, carbon stabilized berylium grids.

Sections were examined using a Zeiss EM10C, adapted for scanning transmission electron microscopy (STEM) and energy dispersive x-ray analysis (EDX). Spot size of 15 nm was routinely used. A spot or region scan was used to obtain a characteristic x-ray spectrum. X-ray mapping was performed by interfacing the STEM with a Kontron Image Processing System (IPS). A 128x128 pixel resolution and a dwell time of 2 seconds were used.

Quantification of Endocytosis

Fifteen individual roots were trimmed and sectioned for each treatment. From each individual root tip, three cells from each the three developmental stages (meristem, elongating, and vacuolate) were measured. This gave a sample size of 45 cells/developmental stage. The vesicle diameter, number of vesicles/cell, and cytoplasmic area (excluding vacuoles and nuclei) were measured using the Kontron IPS interactively with the TEM. The number of vesicles/cell was divided by the cytoplasmic area/cell to get vesicles/um^2/cell; this allows comparison between cells of different sizes. Frequency distributions were generated and non-parametric statistical tests performed (Kruskel-Wallace and Mann-Whitney U test).

Measurements of cell dimensions

Five to ten individual roots were trimmed and sectioned for each treatment. From each root four to five cells from each developmental stage were measured using a Zeiss photomicroscope with a video attachment. The video signal was analyzed using the Kontron IPS.

RESULTS

Three stages of cell development were distinguished for the purpose of this study: meristematic, elongating and vacuolate (Fig. 1-3). Meristematic cells are apical cells prior to differentiation; for the last two stages, the epidermal and underlying two to three layers of cortical cells were studied. The cells increase in length as they mature, while the cell wall width stays the same or increases slightly (Table 1).

Both lanthanum and lead were tested as markers for endocytosis (Figs. 4-6); lanthanum proved to be more effective and was used in subsequent experiments. To confirm the identity of the heavy electron dense deposits in the tissues as lanthanum, x-ray microanalysis was performed. When the electron beam was scanned over the deposits in the cell wall, a spectrum with characteristic lanthanum peaks was collected (Fig. 7). Mapping the location of the x-rays indicated the majority of the signal emanated from the heavy deposits in the cell wall (Fig. 8).

In addition to apoplastic labelling, electron dense label appeared along the cell surface, in coated pits, in membrane invaginations, and in

Table 1: Cell lengths and cell wall widths of differentiating primary root cells of Lobelia erinus.

cell length developmental stage	mean	standard deviation	sample size
meristem	18 um ±	4 um	44
elongating	30 um ±	14 um	44
vacuolate	80 um ±	14 um	22

cell wall width developmental stage	mean	standard deviation	sample size
meristem	0.15 um ±	0.3 um	38
elongating	0.21 um ±	0.7 um	50
vacuolate	0.40 um ±	0.2 um	50

coated and smooth vesicles of all cell types. The smooth membrane infoldings were often long necked structures (Fig. 18) similar to those described by Staehelin and Chapman (1987).

The criterion for considering a structure as labelled was the presence of dark electron dense deposits with densities similar to deposits in the cell wall which were identified by x-ray microanalysis as lanthanum. These could be distinguished from the fibrillar, less electron dense deposits seen in the structures of the distilled water treated control specimens (Fig. 10). Uranyl acetate post staining was necessary to visualize coated membranes during counting, and comparisons with unstained lanthanum sections provided a control for this step. Lanthanum treatment did not result in clear labelling of all vesicles (Fig. 9). The apparently unlabelled vesicles could be Golgi derived secretory vesicles or endosomes whose deposits are not in the plane of section.

Lanthanum deposits were detected in coated vesicles which displayed the characteristic bristles on their cytoplasmic surface (Fig. 12, 14; Table 2). Smooth vesicles, i.e. lacking a

Table 2: Lanthanum labelled vesicle diameters

type of vesicle	mean diameter	standard deviation	sample size
coated vesicle	101 nm ±	14 nm	129
smooth vesicle	106 nm ±	34 nm	1037

Table 3: Total number of coated vs. smooth lanthanum labelled vesicles. Total vesicles found in 27 cells counted for each stage of development.

developmental stage	coated vesicles	smooth vesicles	ratio cv:sv
meristem	16	143	1:11
elongating	42	358	1:12
vacuolate	17	188	1:9

cytoplasmic coat were also labelled (Fig. 11, 13, 15, 17; Table 2). The ratio of smooth: coated vesicles was approximately 10:1 for all cell types (Table 3).

Both coated and smooth vesicles were often associated with cortical microtubules which underlie the plasma membrane (Fig. 13, 15). In some cases fibrillar connections between the microtubule and vesicle could be seen (Fig. 17).

The amount of endocytosis occurring in each developmental stage in terms of the number of endosomes/um^2/cell are presented in Fig. 20. The elongating cells had the most labelled vesicles/um^2/cell and the vacuolate cells had the lowest number. Despite an adequate sample size, there were a few cells which contained unusually high values of labelled vesicles/um^2, and this is reflected by the high standard deviations. According to the nonparametric statistical tests, the three developmental stages have significantly different amounts of endocytosis.

Small vacuoles (0.2-0.5 um in diameter) containing numerous vesicles in their lumina were labelled with the lanthanum treatment (Fig. 19).

These can be interpreted to be the multivesicular bodies (MVB) described by Tanchak and Fowke (1987), in their description of endocytosis in the soybean protoplast.

The dictyosomes did not appear to be labelled following lanthanum treatment (Fig. 16). Labelled vesicles could be seen in the vicinity of the Golgi, but not in direct connection to the cisternae. No structure corresponding to the partially coated reticulum (Pesacreta and Lucas 1985) could be seen, although some vesicles were slightly elongate and may represent a section through a similar structure. The occurrence of deposits in the endoplasmic reticulum must be noted, however the frequency of their occurrence was extremely low. Approximately 5% of the cells displayed some deposits in the endoplasmic reticulum.

Figs. 1-3: Differentiation of primary root cells from meristem region to mature, vacuolate cells.

Fig 1:meristematic cells are characterized by dense cytoplasm, prominent central nuclei, and provacuoles.

Fig. 2:elongating cells have a rectangular shape, and provacuoles coalescing.

Fig 3:vacuolate, mature cells display large central vacuole, with a peripheral cytoplasm.

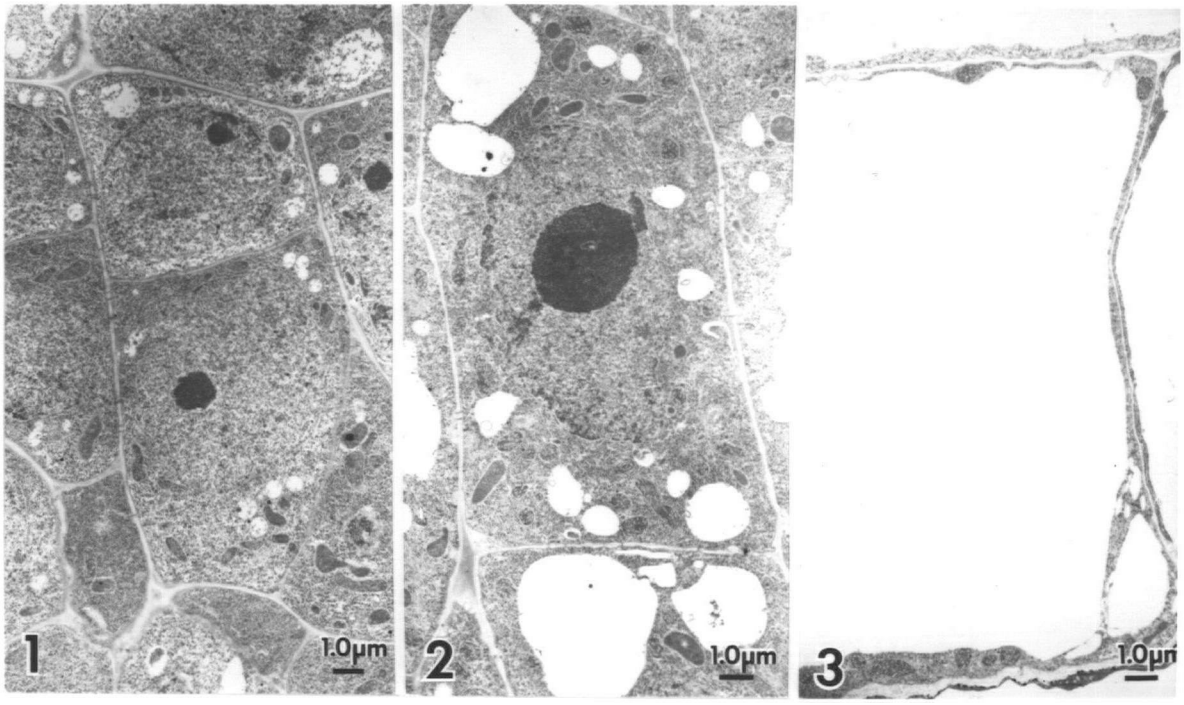
1
1.0μm
2
1.0μm
3
1.0μm

Figs. 4-8: comparison of different heavy metal treatments (La, Pb) vs. control (distilled water).

Fig. 4: lanthanum forms heavy deposits in radial crosswalls, but does not appear in ground cytoplasm.

Fig. 5: normal ultrastructure of Lobelia seedling root treated with water.

Fig. 6: lead deposits can be seen in the cell wall as well as ground cytoplasm and organelles.

Fig. 7:x-ray spectrum generated by region scan of heavy deposit in cell wall found in lanthanum treated root, x-rays used for mapping are indicated.

Fig. 8:x-ray map shows location of x-rays with characteristic energy level for lanthanum.

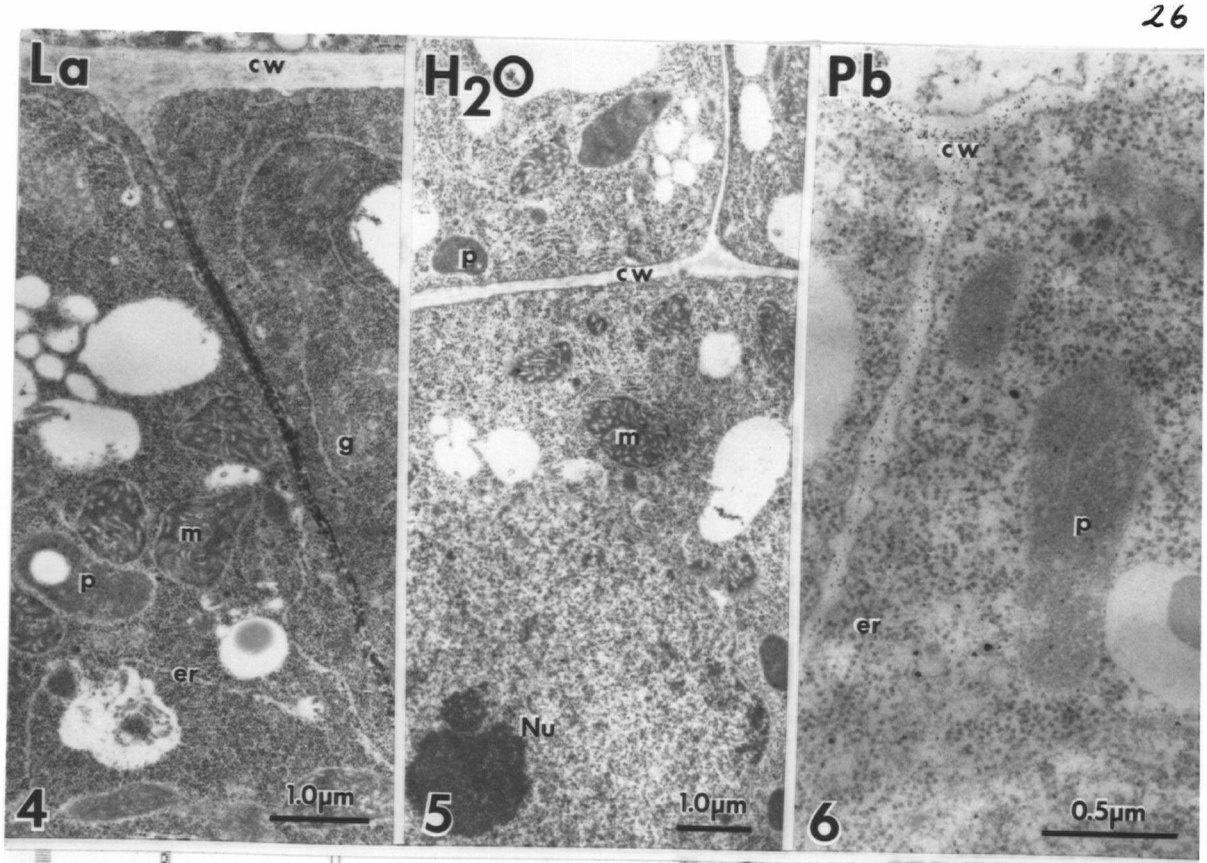
La
cw
g
m
p
er
1.0µm
4
H_2O
p
cw
m
Nu
1.0µm
5
Pb
cw
p
er
0.5µm
6

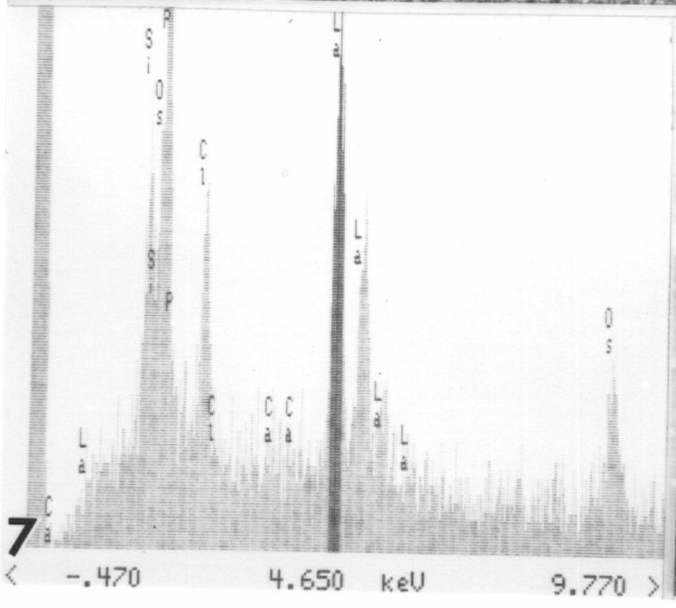
Si
Os
Cl
Ca
La
-.470
4.650
keV
9.770
7

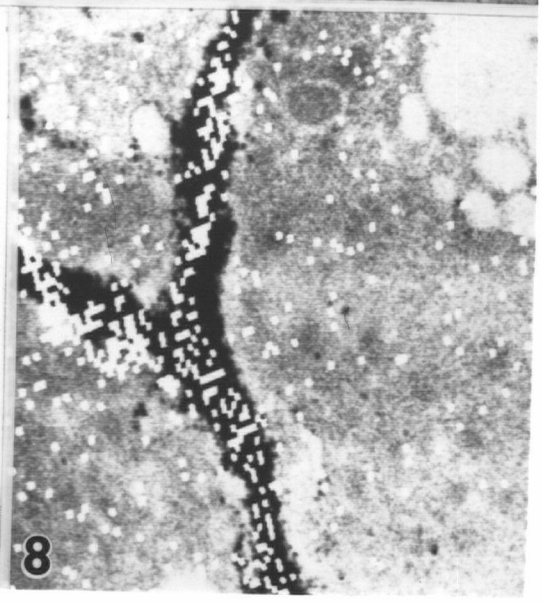
8

Figs. 9-14: Coated and smooth vesicles found in root cells of Lobelia erinus.

Fig. 9: lanthanum treated sample; apparently unlabelled coated vesicle associated with microtubule.

Fig. 10: distilled water treated; cell wall does not have electron dense deposits.

Figs. 11-14:lanthanum treated.

arrow indicates lanthanum label, arrowhead indicates coated membrane, pm=plasma membrane, mt=microtubule, cw=cell wall. All bars=100nm.

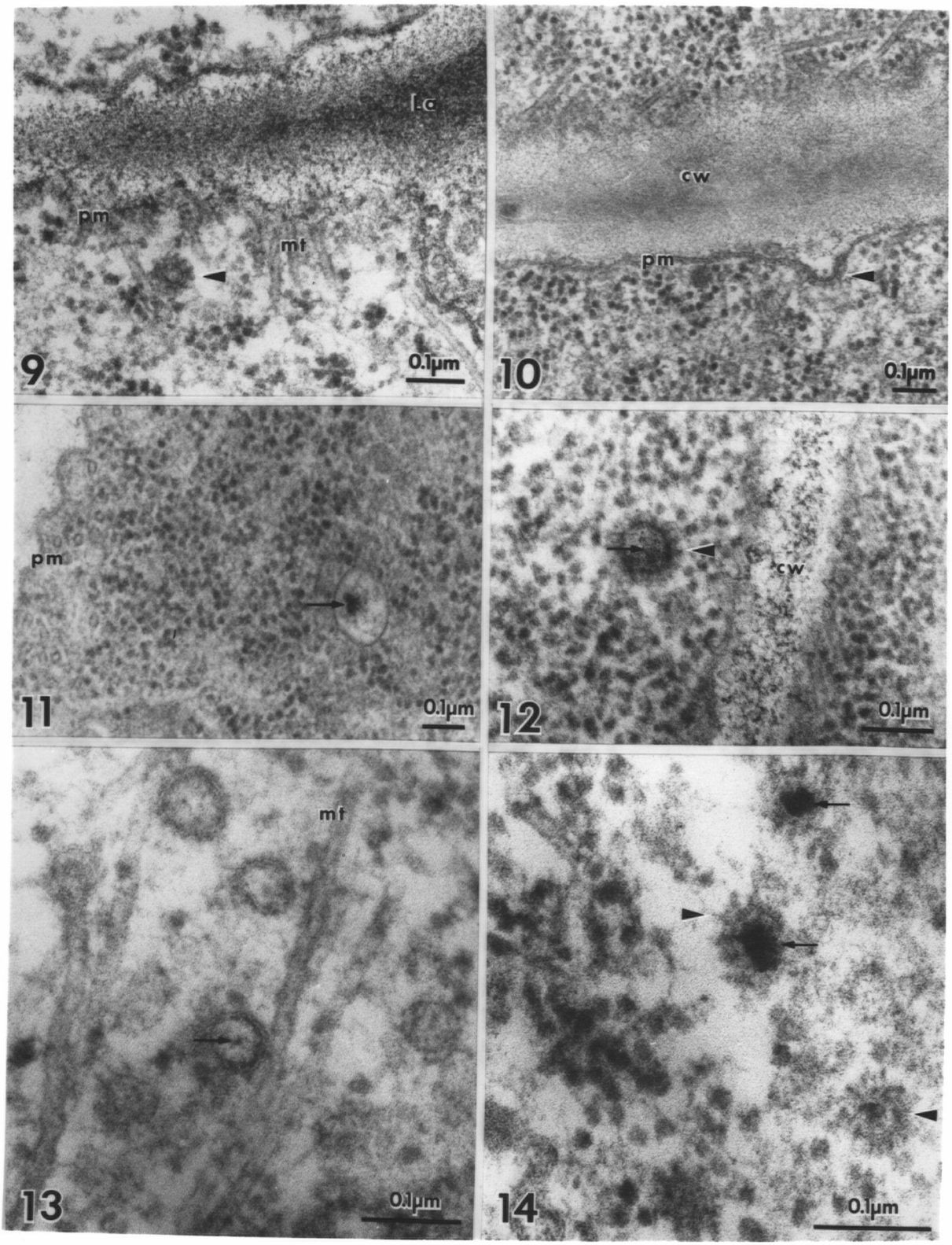
Lc
pm
mt
9
0.1μm
cw
pm
10
0.1μm
pm
11
0.1μm
cw
12
0.1μm
mt
13
0.1μm
14
0.1μm

Figs. 15-19: Intracellular structures labelled with lanthanum.

all lanthanum treated.

Fig. 15:smooth endocytotic vesicles associated with microtubule

Fig. 16: elongating epidermal cell with apparently unlabelled cell wall, Golgi, and provacuoles; arrow indicates lanthanum deposit.

Fig. 17: Vesicle-microtubule connection (arrowhead).

Fig. 18: membrane infoldings form long-necked structures.

Fig. 19: multivesicular body. All bars=100 nm.

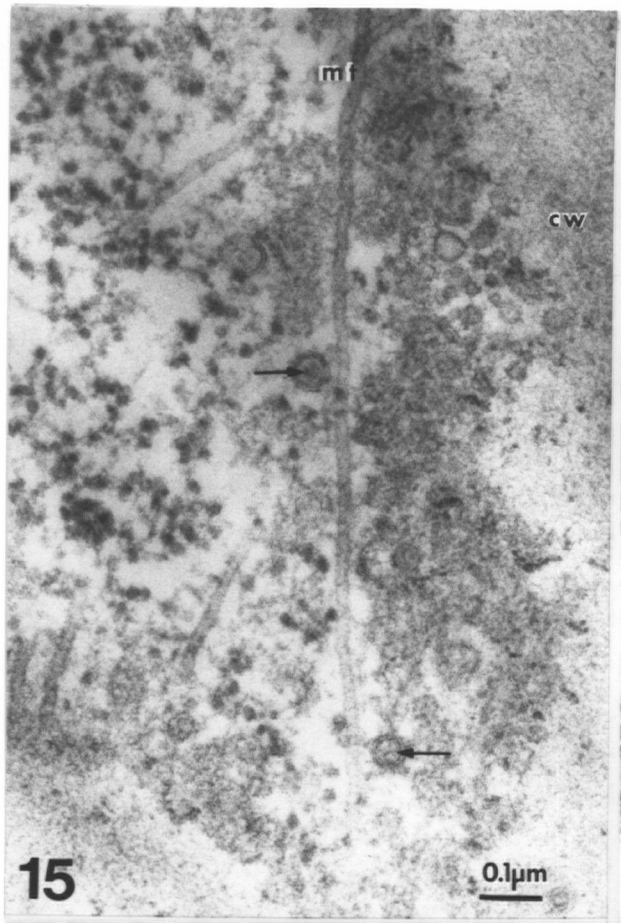
mf
cw
15
0.1µm

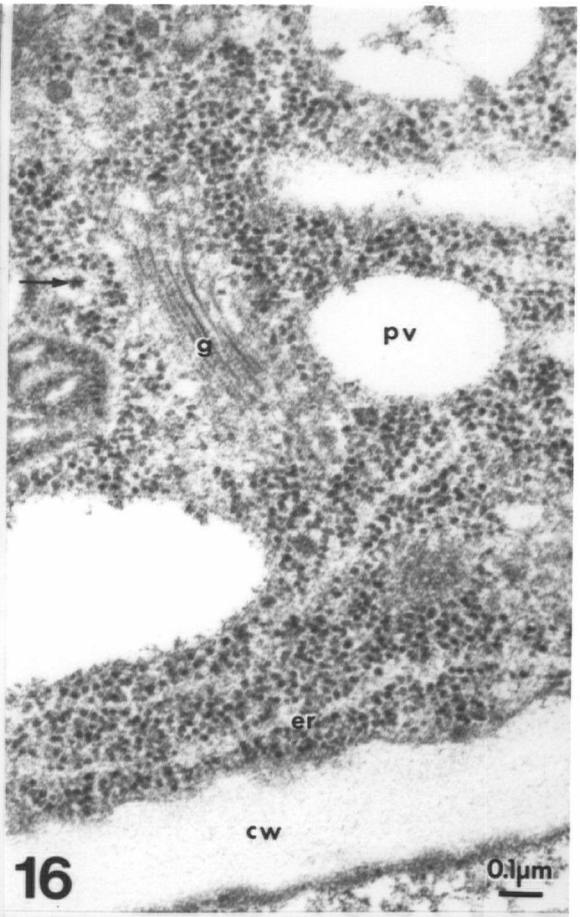
g
pv
er
cw
16
0.1µm

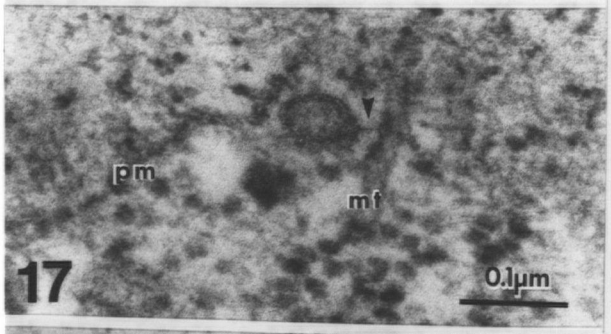
pm
mf
17
0.1µm

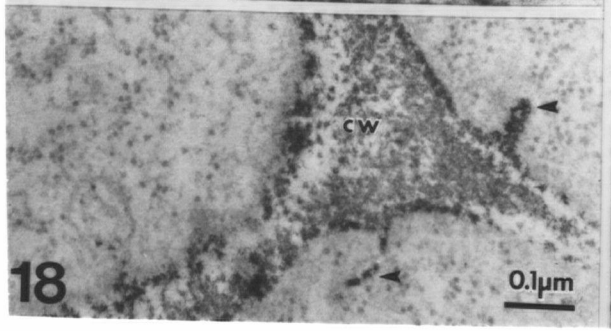
cw
18
0.1µm

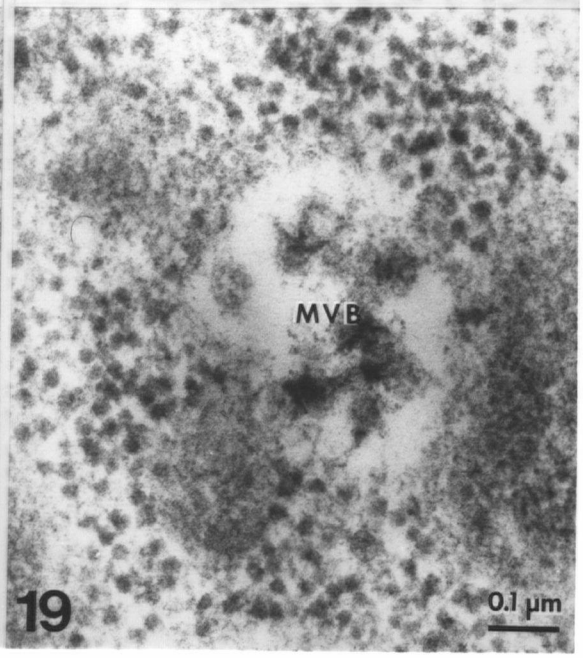
MVB
19
0.1 µm

Fig. 20: Density of endocytotic vesicles along axis of differentiation in primary root cell. Meristematic cells have relatively high amount of endocytosis; elongating cells have highest. The mature, vacuolate cells have lowest amount of endocytosis. Sample size for each stage was 45 cells.

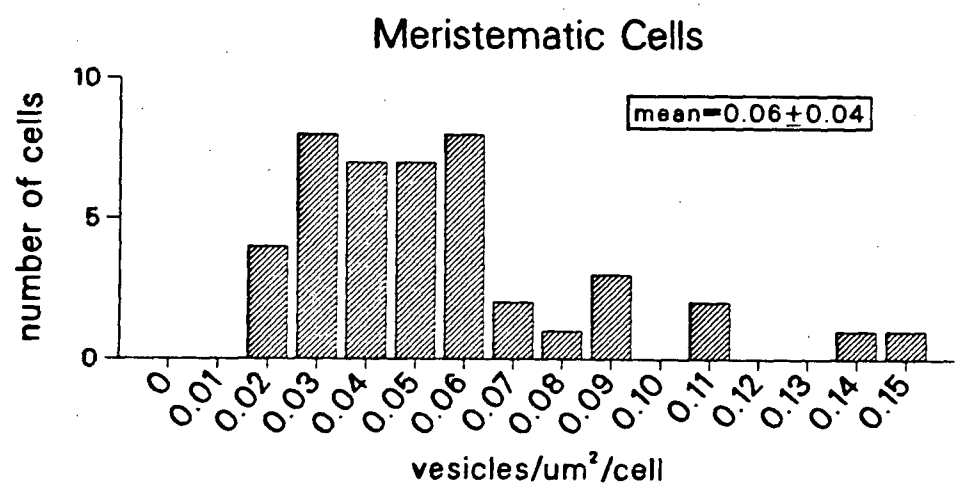
Meristematic Cells
mean=0.06±0.04
number of cells
10
5
0
0 0.01 0.02 0.03 0.04 0.05 0.06 0.07 0.08 0.09 0.10 0.11 0.12 0.13 0.14 0.15
vesicles/um²/cell

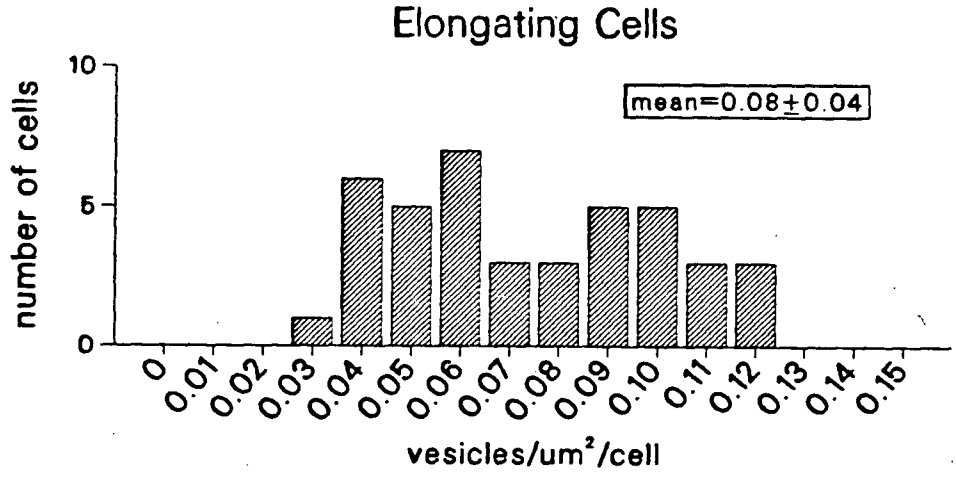
Elongating Cells
mean=0.08±0.04
number of cells
10
5
0
0 0.01 0.02 0.03 0.04 0.05 0.06 0.07 0.08 0.09 0.10 0.11 0.12 0.13 0.14 0.15
vesicles/um²/cell

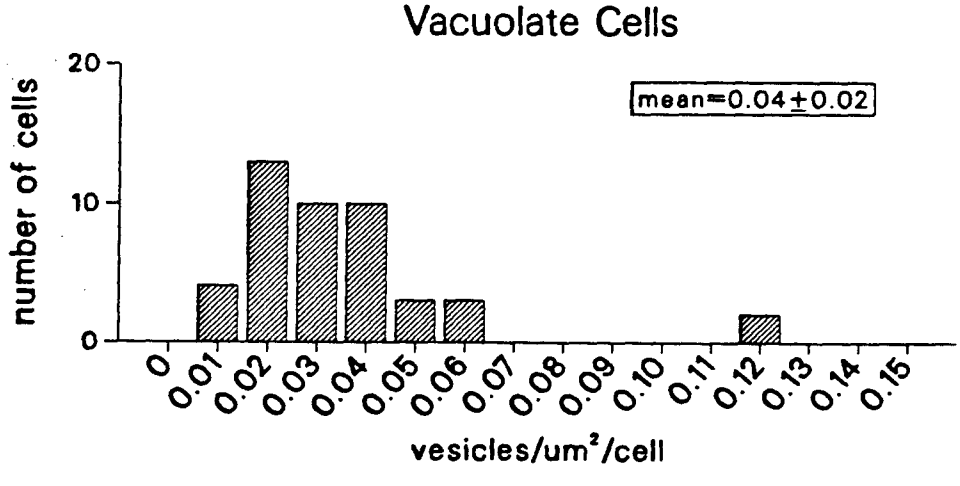
Vacuolate Cells
mean=0.04±0.02
number of cells
20
10
0
0 0.01 0.02 0.03 0.04 0.05 0.06 0.07 0.08 0.09 0.10 0.11 0.12 0.13 0.14 0.15
vesicles/um²/cell

DISCUSSION

In previous studies of endocytosis in higher plant cells, a high degree of variability in the amount of endocytosis has been reported (Joachim and Robinson 1984, Tanchak and Fowke 1987). For this reason, quantification of endocytosis was necessary to compare different cell types. One explanation for the high variance is the effect of plane of section on the occurrence of labelled vesicles. A section adjacent to the plasma membrane could have more vesicles than a section through the perinuclear region, where the vesicles could have already fused with multivesicular bodies.

In contrast to the results for maize root cap (Hubner *et al*. 1985) lanthanum, not lead, seems to be the superior marker for endocytosis in primary root cells of *Lobelia erinus*. Lanthanum did not appear to cross the plasma membrane; this is consistent with earlier findings (Revel and Karnovsky 1967, Taylor and Hall 1979). In previous studies where lanthanum was reported in the cytoplasm, incubations of up to 15 hours in high concentrations of lanthanum were used (Van Steveninck *et al*. 1976). In the present study, short time exposure (1 hour) and relatively low

concentrations (5 mM La) were utilized. It must be noted that lanthanum may displace calcium ions (Martin and Richardson 1979), which could bring about changes in phospholipid domains, pectic bridges in the cell wall, and the calcium metabolism of the cell. Calmodulin function did not seem to be impaired because cytoplasmic systems controlled by this protein appear normal, e.g. microtubules (Keith et al. 1983).

The lanthanum labelling of cellular structures found here agrees well with the results from studies of endocytosis in plant protoplasts and animal cells. The presence of turgor pressure may account for some characteristic differences in differentiating root cells. The smooth membrane intermediate structures first described by Staehelin and Chapman (1987) for secretion under turgor and observed in this study, may represent a mechanism for endocytotic invagination. In addition, the basket of the coated membrane forms a geodesic dome structure that could support the membrane against turgor (Pesacreta and Lucas 1985).

In animal cells, coated vesicles have been shown to play a role in receptor mediated endocytosis; relatively little is known about the

function of coated vesicles from plant cells (Robinson and Depta 1988). In animal cells, coated vesicles are active in selectively concentrating integral membrane proteins during receptor mediated endocytosis (Brown et al. 1983). The processes of differentiation could require a changing complement of enzymes, secretory products, membrane pumps or pores over time.

Coated vesicles could be carrying some of these proteins to and from the endomembrane system of the plant in a manner analogous to receptor mediated endocytosis in animals. The localization of peroxidase (Griffing and Fowke 1985) and glucan synthases (Griffing et al. 1986; Depta et al. 1987) in coated vesicles is consistent with this hypothesis. On theoretical considerations, it is possible that receptor mediated endocytosis occurs in the turgid higher plant cell (Saxton and Breidenbach 1988). The internalization of coated vesicles observed in these experiments may represent specific uptake of integral membrane proteins but further work is required in this area.

This is the first report of cytoskeletal elements associated with endocytosis in plants. It is possible that in differentiating plant cells

microtubules appear close to the endosomes as a fortuitous consequence of the close packing of microtubules as they form a coil restricting lateral expansion (Lloyd and Seagull 1985). However, the presence of fibrillar connections between vesicles and microtubules can be interpreted as evidence of a functional role for microtubules in endosome transport.

The relationship between endosomes and microtubules in Lobelia root cells agrees with the reported transport of endosomes in animal cells (Kolset et al. 1979, Vale 1987). It is possible to speculate that kinesin or an analogous "microtubule motor" protein may be acting in vesicular transport in elongating root cells as it does in amoeba, neurons, and fibroblasts (Vale 1987). The association between microtubules and coated vesicles has been noted many times in higher plant cells (Doohan and Palevitz 1980, Ryser 1979, Emons and Traas 1986).

The increased uptake of extracellular medium in elongating secretory cells compared to vacuolated non-secretory cells, as described in this work, supports the concept that endocytosis is at least one of the mechanisms for balancing

exocytosis. The quantitative data in this study is consistent with a report that there were more coated vesicles in "growing cells" than non-growing cells (Emons and Traas 1986). However, in the absence of endocytotic markers, it is impossible to tell if those coated vesicles were involved in endocytosis or exocytosis. Vesicular membrane recycling during wounding has been demonstrated in an alga, Boergesenia (O'Neil and LaClaire 1988).

Based on the results of this study and similar results in protoplasts, a model of membrane cycling in elongating root cells can be proposed (Fig. 21). Coated and smooth vesicles could invaginate from the plasma membrane, pulled against the forces of turgor by the cytoskeleton. Uncoating of the endocytotic vesicle would then occur fairly rapidly, which could account for the greater number of smooth vesicles than coated vesicles. Smooth vesicles could also bud off the plasma membrane, perhaps via the formation of intermediate structures described by Chapman and Staehelin (1987) for secretion. In this study, similar structures were observed labelled with lanthanum, suggesting endocytosis under turgor does occur.

After formation of endocytotic vesicles, the microtubule system may transport vesicles to the multivesicular bodies. Lanthanum accumulates in the multivesicular body. This is consistent with reports on animal cells where horseradish peroxidase was used as a fluid phase marker; it appeared only in the endosomal and lysosomal compartments but not in the Golgi (Farquhar 1981, de Chastellier et al. 1987, Storrie et al. 1984).

For membrane recycling to occur, the internalized membrane must make its way back to the Golgi, to package the cell wall material being secreted. Because vesicles associated with the Golgi were not labelled in this study, a direct fusion between endocytotic vesicles and Golgi does not appear likely. Vesicular membrane recycling could still occur if small vesicles, (e.g. with diameter of 50 nm, and with a high surface area to volume ratio) pinch off the multivesicular body or endosome. The formation of tubules or small vesicles has been proposed as a mechanism of extruding the aqueous contents of the endosome, allowing concentration of membrane components (Rome 1985, Geuze et al. 1984). Thus membrane recycling could be a two step process, first the internalized

membrane reaches the multivesicular body, then membrane material is shuttled back to the Golgi for the next round of secretion.

It should be noted, however, that phospholipid transfer proteins or micelles could also play a role in membrane cycling (Robinson 1984, Steer 1985, Staehelin and Chapman 1987).

There are many unanswered questions in the area of endocytosis in plants regarding possible receptors and ligands, cytoskeletal connections, and the role of the lysosome/central vacuole in the ultimate fate of the material internalized. The present study is part of a growing body of literature that supports the view that plant cells have the ultrastructural apparatus to undergo endocytosis and that endocytosis is an integral part of the membrane homeostasis of the endomembrane system.

Fig. 21: Model of membrane recycling during cell wall secretion.

cv= coated vesicle, sv= smooth vesicle, mt= microtubules stipple= lanthanum, squares= secretory product, triangles= clathrin coat protein.

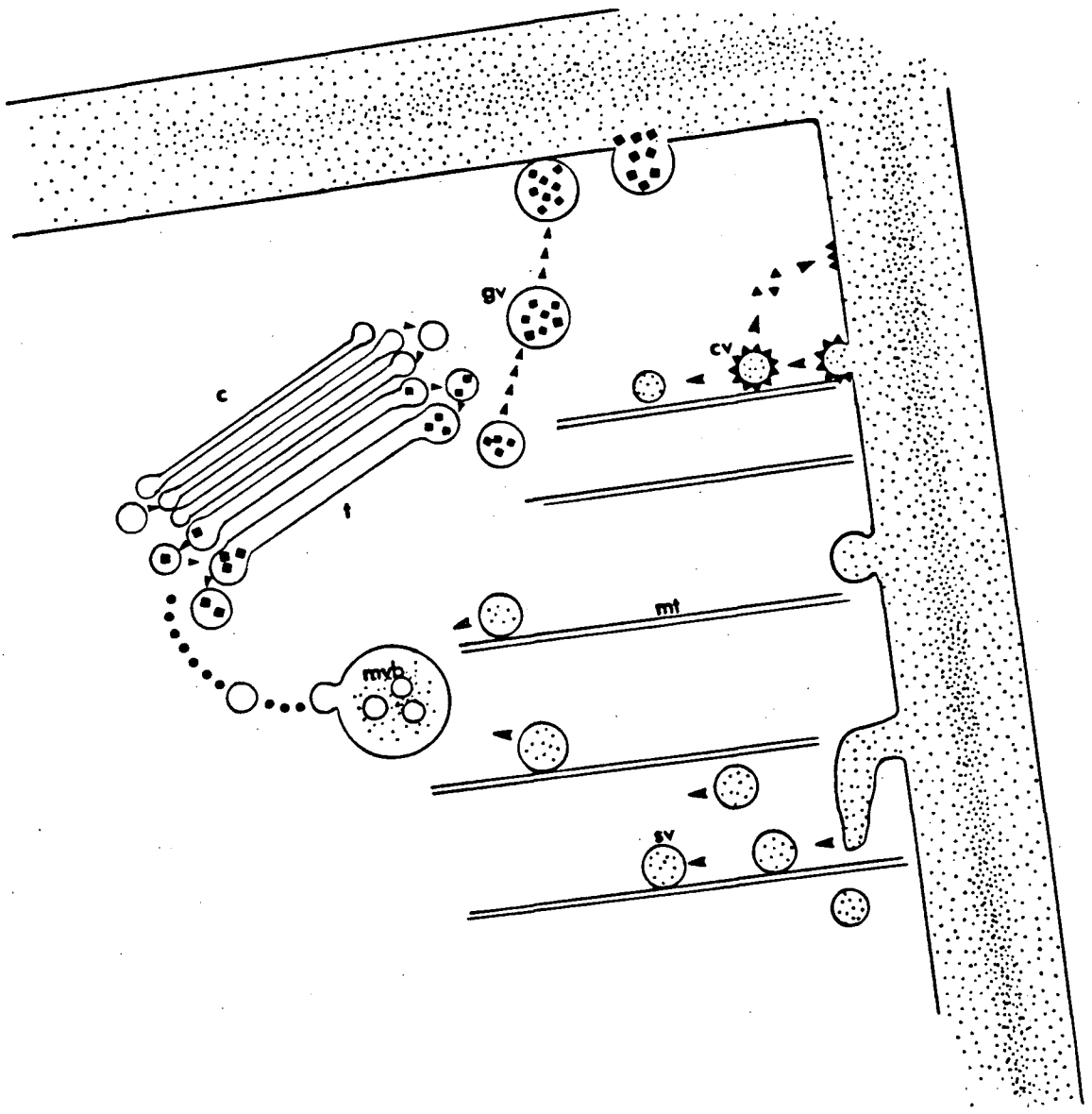

Chapter 2

SECRETION OF CELL WALL COMPONENTS IN ELONGATING ROOT CELLS OF *LOBELIA ERINUS*

In a study of endocytosis it is appropriate to examine the environment in which endocytosis occurs. The objective of this study was to examine the intracellular conditions and factors directly related to endocytosis, with emphasis on the interrelationship between this process and secretion. Granulocrine secretion can be considered the opposite of endocytosis, as it represents the vesicle mediated addition of membrane material to the plasma membrane through membrane fusion. The aqueous contents of the vesicle are released, resulting in the extrusion of secretory product into the external environment.

The membrane in the secretory cell flows from endoplasmic reticulum (ER) to dictyosomes, collectively called the Golgi apparatus, to plasma membrane (PM) (the endomembrane hypothesis of Morre and Mollenhauer 1974, Harris 1986). The endomembrane system can be roughly divided into ER-like membranes (nuclear envelope, ER, transition vesicles, cisternae of the cis Golgi) and PM-like membranes (cisternae of the trans Golgi, trans Golgi network, secretory vesicles, endosomes,PM).

New membrane material would mature from the ER

type composition to the PM type composition as it moves across the dictyosome stack (Morre and Mollenhauer 1983). The characteristic endoplasmic reticulum lipids are phosphatidyl choline (PC), phosphatidyl ethanolamine (PE) with phosphatidyl inositol (PI) and phosphatidyl glycerol as minor components (Chrispeels 1980). Free sterols, glucocerebroside, PC and PE are the principle lipid components in the plasma membrane (Rochester et al. 1987). Both plant and animal cells exhibit this high sterol:phospholipid ratio at the plasma membrane (Leonard and Hodges 1980).

The organelles of the endomembrane system also show polarity in terms of heterogenous protein compositions (Morre 1975). Coinciding with biochemical determinations is the evidence from freeze fracture studies, which show "membrane differentiation" with respect to the protein composition, i.e. changes in intra membrane particles (IMP) across the Golgi (Staehelin and Kiermayer 1970, Northcote and Lewis 1968).

The endoplasmic reticulum is the major site of phospholipid synthesis (Montague and Ray 1977, Morre 1970) and cotranslational insertion of integral membrane proteins (Walter and Blobel 1982,

Walter et al. 1984, Wickner and Lodish 1985, Von Heijne 1985, Boston et al. 1982). This production of membrane components in the ER supplies the organelles of the cell with membrane either by vesicular transport or phospholipid transfer proteins (Robinson 1985, Morre and Mollenhauer 1980). The ER must be considered a dynamic structure: resident proteins as well as transitory proteins are found there. In cultured animal cells, the retention of resident proteins in the ER is highly selective; proteins lacking retention signal are exported through the Golgi to the PM (Wieland et al. 1987).

In higher plant cells, the ER is often observed lying parallel to the plasma membrane, separated from it by the cortical cytoplasm (Chrispeels 1976, Craig and Staehelin 1988). This configuration may be related to the importance of the ER in maintaining low intracellular calcium concentrations (Buckhout 1984, Moore 1986). There are many structural elements in cortical cytoplasm that are controlled by Ca^{2+} concentration changes, eg. vesicle fusion, polymerization of cytoskeletal elements, and membrane fluidity (Picton and Steer 1985).

In higher plants, the morphological and functional relationships observed between the ER and Golgi have some special features (Chrispeels 1976, Mollenhauer and Morre 1976, Robinson 1980). In contrast to protein secreting animal cells, there are few transition vesicles between the ER and Golgi in plant cells (Morre and Mollenhauer 1976, Robinson 1980, Dauwalder and Whaley 1982).

It has been suggested that fewer transition vesicles are required between the ER and Golgi because less protein is being produced in the plant cell (Robinson and Kristen 1982). However, the polysaccharides produced in the plant cell will require membrane packaging; the amount of membrane required on the maturing face of the Golgi should be independent of the chemical composition of the vesicle contents. Less membrane addition to the cis face of the Golgi could be interpreted as support for an efficient membrane recycling mechanism on the trans face. Direct connections between the ER and the trans Golgi have been interpreted as a GERL (Golgi ER Lysosome) network, similar to that described by Novikoff in animals (Harris and Oparka 1983, Harris 1986). Ultrarapidly frozen root cells did not show

connections between the ER and Golgi (Craig and Staehelin 1988).

The functions of the Golgi in plants, animals, and fungi include glycosylation, sorting, and packaging of secretory products. The dictyosome usually consists of 4-8 stacked cisternae. Each cisterna is characterized by a comparatively stable central plate containing resident proteins and a peripheral network from which vesicles bud.

There are several models of cisterna formation, maintenance, and maturation (Farquhar 1985, Shannon et al. 1982, Robinson 1985). The cisternal progression model suggests the entire cisterna moves through the dictyosome stack, maturing as it goes from cis to trans faces (Farquhar 1985). This model is supported by the work of Brown and coworkers who studied scale secretion in a Chrysophycean alga. One scale per cisterna is produced and the entire cisterna is shed from the dictyosome as the scale matures (Brown 1969).

An alternate hypothesis is a fixed cisterna model, where each cisternae is specialized for a subset of glycosylation or sorting functions. In this model, resident enzymes would be stationary in

the cisterna with membrane and substrate being transferred by vesicles from cisterna to cisterna. This model has received support from a variety of sources. Specific cytochemical reactions and glycosyl transferases have been localized in cis, medial, or trans cisternae (Pavelka 1987). Vesicular transport has been simulated in vitro, demonstrating that intercisternal transport is unidirectional and sequential (Balch et al. 1984). Recently the view of the Golgi as a relatively fixed structure with dynamic flow of membrane and products has emerged (Farquhar 1985, Orci et al. 1989). The nature of the intercisternal transport vesicles is currently the subject of investigation; the vesicles are coated but the coat does not appear to consist of clathrin (Griffiths et al. 1985, Orci et al. 1986).

The products of the Golgi include extracellular matrices, membrane proteins, glycolipids, and lysosomal proteins. These products must be sorted to the correct intracellular destination. In animal cells, the extensive network of vesicles and tubules at the trans face of the Golgi is believed to be the region where sorting occurs (Van Deurs et al. 1988).

The reticular nature of this region was originally interpreted as a specialized domain of ER, and based on its alkaline phosphatase activity it was named GERL, for Golgi-ER producing lysosomes (Novikoff 1964). Recognition of the variety of Golgi products which traverse this trans Golgi region, and the lack of evidence for ER connections, have led to its redefinition as the trans Golgi network (TGN) (Griffiths and Simon 1986).

The TGN has been characterized using the transport of lysosome enzymes via the mannose-6-phosphate receptor and the transport of the vesicular stomatitus virus G protein as models (Kornfeld and Kornfeld 1985, Griffiths et al. 1985). Analogous models have not been developed for plant cells, and little is known about the mechanism of sorting of Golgi products. The situation is further complicated by an additional sorting destination, the vacuole (Dorel et al. 1989).

While the basic functions of the Golgi can be considered universal (Farquhar and Palade 1981), differences between phyla can be seen. In higher plants, the Golgi tend to occur as individual

dicytosomes, with seemingly random orientation; animal dictyosomes tend to occur as a perinuclear complex, peripherally associated and with similar polarity. The cis to trans polarity is more pronounced in plant dictyosomes; the lumen of the cisternae gradually narrows in the trans direction (Morre and Mollenhauer 1983, Robinson 1985). The complex membrane arrangements at the trans face of the plant dictyosome have been interpreted as the fragmentation or sloughing off of the trans cisterna (Mollenhauer 1971, Robinson 1985).

A partially coated reticulum (PCR), located near the dictyosome, has been described in higher plant cells (Pesacreta and Lucas 1985). The PCR is an anastomosing network of vesicles and tubules. There is now a "developing controversy" as to the nature of the PCR (Tanchak et al. 1988). It has been interpreted as an endosome, distinct from the dictyosome (ibid.); it has been called an extension of the trans Golgi cisternae (Hillmer et al. 1988, Robinson and Depta 1988). Robinson and coworkers suggest the PCR would become separated from the dictyosome by the sloughing off of the trans cisternae (Hillmer et al. 1988). In view of the

confusion surrounding the PCR and trans Golgi membranes in higher plants, cytochemical and ultrarapid freezing studies were undertaken to examine these PM-related membranes.

The major component of secretion in wall secreting cells is polysaccharides. To observe polysaccharides, cytochemical stains specific for polyhydroxy compounds can be used. There are several protocols for staining polysaccharides (Roland 1978) such as modified periodic acid-Schiffs (Thiery 1967, Ryser 1979), alkaline bismuth (Park et al. 1987, Shinji et al. 1976), ruthenium red (Vian and Reis 1972) or alcian blue (Trachtenberg and Fahn 1981). The use of these stains has provided morphological evidence that complements biochemical and autoradiographic evidence that polysaccharides are assembled in the Golgi (Dixon and Northcote 1985, Dauwalder and Whaley 1982). In this study, the Golgi was only a part of the overall membrane systems examined for polysaccharide content. The partially coated reticulum and multivesicular body, as elements of the PM-like endomembrane system were also examined. Conventional transmission electron microscopy sample preparation was compared with ultrarapid

freezing on a polished copper block held at liquid nitrogen temperature, followed by freeze substitution.

In summary, the objectives of this study were:

1. In view of the confusion surrounding the PCR and trans Golgi membranes in higher plants, cytochemical and ultrarapid freezing studies were undertaken to examine these PM-related membranes.

2. The Golgi and associated membrane systems were examined for polysaccharide content, indicating cell wall matrix synthesis.

3. Ultrarapid freezing and staining for polysaccharides should identify which compartments are part of the pathway of exocytosis. This technique immobilizes membranes at the instant of freezing and should provide an accurate picture of the endomembrane system

4. The pathway of exocytosis can be compared with the pathway of endocytosis shown in chapter 1.

Conventional TEM Fixation

Lobelia erinus seedlings were germinated on filter paper moistened with distilled water for 7 days. The plants were manipulated by the cotyledons, under a dissecting microscope. The seedlings were fixed for 1 hour in a dilute Karnovsky's fixative consisting of 1 % glutaraldehyde and 1.5 % formaldehyde, freshly prepared from paraformaldehyde powder in 50 mM PIPES pH 7.4. After 2 rinses of 10 minutes each in buffer, the samples were postfixed in 1 % OsO_4, buffered as above, overnight at 4^{o} C.

After a rinse in buffer, the samples were dehydrated through a series of increasing concentration of methanol. Propylene oxide was used as a transition solvent between methanol and resin. The seedlings were infiltrated and embedded in epon. Silver sections were obtained using a diamond knife on a Reichert OMU3 or a Reichert Ultracut E and mounted on uncoated 200 mesh copper grids. The grids were stained in saturated uranyl acetate for 25 minutes, followed by rinsing in distilled water. Sato's lead citrate was used for 5-7 minutes in a low carbon dioxide environment.

Peroxidase Cytochemistry

Seedlings were treated to localize endogenous peroxidase following the methods of Griffing and Fowke (1985). The cells were fixed in 1 % glutuaraldehyde in 60 mM sodium phosphate buffer, pH 7.4, followed by 5 washes in the buffer over 1 hour, with the pH decreasing stepwise from 7.4 to 5.4. The peroxidase substrate and cytochemical reagents were 5 mM hydrogen peroxide and 4 mg/ml diaminobenzidine (DAB). The seedlings were incubated with the substrate/reagent mix for 10 minutes, 30 minutes, or 60 minutes. For control treatment, samples were incubated in DAB alone or buffer alone. At the end of the incubation period, the samples were put on ice and again rinsed thoroughly over 1 hour. Postfixation using 1 % OsO_4 was carried out overnight at 4^{o} C. After several washes in buffer, methanolic dehydration and epon embedding was performed as described above for TEM. Sections were observed under the Zeiss 10C TEM without poststain to improve the relative contrast of the peroxidase reaction product.

Ultrarapid Freezing/ Freeze Substitution

For ultrarapid freezing, seeds were germinated as described above and frozen at 7 days postimbibition. Seedlings were placed on a layer of filter paper, on a layer of parafilm which was stuck on a soft foam pad with a gluestick. The soft foam pad was backed with a metal planchette that magnetically attaches to the MM80 attachment of the Reichert-Jung KF80 freezing apparatus. The samples were mounted and kept in a humid environment while the polished copper mirror ("metal mirror") equilibriated to liquid nitrogen temperature (-196° C). The planchette, with attached sample, was then rapidly transferred to the MM80 arm and slammed against the metal mirror. The samples on the filter paper were then separated from the soft foam by removing the now brittle parafilm. The samples were transferred, under liquid nitrogen, to the Reichert-Jung CSAuto for freeze substitution.

The substitution was carried out in 1 % OsO_4 at -80° C for 55 hours. During this time, the water in the sample was replaced with acetone. The temperature was increased at a rate of 10° C per hour until it reached 0° C. At this time, the

osmium acetone mix was replaced and rinsed with ice cold absolute acetone. After several rinses, the samples were allowed to come to room temperature and infiltrated in Spurr's resin. After embedding and curing the resin, silver sections were cut on the Ultracut E.

Polysaccharide cytochemistry

Several cytochemical techniques for polysaccharides were tested in preliminary experiments (see references Appendix 2 for details of methods).

Both conventionally fixed and ultrarapidly frozen material was stained in alkaline bismuth, following the procedure of Shinji et al. 1976). A stock solution of 1 g bismuth subnitrate, 2 g sodium tartrate, 5 g sodium hydroxide and 50 ml deionized distilled water was prepared. This was diluted 1 ml in 40 ml deionized distilled water to give the working solution. The grids were stained at 40^{o} C for 40 minutes in a humid environment, then rinsed by gently agitating in beakers of deionized distilled water.

The sections were examined and photographed on the Zeiss 10C operated at 60 kV.

The endogenous peroxidases of the root tip of L. erinus were localized with the classical cytochemical technique of Graham and Karnovsky (1966). The production of this enzyme can be considered an example of constitutive protein secretion. The reaction product for peroxidase was found in the cell wall, vesicles associated with the cortical cytoplasm, and intraluminal vesicles of the vacuoles (Figs. 22-25). In the cell wall, the peroxidase reaction product is stratified into several wall layers (Figs. 22-24). The epidermal mucilage layer is more darkly stained than the cellulosic layer (Fig. 24). The plasma membrane and nearby vesicles also contain reaction product (Figs. 23, 24). The dictyosome vesicles were amorphous in terms of membrane and contents (Fig. 25). In some areas the cytochemical reagents did not penetrate into the tissue making it impossible to draw any conclusion about peroxidase levels between tissues.

To examine organelles related to cell wall synthesis, cytochemical stains for polysaccharide were used. Of the several stains tested (Table 4) alkaline bismuth staining gave most consistent results on both conventionally fixed (Figs. 26-36)

Table 4: Comparison of cytochemical stains labelling pattern on L. erinus root tips. All stains were visualized by TEM.

Stain	Structures labelled
periodate-silvermethenamine post stain	cell wall; cells easily digested with periodate.
ruthenium red en bloc	outermost cell wall layer; root hairs; root cap.
alcian blue en bloc	root cap mucilage; epidermal outer wall layer.
pectinase-colloidal gold on Epon sections	no signal above noise.
alkaline bismuth post stain	dictyosomes; vesicles; partially coated reticulum; plasma membrane; cell wall

and freeze substituted tissue (Figs. 36-38). This method has been used to stain Golgi vesicles, cell wall and plasma membrane of pear leaves (Park et al. 1987).

In Lobelia erinus root cells, well characterized carbohydrate containing structures were stained with alkaline bismuth. Examples of these are the starch granules (Fig. 22, compare control Fig. 23) and the cell wall (Figs. 26, 28, 32-34; compare controls Figs. 27, 29, 35). The starch granules are more prominent in the plastids of the root cap than in the plastids of epidermal or cortical cells. The positive reaction of starch granules to alkaline bismuth confirms the specificity of this stain for polysaccharide.

The cell wall appeared stratified into several layers that varied depending on the cell type and sectioning effects (Fig. 26 vs. 28). In general the pattern of cell wall staining observed was (from the cell surface): a darkly staining extracellular surface of the plasma membrane, a zone of decreased density into which fibrils from the cell surface projected, a dense cellulosic layer, and a darkly stained middle lamella zone.

In conventionally fixed material, the region between the plasma membrane and cell wall contained alkaline bismuth reactive vesicles which can be identified as lomasomes (Fowke and Setterfield 1969 Figs. 28, 29, 34, 35). No such vesicles were identified in ultrarapidly frozen material (Figs. 36, 37). Fibrillar connections between the plasma membrane and cell wall could be visualized with alkaline bismuth (Fig. 28, 33, 34). The plasma membrane often had cortical microtubules lining the cytoplasmic surface; the cell wall stain in these regions had no obvious relationship to the microtubules (Fig. 32).

It is common to observe vesicles in the cortical cytoplasm in both the conventionally fixed and the ultrarapidly frozen; some of these stained positively with alkaline bismuth (Figs. 28, 30, 32-34, 36-38). It is interesting to note however that there is a wide variety of staining intensities between vesicles (Fig. 30, 34, 36). It was often difficult to distinguish coated membranes in the ground cytoplasm on sections that were stained for polysaccharides only (Fig. 33). This could be because the protein coat on the membrane does not react with the stain for polysaccharide.

The conventional TEM fixation did not preserve the vesicles of the dictyosomes (Figs. 29, 30). Fixation conditions were varied in an attempt to improve the Golgi preservation, but these structures were easily disrupted. Different combinations of buffers, divalent cations, or formaldehyde : glutaraldehyde ratios were tested (data not shown). Under these conditions of poor preservation it was difficult to assess the number of transition vesicles between the ER and dictyosome, or the staining properties of the dictyosome cisterna (Fig. 30). This can be compared with the material that was ultrarapidly frozen where the dictyosomes and adjacent vesicles are clearly delineated (Figs. 36-38). Vesicles were observed in between the ER and dictyosomes; these vesicles have small diameters (about 50 nm).

After ultrarapid freezing, dictyosomes displayed cis to trans polarity similar to that described by Robinson and Kristen (1982) where the cisterna width decreases in the cis to trans direction (Fig. 36). Alkaline bismuth staining intensity also displayed a definite polarity, with highest density in the trans cisternae (Figs. 36-38)

The trans face of the Golgi shows a reticulum of tubules and vesicles; one subset of these vesicles are larger (diameter about 100-150 nm) than the peripheral vesicles of the dictyosome (diameter about 50-100 nm). These larger vesicles resembled some of the darkly staining cortical vesicles, thus they may represent secretory vesicles (Fig. 36) . The reticulum at the trans Golgi face can be distinguished by the presence of these larger vesicles.

In addition to the trans Golgi associated reticulum, a separate complex with small vesicles and staining characteristics similar to the plasma membrane were observed (Figs. 36-38). This system of anastamosing tubules and vesicles can be interpreted as the partially coated reticulum (Pesacreta and Lucas 1985). This structure was commonly observed in the ultrarapidly frozen cells, but rarely in the conventionally fixed cells.

Multivesicular bodies were lightly stained with alkaline bismuth (Figs. 30, 34, compare control Fig. 31). After conventional fixation, a population of small vesicles in the cytoplasm surrounding the multivesicular body are stained with alkaline bismuth. After ultrarapid freezing,

similar vesicles can be seen budding from or fusing with the multivesicular body (Fig. 38).

The most distinctive features seen in the ultrarapidly frozen material compared to conventionally fixed tissue are the presence of an elaborate network on the trans Golgi face, absence of lomasomes, and the presence of many small shuttle or transition vesicles between organelles of the endomembrane system. The provacuoles and central vacuole showed the same relative alkaline bismuth reactivity (Figs. 28, compare control Fig. 29). It was difficult to interpret the nature of the material associated with the inner surface of the vacuole; the tonoplast was stained by lead and uranyl acetate as well. It is interesting to compare the poststained material (Figs. 26-38) with the peroxidase material which was unstained (Figs. 22-25).

Figs. 22-25: Endogenous peroxidase activity in elongating Lobelia root cells.

Fig. 22: survey of first cell layer showing penetration of DAB product in cell wall. Arrow shows intraluminal vesicle in central vacuole.

Fig. 23: epidermal cells labelled along cell wall and in cortical vesicles (arrow).

Fig. 24: cell wall layers show differential staining; cortical vesicles stained.

Fig. 25: poor dictyosome perservation.

V=vacuole, cw=cell wall, pm=plasma membrane, pv=provacuole, c=cellulosic layer, m=mucilage, d=dictyosome.

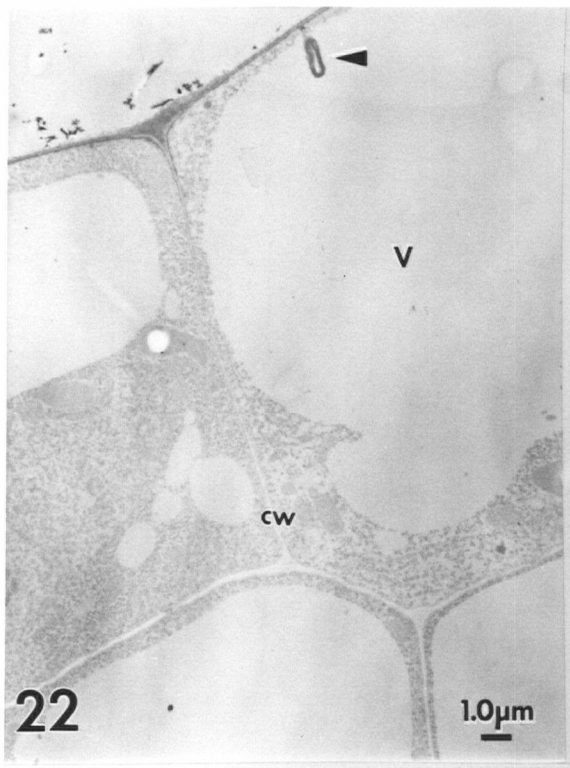
V
cw
22
1.0µm

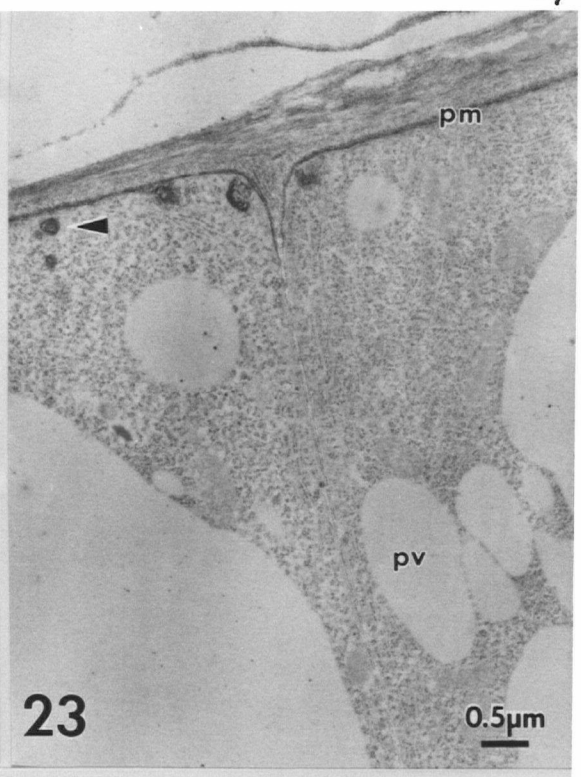
pm
pv
23
0.5µm

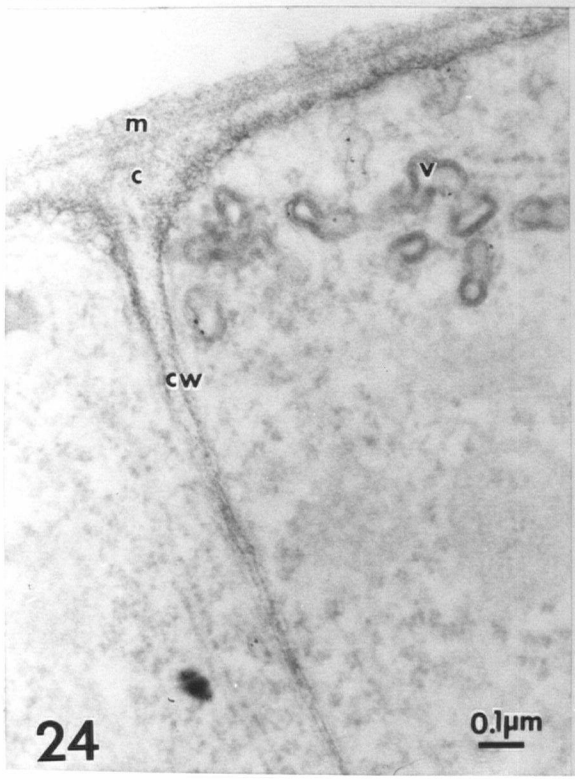
m
c
v
cw
24
0.1µm

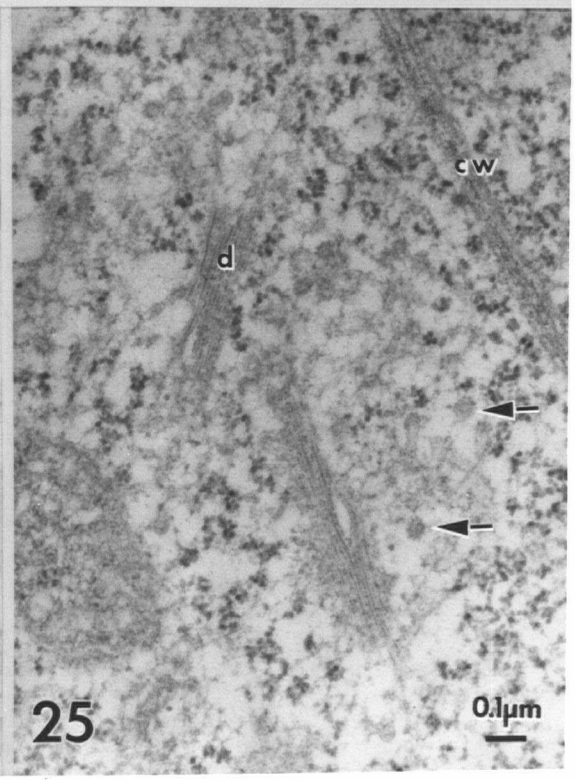
cw
d
25
0.1µm

Figs. 26-31: Alkaline bismuth staining of conventional TEM preparations.

Fig. 26: starch granule stained with alkaline bismuth.

Fig. 27: control starch granule stained with uranyl acetate/ lead citrate.

Fig. 28: secretory granule (arrow) and cell wall stained with alkaline bismuth.

Fig. 29: control stained with uranyl acetate/ lead citrate.

Fig. 30: dictyosome, multivesicular body stained with alkaline bismuth.

Fig. 31: control multivesicular body stained with uranyl acetate/ lead citrate. Note: plaque on MVB. cw=cell wall, s=starch granule, pv=provacuole, d=dictyosome, mvb=multivesicular body.

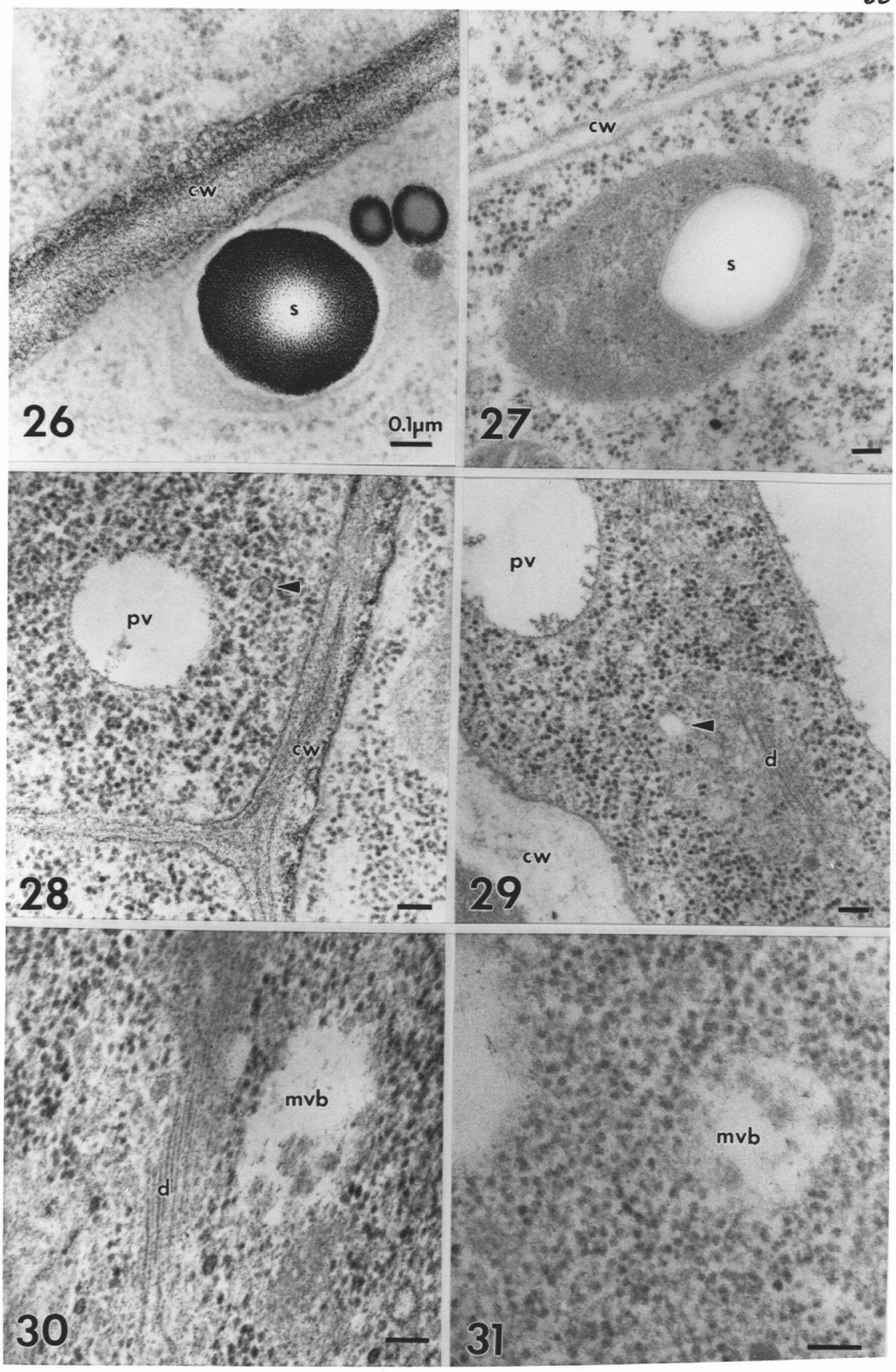
cw
s
26
0.1µm
cw
s
27
pv
cw
28
pv
d
cw
29
mvb
d
30
mvb
31

Figs. 32-35: Alkaline bismuth staining of conventional TEM preparations.

Fig. 32: tangential section through cortical cytoplasm showing secretory vesicle (arrow), and cell wall stain positive for polysaccharides.

Fig. 33: cortical vesicle, plasma membrane, and cell wall in elongating cell.

Fig. 34: differential staining of cortical vesicles; multivesicular body does not stain for polysaccharides.

Fig. 35: control section stained with uranyl acetate/ lead citrate. arrow indicates vesicle, asterisk indicates unusual polygonal structure that resembles coated membranes.

mt=microtubules, cw=cell wall, l=lomasome, mvb=multivesicular body.

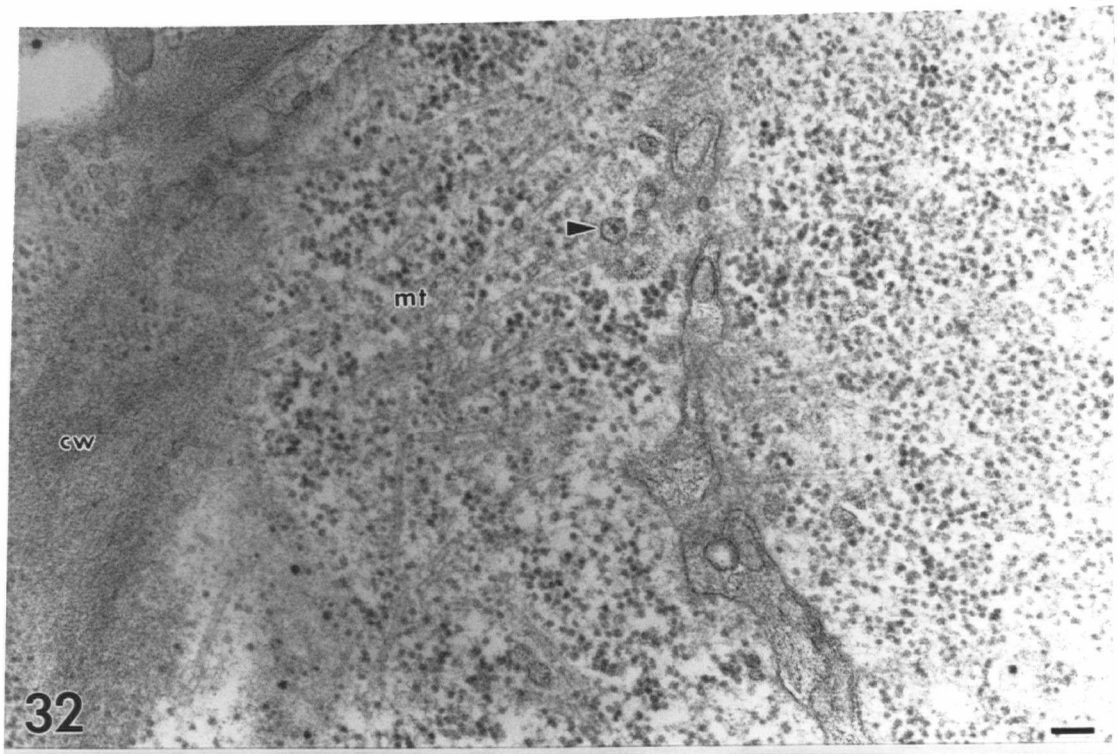
mt
cw
32

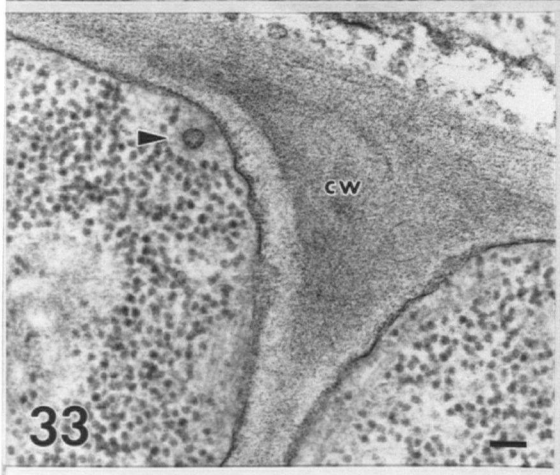
cw
33

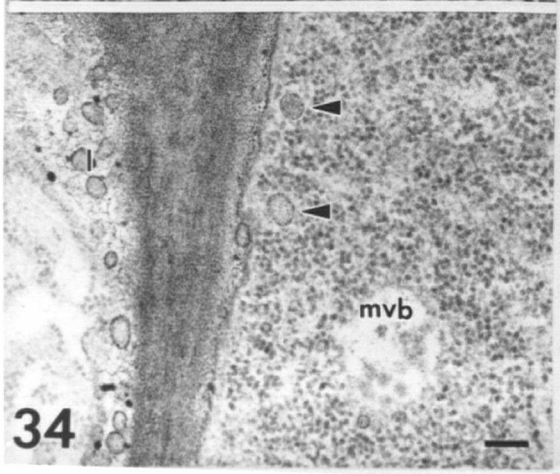
mvb
34

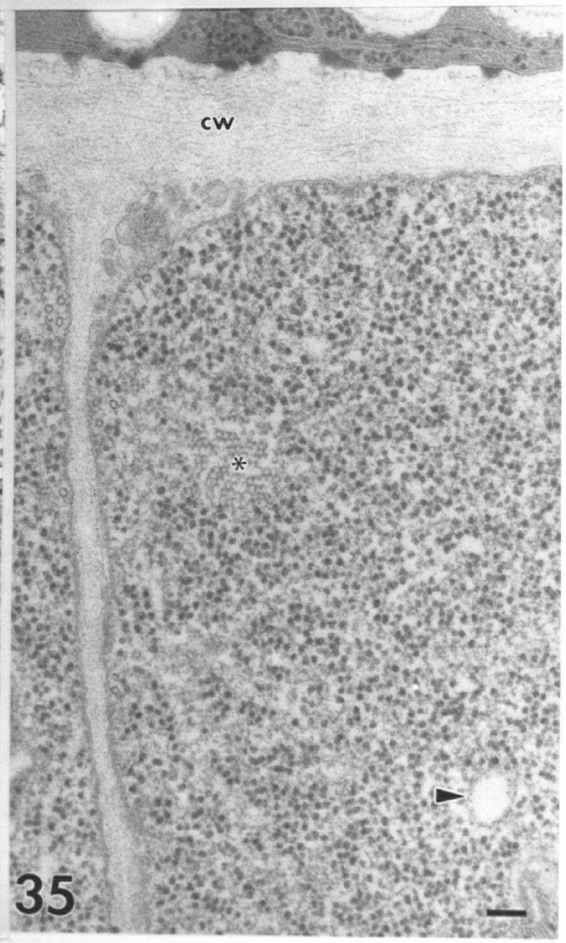
cw
35

Figs. 36-38: Alkaline bismuth staining of ultrarapidly frozen, freeze substituted material.

Fig. 36: example of epidermal cell ultrastructure. ER not stained, dictyosome exhibits polarity from cis to trans, secretory vesicles at trans Golgi and in cortical cytoplasm (arrows).

Fig. 37: dictyosome between plasma membrane and developing central vacuole.

Fig. 38: dictyosome with extensive trans Golgi reticulum, separate from partially coated reticulum, multivesicular body.

pcr=partially coated reticulum, c=cis Golgi face, t=trans Golgi face, mvb=multivesicular body, d=dictyosome, er=endoplasmic reticulum, t=tonoplast.

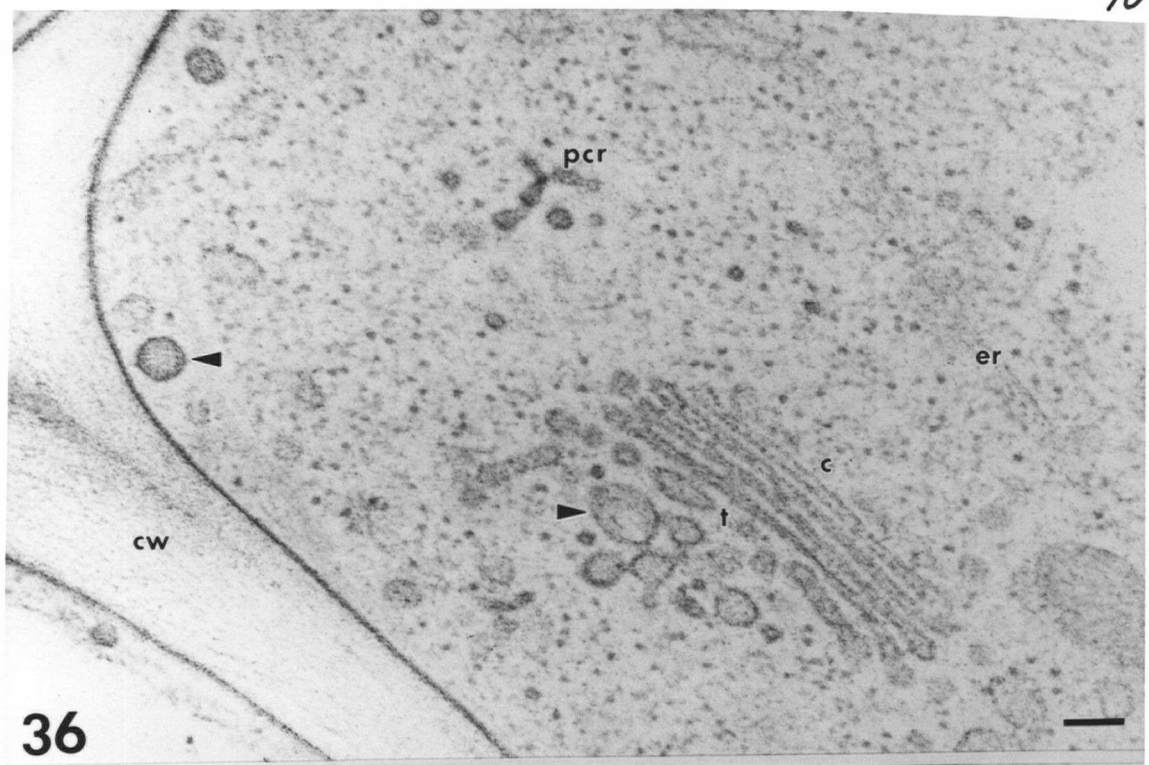

36

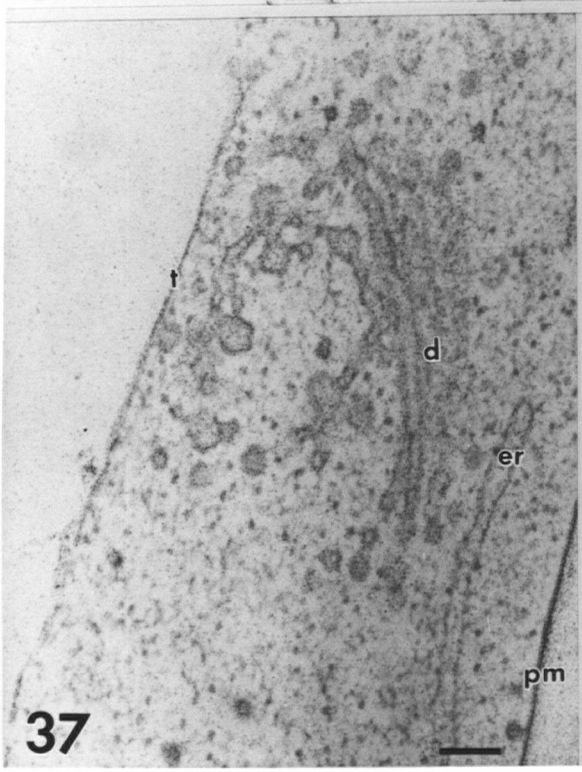

37

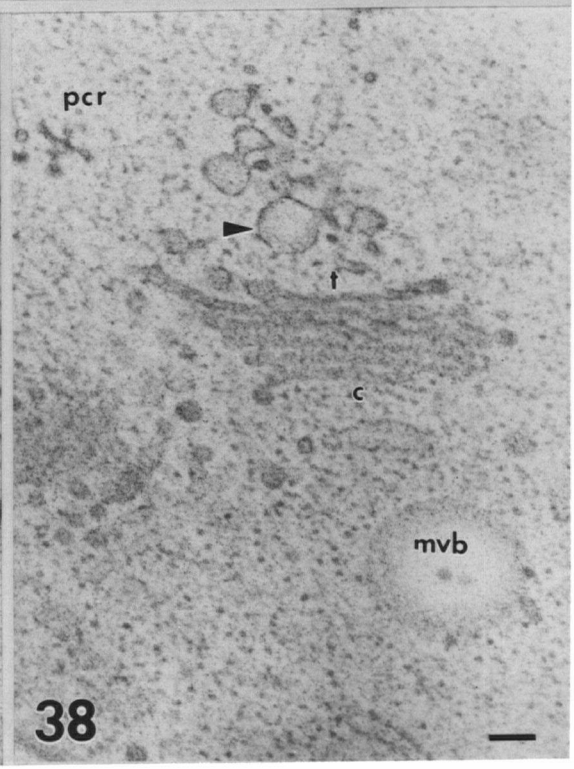

38

The PM-related membranes of the endomembrane system may be considered the environment for the overlapping pathways of exocytosis and endocytosis. The exocytotic pathways shown in this study were peroxidase secretion and cell wall matrix secretion. The results of the cytochemical studies of conventionally prepared TEM samples agree well with results reported in other higher plant (Vian and Reis 1972, Ryser 1979) and animal species (Thiery 1967).

The cellular location of peroxidase in cortical vesicles, cell wall, and vacuole is consistent with the functions postulated for this enzyme. Peroxidase in the cell wall may play a role in cross linking tyrosine units of extensin during cell wall synthesis, and in cross linking phenolic units during lignification (Fry 1986). Since lignification does not begin until the cell is fully elongated, the latter function is probably not critical in the elongating cell.

In a similar cytochemical study of soybean suspension cultured cells, peroxidase was found in the cell wall and vacuoles (Griffing and Fowke 1985). In cultured cells, peroxidase reaction product was faint in the trans dictyosome, but did

not appear on the surface of the plasma membrane. The Lobelia root cells' dictyosomes were not labelled, whereas the plasma membrane and some associated vesicles were heavily labelled. The cortical vesicles which show peroxidase activity may represent secretory vesicles delivering peroxidase to the cell wall. The label on the cell surface would then be recently extruded secretory product, before its incorporation into the wall.

It is unexpected that the endoplasmic reticulum and dictyosome are not labelled by this technique, as these organelles are the sites of protein synthesis and modification. The pH at which the cytochemical tests are carried out and the fixation protocol which precedes the cytochemical test may have created unfavorable conditions for enzyme activity; the parameters employed had been used to localize peroxidase in cultured cells (Griffing and Fowke 1985). It was difficult to judge the dictyosome peroxidase content due to poor preservation of these organelles in conventional preparations. This is an area that cryotechniques could be applied to in the future.

The high level of endogenous peroxidase found in the elongating root cells, and in other higher plant species, eliminate peroxidase as a useful marker for endocytosis in higher plants. Horseradish peroxidase is widely used in animal cell biology to study the endomembranes and kinetics of endocytosis (Steinman et al. 1983).

The cytoplasmic synthesis and eventual deposition of peroxidase can be used as an example of protein secretion. However, proteins only make up about 10 % of the cell wall; 90 % of the wall is polysaccharide (McNeil et al. 1984). To get a complete picture of the exocytotic pathway in the elongating cells, it was necessary to use stains for polysaccharides. Although historically other methods, such as the modified PAS reaction, have been used to detect polysaccharides, alkaline bismuth staining was the most reproducible and distinctive stain for this tissue.

In conventionally fixed samples, the cell wall, extracellular face of the plasma membrane, and vesicles reacted strongly with alkaline bismuth. The intensity of staining of vesicles was highly variable. The heavily stained vesicles could be secretory vesicles carrying cell wall

precursors since the density of stain in these vesicles resembles the density of stain in the cell wall. The lightly stained vesicles could represent endocytotic vesicles, but in the absence of markers for endocytosis this interpretation is speculative. Due to the process of membrane recycling, some endosomes may stain positively for secretory product. In rat acinar cell, it was shown that the a portion of the protein secretory product was reinternalized by endocytosis (Romagnoli and Herzog 1987). This apparent paradox illustrates the difficulty of interpreting this type of experiment.

The cell wall has been considered as little more than a technical impediment to the study of the plasma membrane and the intimate relationship between these structures is ignored. The wall may influence the plasma membrane in a manner analogous to the restraints imposed on the plasma membrane by the cytoskeleton. In this study, structural continuity was observed between the extracellular face of the plasma membrane and the cell wall. The fibrils projecting from the cell surface may be cell wall components that have been secreted and are coalescing with the existing cell wall. Alternatively, the fibrils seen projecting from the

cell wall could be components of the glycocalyx, the carbohydrate coat on the cell surface. If this coat is linked to the cell wall matrix, the extracellular connections could restrict the mobility of the glycolipids and glycoproteins in the membrane.

The vesicles found in the periplasmic space between the cell wall and plasma membrane, called lomasomes, are only observed in conventionally fixed material, not in ultrarapidly frozen material. In other studies of ultrarapidly frozen plant cells, the plasma membrane was reported as smooth and unperturbed (Fernandez and Staehelin 1985). This suggests lomasomes are an artifact of chemical fixation, as suggested many years ago by Fowke and Setterfield (1969). One possible mechanism of generation of lomasomes could be the stabilization of plasma membrane-cell wall connections by glutaraldehyde during primary fixation. During aldehyde fixation, lipids are not stabilized so the membrane may be contracting and expanding over the fixation and rinse period. If some domains of the membrane are held in place by association with the extracellular matrix, these domains could be torn out of the membrane.

Membrane fragments would then vesiculate to form lomasomes.

In the conventional TEM micrographs, plant cells often show a "typical undulating appearance of plasma membrane" (Leonard and Hodges 1980). In contrast, one of the criteria for judging the success of ultrarapid freezing is the smooth, unperturbed appearance of the membranes (Gilkey and Staehelin 1986). The endomembranes seen in zones of well frozen material in this study have distinctive appearances. There are many more vesicles present and the dictysome associated network is extensive. When stained with alkaline bismuth, these sections provide information on the location of polysaccharide in the unperturbed cell.

In ultrarapidly frozen material, there are small vesicles in the zone of cytoplasm between ER and the Golgi. This is predicted by the endomembrane concept (Morre and Mollenhauer 1974), but has not been commonly observed in conventional preparations (Steer 1985). The presence of these vesicles suggests that one mechanism for transport of membrane subunits between the ER and the Golgi is by vesicles, another possible mechanism is phospholipid transfer proteins (Robinson 1985, Fernandez and Staehelin 1985).

The ER elements do not contain enough polysaccharide to give a positive alkaline bismuth reaction. Although fractionation studies have suggested that some cell wall matrix components are assembled in the ER (Bowles and Northcote 1972, 1974), the ER is a minor component when compared to the Golgi, the predominant site of cell wall matrix synthesis (Fincher and Stone 1981).

In ultrarapidly frozen preparations, the Golgi cisternae showed polarity across the stack of the dictyosome with respect to cisternae width and alkaline bismuth staining properties. The polarity has been noted for a variety of characteristics, i.e. phosphotungstic acid-chromic acid staining, intercisternal elements, and osmium staining (Robinson and Kristen 1982, Shannon et al. 1982).

A model formulated to explain sensitivity of the Golgi to ionophores suggests a mechanism for maintaining polarity (Griffing and Ray 1985). In this model, proton transporting ATPases in the cisterna membrane would create a pH gradient; the protons would associate with ionized carboxyl groups of the pectins in the cisterna lumen. Osmotic effects would then cause water to leave the lumen of the cisterna and force secretory product

out to the peripheral vesicles.

It has been suggested that there are two pathways where sorting of membrane components and secretory products occurs: the endosome pathway and the trans Golgi network (Van Deurs et al. 1988). In plants and animals multivesicular bodies are recognized as endosomes (Tanchak and Fowke 1987, Friend 1969). The multivesicular bodies were not stained for polysaccharides in both conventionally fixed and ultrarapidly frozen Lobelia roots. This suggests the endocytic pathway and exocytic pathway are separate at this point.

The endosome in animal cells has been divided into two morphological and functional compartments: the peripheral tubular network and the perinuclear multivesicular bodies (Miller et al. 1986). Functionally these correspond to early and late endosomes. In the early stage, endosomes serve as compartments for uncoupling receptors and ligands (CURL) (Geuze et al. 1984, Schmid et al. 1988). The late endosome is believed to be involved in transit to the lysosome (ibid., Griffiths et al. 1988). The partially coated reticulum observed in the ultrarapidly frozen Lobelia root cells is morphologically similar to the early endosome in

animals. Further support to the theory that PCR may be an endosome, analogous to those of animals, comes from enzyme cytochemistry. Acid phosphatase, the marker enzyme for lysosomes, was not found in the PCR in higher plant protoplasts, suggesting they are prelysosomal compartments (Record and Griffing 1988).

Thus in Lobelia root tip cells the biosynthetic pathway for polysaccharides is via Golgi, trans Golgi network, secretory vesicle, and plasma membrane. Organelles that did not stain strongly for polysaccharides coincide with the pathway for endocytosis as outlined in Chapter 1. If the partially coated reticulum does represent an early endosome, then microtubules may play a role in transporting the endosome through the cytoplasm as it matures into a multivesicular body, as they do in animal cells (Miller et al. 1986). The following chapter examines the roles microtubules play in elongating cells of Lobelia.

Chapter 3

MICROTUBULES IN ELONGATING ROOT CELLS OF *LOBELIA ERINUS*: EFFECT OF COLCHICINE ON ENDOCYTOSIS

INTRODUCTION

The objective of this study was to examine the microtubules in elongating root cells of *Lobelia erinus*. Immunofluorescence and TEM were used to study the cytoskeleton, with emphasis on the role of the microtubules in endocytosis during cell wall synthesis. The study of microtubules in the deposition of cellulose microfibrils has overshadowed other aspects of the role of the cytoskeleton in cell wall secretion. There is little information on how vesicles are moved from the Golgi to the plasma membrane during secretion, or from the plasma membrane to internal endomembranes during endocytosis.

In the animal systems in general, vesicle transport has been shown to be primarily microtubule based (Kolset *et al.* 1979, Sheetz *et al.* 1986). Vesicle transport has been dissected *in vitro* to isolate the force generating proteins, e.g. kinesin (Schnapp *et al.* 1985, Vale 1987).

In elongating root cells the microtubules are a prominent feature of the cytoskeleton. Microtubules, first observed transversely around the longitudinal axis of the cell, were interpreted as hoops of microtubules around the cell (Ledbetter

and Porter 1963). Immunofluorescence techniques have altered this view: the array of microtubules in elongating cells has been described as a "helical array" (Lloyd and Seagull 1985).

The theory that microtubules act as guide elements for the deposition of cellulose microfibrils has received support from a variety of sources (Heath 1974, Seagull 1983, Hepler 1985). In general, the orientation of newly deposited cellulose microfibrils has been found to be parallel to the microtubules underlying the cell wall (Robinson et al. 1976). Treatment with the drug colchicine disrupts cortical microtubules, subsequently cellulose microfibril pattern becomes random (Pickett-Heaps 1967). The development of secondary wall patterns during xylogenesis has been cited as "one of the best examples of the relationship between microtubule disposition and microfibril orientation" (Falconer and Seagull 1985).

The consequence of deposition of cellulose microfibrils transverse to the long axis of the cell is the restriction of lateral expansion. The meristem cells have sides which are roughly square, but which become rectangular as the cell elongates.

The role of microtubules in this morphogenic event is illustrated by the changes that occur when cells are treated with ethylene (Roberts *et al*. 1985). Ethylene treatment inhibits cellular elongation and stimulates lateral expansion. Using immuno-fluorescence, the authors demonstated that the changes in cell shape were preceded by changes in microtubule orientation from a transverse to oblique pattern. The prominent microtubule network in the elongating cell appears to play important roles in the synthesis of the fibrillar component of the cell wall and in morphogenesis. It is not known what role, if any, this network plays in endomembrane turnover during synthesis of the matrix component of the cell wall.

Elongation is accompanied by the addition of exocytotic secretory vesicles (see chapter 2), and the removal of membrane material by endocytotic vesicles (see chapter 1). The microtubules present in elongating cells are good candidates for guiding vesicle movement. However, microtubules are only one part of the complex cytoskeleton found in higher plant cells which consists of microtubules, actin microfilaments (Palevitz 1987, McCurdy *et al*. 1988), and intermediate filaments (Powell *et al*.

1982, Dawson et al. 1985). In addition, the microtrabecular network interconnects the elements of the cytoskeleton listed above and the cellular organelles (Kobayashi et al. 1988, Cox et al. 1986).

The microtubules which underlie the plasma membrane were observed amongst lanthanum labelled endosomes (see chapter 1). Depending on the plane of sectioning, fibrillar connections can be observed between the endosome and microtubule. The microtubules are closely packed along the cytoplasmic face of the membrane; the endocytotic vesicles may simply be migrating freely past this region when they are fixed. Alternatively the mechanism of endocytotic vesicle transport could be along microtubules. To distinguish between these possibilities, elongating root cells were treated with colchicine to disrupt the microtubules and the pattern of vesicular transport compared with normal cells.

Plant cells are considerably less sensitive to colchicine than animal cells (Morejohn and Fosket 1986). In animal cells, nanomolar amounts of colchicine interfere with mitosis. Plant cells require millimolar amounts to produce the same

effect. In this work, immunofluorescence was used to determine the concentration of colchicine required to disrupt the microtubular array in Lobelia erinus. This colchicine level was then used in conjunction with lanthanum as a marker for endocytosis.

METHODS AND MATERIALS

Immunofluorescence

The buffer for all immunofluorescence experiments was microtubule stabilizing buffer (MSB), consisting of 50 mM PIPES, 5 mM EGTA, and 5 mM $MgSO_4$ pH 7.2. 7 day old Lobelia erinus seedlings were fixed for 40 minutes, 20 minutes, or 10 minutes in 4 % buffered formaldehyde, freshly prepared from paraformaldehyde. After 3 washes over 15 minutes the cell wall was partially digested for 20 minutes in 1 % cellulase (Sigma C-7377 from Aspergillus niger), and 0.5 % pectinase (Sigma P-2401 from Rhizopus species).

Poly-l-lysine (PLL) coated cover slips were prepared following the procedure of Fisher (1982). Square #1 coverslips were sonicated in hot soapy water for 5 minutes, followed by a rinse in distilled water. The coverslips were immersed in hot chromic acid-sulfuric acid for 1-2 hours at 70° C, then rinsed again in distilled water. A drop of one hundred microlitres of 2.5 mg/ml PLL was layered on the cover slip and allowed to stand for 5 minutes. If the coverslips were at all dirty, there would be hydrophobic repulsion, and neither the PLL nor the cells would adhere to the

coverslip. After 5 minutes, the PLL was drained off the slide and it was given a quick wash in distilled water. The coverslips were air dried and used within 1 hour.

The enzyme digested root tips were dissected away from the seedlings under a dissecting microscope. About 30 root tips would be placed in a drop of buffer on the PLL coated cover slip. A clean uncoated coverslip was used to squash the root tips and the squashes allowed to settle on the PLL for 1-2 hours, in a humid environment. The cells were made permeable to antibodies using either 1 % Triton-X-100 for 1 hour or by plunging the coverslips into 50 % methanol at -10° C for 10 minutes. Non specific protein binding sites were blocked with a "preincubation" of 1 % BSA for 10-20 minutes. Aldehydes were reduced with 3 washes of 3 minutes each in 1 mg/ml sodium or potassium borohydride. After 3 washes over 15 minutes, the cells were ready for antibody treatment.

Staining chambers were made by attaching strips of coverslip glass to a light microscope slide with silicone sealant. The coverslip with the cells was inverted over the strips, suspending

the cell into 100 microlitres of antibody solution. The benefit of this system is that small volumes of antibody are sufficient to evenly bath the cells. The staining chambers were set in a humid environment and maintained at 37^{o} C.

The primary antibody was anti-tubulin, raised in rabbit against chick fibroblast tubulin (polyclonal, Sigma T3536); the antibody was diluted from its stock solution 1:40 or 1:50 in 50 mM sodium phosphate buffer. The root cells were incubated with the anti-tubulin for 30 minutes or 1 hour in the staining chamber as described above. Excess antibody was removed with 3 washes in buffer of 10 minutes each. The slides were drained of buffer and stained with the secondary antibody, anti-rabbit IgG conjugated to fluoroscein isothiocyanate (FITC) (Sigma F0382), diluted 1:50 in 50 mM sodium phosphate buffer. This was the level at which staining with secondary antibody alone did not produce significant fluorescence. Anti- rabbit IgG conjugated to rhodamine was used in preliminary experiments but the level of background staining was unacceptably high. After a final series of 3 terminal washes buffer of 10 minutes each, the coverslips were mounted in 90 %

glycerol and viewed with a Leitz Dialux microscope fitted with epifluorescence illumination. All fluorescence photographs were taken with a standard 2 minute exposure to allow comparison between treatment (primary and secondary antibody) and controls (no primary antibody; secondary antibody only). Roots were treated with 10 mM colchicine for 2 hours at room temperature and fixed immediately in 4 % formaldehyde. The samples were then processed for immunofluorescence as outlined above alongside control (no colchicine) roots.

Results from 5 immunofluorescence experiments were analyzed using the Kontron Image Processing System (IPS). Negatives were illuminated on a light table; the image of the negative was recorded with a video camera which was operated on line with the IPS. The image was digitized, and the cells were edited out of the background. The integrated optical density, which describes the grey levels of the area of the cell, was measured for cells photographed at the same magnification (315X) and exposure (2 minutes). Standard black and white levels were set, taking into account the effect of stray light. Absolute numbers between experiments were variable but the amount of

fluorescence in samples treated with antitubulin could be compared to the amount of fluorescence in control samples (no antitubulin). When fluorescence within experiments was expressed as a percentage of the control fluorescence, the between experiment variation was small.

Transmission Electron Microscopy

Seven day old seedlings were pretreated with 10 mM colchicine, for 2 hours at room temperature. 5 mM lanthanum nitrate was added to the 10 mM colchicine solution to test for endocytosis after microtubule disruption. Pretreated seedlings were incubated in the lanthanum/colchicine for 1 hour. As controls, seedlings were treated with distilled deionized water, lanthanum only, or colchicine only. Samples were fixed without rinsing in dilute Karnovsky's fixative (1.5 % formaldehyde, 2 % glutaraldehyde in 50 mM PIPES buffer pH 7.4) for 1 hour. After 3 rinses of 10 minutes each in buffer, the samples were postfixed in 1 % OsO_4, overnight at 4 ^{o} C. Dehydration in methanol was followed by infiltration and embedding in epon resin. Silver sections were cut on the Reichert-Jung Ultracut E

and stained with methanolic uranyl acetate for 25 minutes. Grids were examined and photographed under the Zeiss TEM 10C.

RESULTS

The elongating Lobelia erinus root cells show the characteristic transverse microtubule arrays underlying the plasma membrane of differentiating higher plant cells (Fig. 39). This arrangement of microtubules was observed in both lanthanum treated (Fig. 46) and untreated control cells (Figs. 39, 40). Vesicles with and without lanthanum label were often associated with microtubules in the cortical cytoplasm (Fig. 46, see also chapter 1). The microtubules are arranged in parallel strands perpendicular to the axis of elongation. In this cell type, groups of 2-3 microtubules were more common than single microtubules (Fig. 40).

The biochemical identity of these hollow rod elements of the cytoskeleton as microtubules was confirmed by immunofluorescence. Incubation in primary antibody specific for tubulin resulted in bright cytoplasmic fluorescence (Fig. 43). There was low fluorescence in the nucleus and cell walls. Fragments of cells adhered to the poly-l-lysine coated coverslips and showed bright fluorescence, indicating the fluorescence was associated with the cortical cytoplasm, i.e. fluorescence was not released by opening the cell. Individual fibrils

usually observed in such immunofluorescence experiments, were not clear.

The bright fluorescence in cells treated with the primary antibody, anti-tubulin, was compared with low fluorescence in control cells which were treated with secondary antibody only (Figs. 43, 44). The brightness of the fluorescence was measured by the parameter of integrated optical density (IOD) on the Kontron IPS; bright fluorescence gives a lower integrated optical density (Fig. 50). For cells treated with anti-tubulin, the integrated optical density was 33 $\pm$ 2.3 % (n=3 replicate experiments) of control cells. The absolute brightness of the cells varied between replicates, but when brightness was expressed as a percentage of the control, the relative brightness did not vary between replicates.

When cells were treated with 10 mM or 100 mM colchicine, the pattern of fluorescence changed (Fig. 45). The peripheral cytoplasm was no longer brightly fluorescent, and the nuclear fluorescence increased. The perinuclear zone appeared as a bright band around the nucleus. The peripheral cytoplasm had uneven fluorescence. When the amount of fluorescence in these cells was quantified, the

integrated optical density in cells treated with colchicine and anti-tubulin was 43 ± 17 % of controls. This indicates that the fluorescence was dimmer in these cells than in cells not treated with colchicine; the fluorescence is more variable as well. Since 10 mM and 100 mM concentration of colchicine gave similar results, the lower concentration was used in all subsequent TEM experiments.

After 2 hour incubation in 10 mM colchicine, the organelles of the elongating root cells showed minor ultrastructural changes (compare control Fig. 41 with Fig. 42). The nuclei in control cells were spherical in shape, whereas in colchicine treated cells the nuclei become irregular in shape. The plasma membrane of colchicine treated cells undulated and showed many more lomasomes and blebs (Fig. 42). Tangential sections through the plasma membrane and cortical cytoplasm displayed the normal transverse microtubule arrays (Fig. 46). After colchicine treatment, these arrays are almost entirely absent (Fig. 47). Occasionally a microtubule would survive the colchicine treatment; these remnants were always seen immediately below the plasma membrane, never deeper in the cytoplasm

than 50 nm from the membrane. The remnants were usually directly connected to the plasma membrane by a thin arm (data not shown).

When cells were pretreated with colchicine, followed by an incubation in lanthanum and colchicine, the effects of microtubule disruption on endocytosis can be seen. There were fewer lanthanum labelled vesicles in the cells treated with colchicine plus lanthanum than in cells treated with lanthanum alone. The multivesicular bodies in colchicine treated cells were not labelled as often as were the multivesicular bodies in control cells (compare control Fig. 48 with Fig. 49). The dictyosomes appeared normal after colchicine treatment. The intercisternal spacing was similar to the dictyosomes in control cells, and a multivesicular body was often observed near by (Fig. 46).

Figs. 39-42: Microtubules in elongating cells.

Fig. 39: Plasma membranes of adjacent cells joined by plasmodesmata. Microtubules line cytoplasmic face of plasma membrane (arrow).

Fig. 40: Tangential section through the cell wall, plasma membrane, and cortical cytoplasm. Microtubules appear in groups (arrow).

Fig. 41: No colchicine control cells have spherical nuclei, smooth membranes.

Fig. 42: Colchicine treated cells have irregular nucleus, wavy membranes.

cw=cell wall, p=plasmodesmata, pm=plasma membrane, m=mitochondrion, v=vesicle, pv=provacuole, Nu=nucleus.

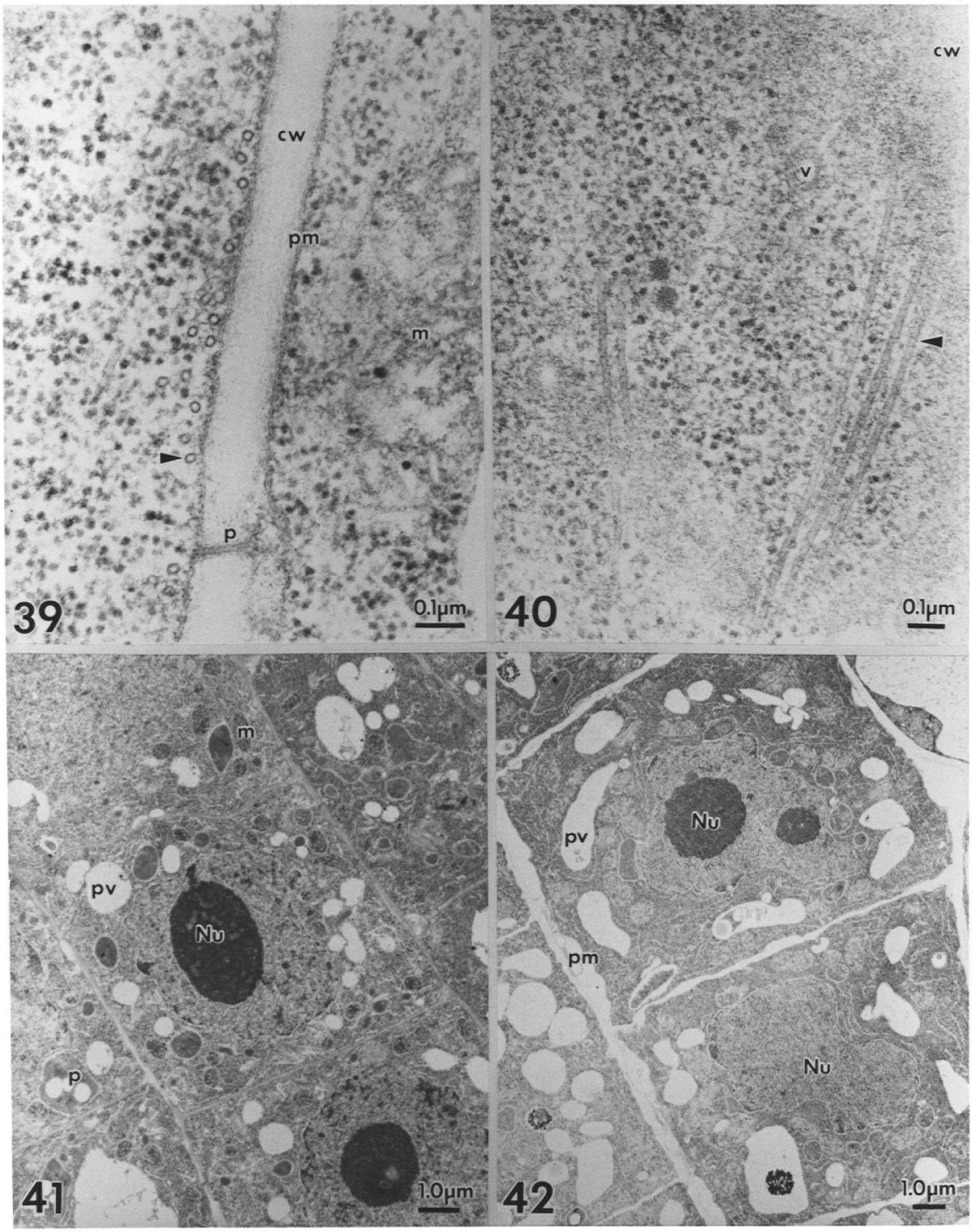
cw
pm
m
p
39
0.1μm
cw
v
40
0.1μm
m
pv
Nu
p
41
1.0μm
pv
Nu
pm
Nu
42
1.0μm

Figs. 43-45: Anti-tubulin Immunofluorescence.

Fig. 43: Cells treated with anti-tubulin primary antibody; antitubulin detected with secondary antibody-FITC. Fluorescence bright in cytoplasm, dim in nucleus and cell wall.

Fig. 44: Cells not treated with anti-tubulin, just secondary antibody-FITC, control for nonspecific binding.

Fig. 45: Colchicine incubation before fixation, anti-tubulin primary antibody, secondary antibody-FITC. Fluorescence in nuclear periphery bright, while cortical cytoplasm fluorescence patchy.

All bars=5 um

All treatments photographed for standard times and conditions.

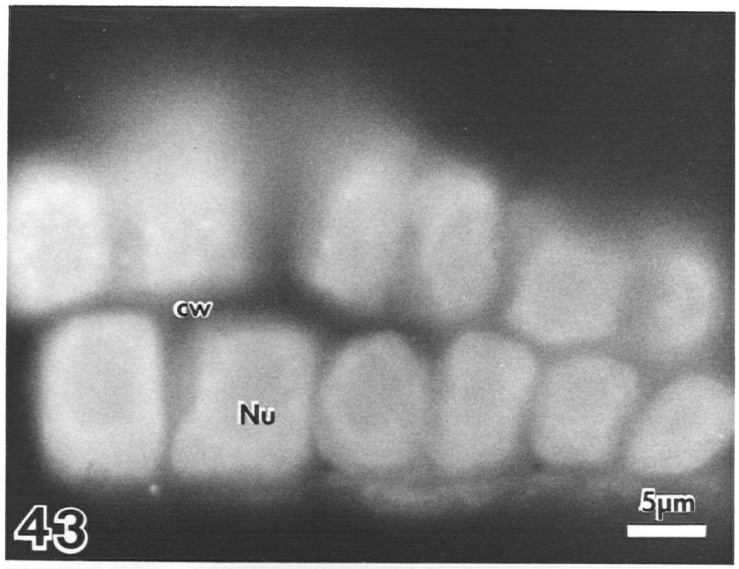
cw
Nu
5μm
43

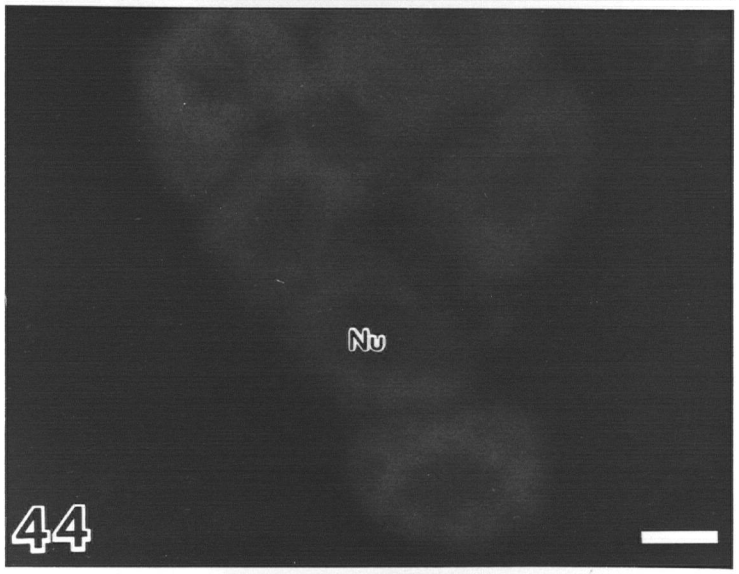
Nu
44

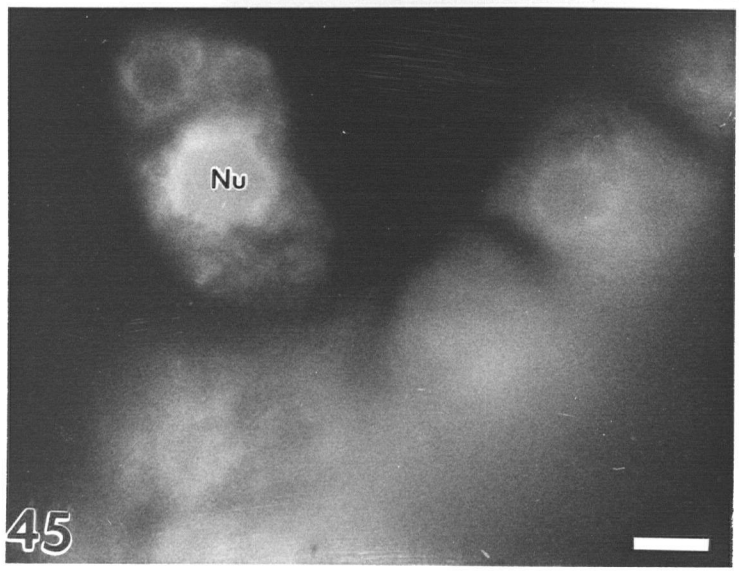
Nu
45

Figs. 46-49: Effect of colchicine on endocytosis in elongating root cells.

Fig. 46: Cell wall and vesicles labelled with lanthanum only, no colchicine. Tangential section through cell wall, plasma membrane, cortical cytoplasm shows microtubule array characteristic of elongating cells. Arrow indicates labelled endocytotic vesicle.

Fig. 47: Region of cortical cytoplasm after colchicine treatment. Wavy plasma membrane; no microtubules present; pattern persists in cellulose microfibrils in cell wall (open arrow).

Fig. 48: Multivesicular body-dictyosome association in colchicine treated cells. MVB unlabelled.

Fig. 49: Multivesicular body in no colchicine, lanthanum only treated cell. Arrow indicates lanthanum deposits.

All bars=0.1 um

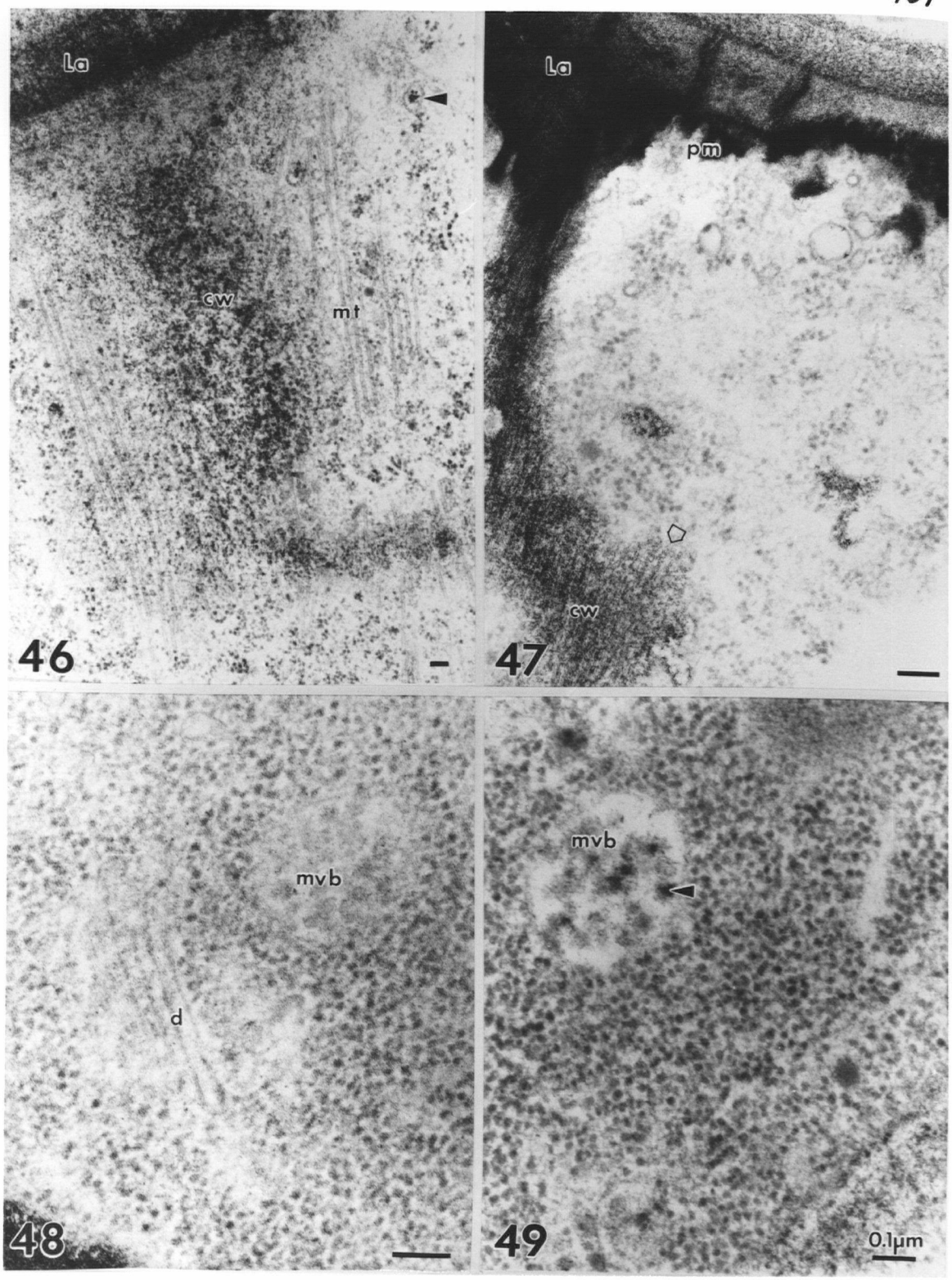
La
cw
mt
46
La
pm
cw
47
mvb
d
48
mvb
49
0.1µm

Fig. 50: Quantification of anti-tubulin immunofluorescence. Integrated optical density (IOD) measures brightness of fluorescence, i.e. brighter fluorescence is less density. "+Ab" indicates treated with anti-tubulin primary antibody. "-Ab" indicates no primary antibody, treated with secondary antibody-FITC only. "+col" indicates treated with 10 mM colchicine.

Microtubule Immunofluorescence

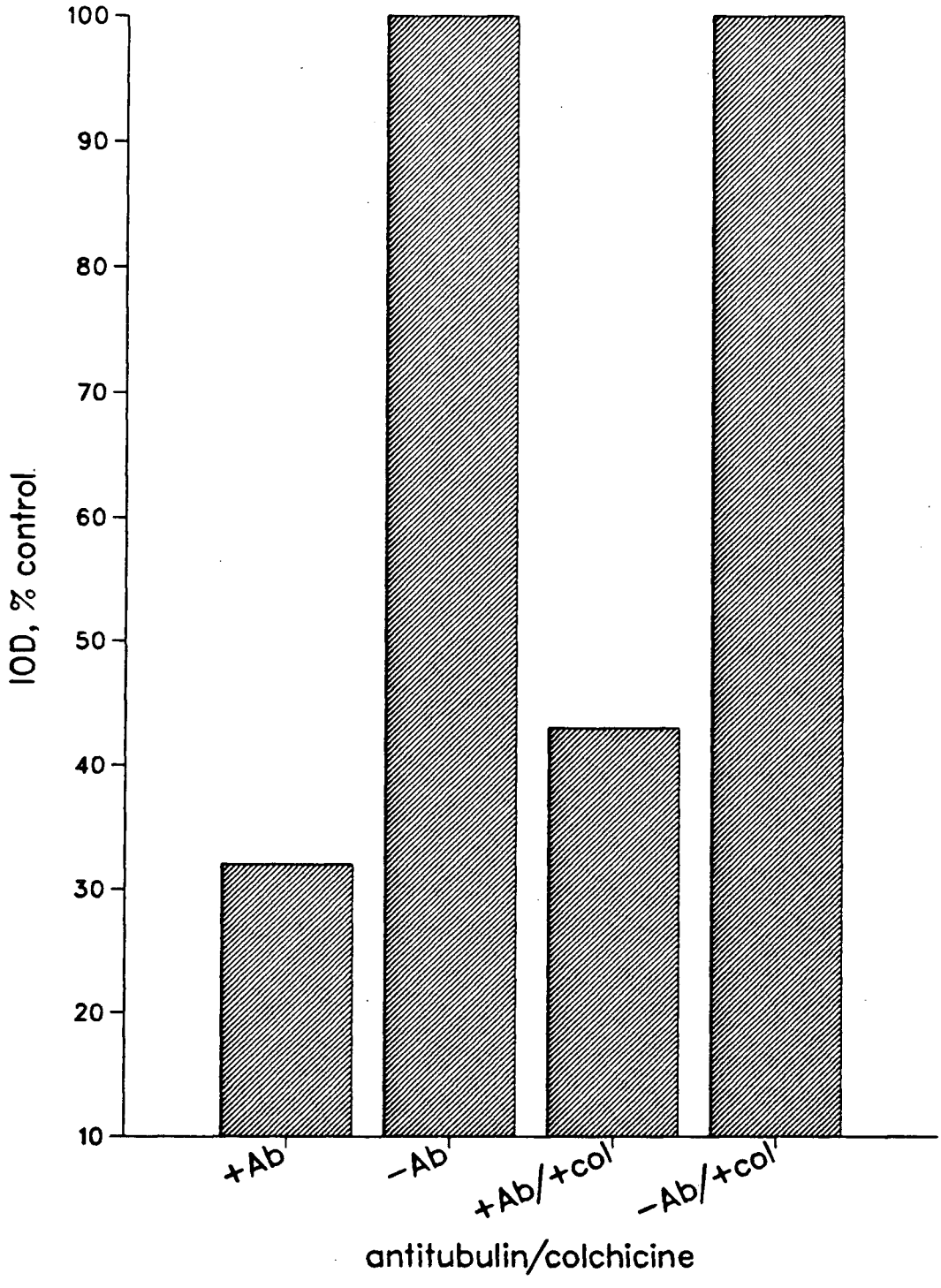

DISCUSSION

Microtubules play an important role in the maintenance of normal cell structure in elongating Lobelia root cells. They can be considered to be a structural framework, maintaining cell shape. Disruption of this cytoskeletal element with colchicine led to the redistribution of immunofluorescence patterns and changes in endocytosis, such as fewer lanthanum labelled vesicles and less multivesicular body labelling.

Whole Lobelia erinus root cells showed bright fluorescence when treated with polyclonal antitubulin antibodies, however, the bright fluorescent strands of microtubule pattern were not clear. The special properties of the plant cell make the observation of individual strands problematic. The thickness of the cell, the presence of the cell wall, and the density of closely packed cortical microtubules can all contribute to obscure the striation in the image (Van der Valk et al. 1980, Wick et al. 1981, Simmonds et al. 1983). In the first report of microtubule immunofluorescence in intact higher plant cells, it was noted that "thickness of an intact cell can make resolution of individual

bundles difficult...where microtubule density is low enough thin fluorescent fibres, almost certainly individual microtubules, can be traced, as in the case of well spread animal cells" (Wick et al. 1981).

The high microtubule density, small size, and boxlike shape of the Lobelia root cells are important considerations when interpreting this type of experiment. Immunofluorescence of cryo sections can be a good alternative to whole mounts (Sakaguchi et al. 1988). The cryo technique would have the added benefit of bypassing the processing steps of cell wall digestion, membrane permeabilizing by Triton or methanol, and squashing on PLL coated coverslips.

The fluorescence observed in the Lobelia root cells appears only in cells treated with the specific primary antibody. Control samples incubated in buffer instead of primary antibody did not show significant fluorescence when incubated with secondary antibody-FITC. It is possible that the bright fluorescence is the result of primary antibody binding nonspecifically to cytoplasmic components. However, the drastic changes in the fluorescence patterns of cells treated

colchicine suggests fluorescence is the result of specific primary antibody binding to microtubules. In addition, the cells were pretreated with bovine serum albumin before antibody incubation to saturate nonspecific protein binding sites.

The change in microtubule immunofluorescence patterns in colchicine treated cells was striking when compared to the ultrastructure of colchicine treated cells viewed under the TEM. The fluorescence pattern was dim and patchy in the cortical cytoplasm in colchicine treated compared to untreated cells. This change in pattern seemed to reflect true differences in the microtubules because with the exception of the disassembly of microtubules, the cortical cytoplasm itself was not radically changed when viewed under the TEM. The membrane profiles are wavy, but there were no gross changes that could account for the change in the immunofluorescence pattern.

The endomembranes involved in endocytosis, as outlined in chapter 1, showed decreased labelling after treatment with colchicine. There was no pronounced gathering of endocytotic vesicles near the plasma membrane, as expected if the vesicles were budding off the membrane but not being

transported. Instead, the disruption of microtubules led to fewer vesicles in the cortical cytoplasm and the membrane had a wavy appearance. This could be the result of fewer vesicles budding off the plasma membrane. It has been noted that endocytosis in plants occurs in a high turgor environment (Cram 1980, Gradmann and Robinson 1989), and this is especially true of elongating cells. Microtubules may act as support beams upon which microtubule associated proteins (MAPs) would brace to move vesicles into the cortical cytoplasm. After disruption of microtubules by colchicine, this mechanism for budding would no longer be active.

There are good precedents for a microtubule-MAP based vesicle transport system. MAPs act as microtubule motors to transport membranous organelles in squid giant axon, bovine brain, and amoeba (Hirokawa et al. 1989). Different motors move vesicles in opposite directions along the polar microtubule: kinesin moves vesicles towards the plus end (Brady et al. 1982, Vale et al. 1985), while dynein (MAP 1C) moves vesicles towards the minus end (Paschel et al. 1987, Gibbons 1988). The three dimensional structure of kinesin

has been described in quick freeze, deep etch studies of reconstituted microtubules, kinesin, and latex beads (Hirokawa et al. 1989). The kinesin head, which has ATPase activity, attaches to the microtubule; the kinesin foot attaches to the latex bead or vesicle (Yang et al. 1989).

The low level of multivesicular body labelling in colchicine treated cells is consistent with reports from the animal literature, where colchicine inhibited uptake of ligand and transfer of ligand to the lysosome (Kolset et al. 1979). In the root cells, the decrease in multivesicular body label may be considered morphological evidence of inhibited transfer of membranes between internal organelles. The lack of vesicles in the cortical cytoplasm, together with the diminished multivesicular body label, support the theory that microtubules are important in endocytosis during elongation in root cells.

It is difficult to chemically dissect one component of the cytoskeleton without effecting the other interacting components. The actin microfilament system is found in the cortical cytoplasm with microtubules (Parthasarathy 1985, Seagull et al. 1987, McCurdy et al. 1988); general

disruption of this microenvironment with colchicine may be producing indirect effects on the microfilaments.

To disrupt microfilaments, cells can be treated with lead, cytochalasin B, or cytochalasin D. There are a variety of changes seen in the treated cells: cytoplasmic streaming is halted in mature vacuolate cells, vesicles are accumulated around the dictyosome, and Golgi cisternae dilate (Yamagoshi and Nagai 1981, Shannon et al. 1984, Vaughn and Vaughn 1987). None of these organelle changes were present in colchicine treated Lobelia root cells, which suggests the integrity of the microfilament system was not significantly disrupted. There were few vesicles around the Golgi, unlike the reported dilated or fragmented Golgi area in cytochalasin treated cells (Mollenhauer and Morre 1976). Dictyosome structure was not altered by colchicine treatment in Lobelia, or in the maize root cap (ibid).

Microfilaments have been shown to be important in secretion of slime in root cap cells (Morre and Mollenhauer 1976, Shannon et al. 1984) and secretion of cell wall in pollen tubes of Tradescantia (Picton and Steer 1981). It is

difficult to visualize microfilaments in thin sections because they are only 6 nm in diameter (in comparison, microtubules are 25 nm in diameter). In sections of Lobelia root cells, microfilaments were rarely observed unlike microtubules which were abundant.

In conclusion, the disruption of microtubules with colchicine produced changes in lanthanum label patterns indicating endocytosis was perturbed. It is not clear from this preliminary study if this is a direct effect on a microtubule-MAP vesicle translocation mechanism or an indirect effect of disrupting this important cytoskeletal element of the elongating cell.

Chapter 4:

PRIMARY CELL WALL POROSITY IN ROOT TIPS OF *LOBELIA ERINUS*

INTRODUCTION

The composition of the extracellular medium bathing the higher plant cell is determined by the physical and chemical barrier of its cell wall. During endocytosis, solutes and solution from the extracellular medium are internalized. This interaction between the cell and its environment is limited to molecules and particles that can cross the cell wall. The environment of the apoplast determines what can be taken up by endocytosis. The objective of this study was to determine the size of the particles capable of diffusing through the pores of the cell wall, and to explore what components of the cell wall define the pore size.

Morphologically the cell wall of the epidermal and cortical cells has an outer pectic layer and an inner cellulosic layer (Setterfield and Bayley 1957, Foster 1982). There are several lines of evidence for this layered structure: light microscope cytochemistry, fluorescence (Miki et al. 1980), TEM cytochemistry, (Moore and Staehelin 1988) , and TEM apoplast tracer studies (Owen et al. 1988, Crowdy and Tanton 1970). The dicot primary cell wall, like many extracellular matrices, is composed of a fibrous network in an

embedding matrix. In higher plants in general, the fibrous network is made up of the crystalline cellulose microfibrils cemented together with a matrix of pectins, hemicelluloses, and proteins (McNeil et al. 1984). In dicots, the predominant pectins are homogalacturons, rhamnogalacturon I and II; the main hemicellulose is xyloglucan (Varner and Lin 1989).

Although the covalent and ionic interactions between the components of the cell wall are not well understood, a working model of a network of cellulose microfibrils coated with xyloglucan in a matrix of pectins and proteins (Keegstra et al. 1973, Preston 1974) will be assumed here. The proteins of the cell wall are enzymes as well as structural proteins (Cassab and Varner 1988). It has been suggested that bonds between structural proteins and polysaccharides "might determine the potential pore size of an intermolecularly crosslinked extensin network" (Cooper et al. 1987).

The pore sizes of higher plant cell walls have been determined using several different methodologies. The ability of a compound to cause plasmolysis or cytorrhysis was used as an assay of the compounds ability to cross the cell wall of

cultured Acer pseudoplatanus; the limiting diameter of pores was reported to be 3-4 nm (Carpita et al. 1979). Cell walls of Phaseolus vulgaris L. seedlings were ground, frozen thawed, and packed into a gel filtration chromatography column; the exclusion of proteins of molecular weight greater than 60 000 daltons was taken as evidence that the pore size is about 3 nm (Tepfer and Taylor 1981a). The passage of fluoresceinated dextrans and proteins into the cell wall and periplasm of cultured, plasmolyzed Glycine max cells showed unhindered porosity of 3.3 nm and a restricted porosity of 6.6-8.6 nm (Baron-Epel et al. 1988). In this study, electron dense markers of a range of sizes were used to determine the pore size in the intact primary root of Lobelia erinus.

METHODS AND MATERIALS

Lobelia erinus seedlings were germinated on filter paper wetted with distilled deionized water. After 7 days, the seedlings were immersed in the apoplast tracer solutions for 2 or 12 hours. The tracers were colloidal gold or 5 mM lanthanum nitrate solutions. For details of lanthanum technique, see chapter 1. Colloidal gold was prepared by the method of Slot and Geuze (1985), using 5 ml of 1 % tannic acid, 5 ml 25 mM K_2CO_3, 4 ml 1 % sodium citrate, 6 ml deionized distilled water to reduce the chloroauric acid solution consisting of 1 ml 1 % chloroauric acid and 89 ml deionized distilled water. The solution was boiled under reflux for 1 hour and allowed to cool to room temperature.

Colloidal gold particle size was measured using the Kontron Image Processing System (IPS) and the Zeiss 10C transmission electron microscope. The microscope was calibrated by measuring the crystal lattice spacing of negatively stained catalase crystals. An aliquot of gold solution was layered on formvar coated grids, excess was blotted off, and the grids were airdried. The colloidal gold particle size was measured as the maximum diameter of each particle.

EGTA treatment consisted of immersing seedlings in microtubule stabilizing buffer (50 mM PIPES pH 6.9, 5 mM $Mg_2(SO_4)$, and 5 mM EGTA) for 1 hour, followed by 12 hours in 3-5 nm colloidal gold solution.

Partial cell wall digestions were carried out on 7 day seedlings for 15 minutes at room temperature in the following enzyme solutions. (i) Pectinase (Sigma P-2401, E.C. 3.2.1.15, from Rhizopus species) was dissolved in 50 mM PIPES buffer pH 7.4 to make a stock solution of 10 mg/ml. This was further diluted to 1 mg/ml, 0.1 mg/ml, 0.025, 0.05 mg/ml, and 0.01 mg/ml. (ii) Protease (Sigma P-5005, type V, from Streptomyces griseus), and (iii) cellulase (Sigma C-7377, E.C. 3.2.1.4, from Aspergillus niger) were dissolved in PIPES at stock concentrations of 10 mg/ml, and further diluted to 1 mg/ml. After 15 minutes, the seedlings were rinsed in buffer 3 times 5 minutes and then incubated in colloidal gold solution for 12 hours.

At the end of the gold incubation, samples were fixed in dilute Karnovsky's fixative (1.5 % formaldehyde, 2 % glutaraldehyde in 50 mM PIPES pH 7.4) for 1 hour. After 3 rinses of 5 minutes each,

postfixation in 1 % OsO_4 was carried out overnight at 4 ^{o} C. Seedlings were dehydrated in methanol and embedded in epon. Silver sections were cut on the Reichert-Jung OMU3 or Ultracut E. Three roots were trimmed and sectioned for each pectinase concentration for 2 replicate fixations. The sections were picked up on uncoated copper grids and examined without poststaining. For each root, the diameter of the colloidal gold particles in the epidermal elongating cells was sampled in at least 5 different cells. The diameter of the gold particles in root sections was measured on the Kontron IPS, as outlined above, for the determination of gold particle size. The mean maximum diameter of gold particle penetrating the cell wall for each pectinase concentration was plotted. Linear regression analysis was used to test the null hypothesis that probe size was independent of pectinase concentration.

Frozen hydrated samples were prepared and viewed in the Biological Sciences Electron Microscopy Laboratory at the University of California at Berkeley. Seven day Lobelia erinus seedlings were mounted on the SEM stub and frozen in liquid nitrogen slush. The stub was

transferred at liquid nitrogen temperature to the cold stage of the SEM, where a controlled rise in temperature to -110 ^{o} C was used to sublime the outer layers of ice covering the sample. The stub was transferred to a cold stage in the coating chamber of the SEM and sputter coated with gold. The roots were returned to the cold stage of the SEM, viewed and photographed at 20 kv accelerating voltage.

RESULTS

The pore size of the primary cell wall of Lobelia erinus was determined using electron dense apoplast markers. Lanthanum freely diffuses across the cell wall (see chapters 1 and 5), suggesting the porosity of the cell wall is at least 0.8 nm. Colloidal gold particles of size range 2 nm-5 nm did not cross the intact cell wall. The only area where colloidal gold was found within the root tip was a scattering of particles in the middle lamellae of the epidermal cells. This appears to be a size restriction and not the consequence of charge, because when colloidal gold particles were coated with amino acids of different charges (lysine, positive charge; glycine, neutral; aspartic acid, negative charge), the colloidal gold was still excluded (data not shown).

The exterior cuticle layer of the intact root acts as a barrier to material entering the cell wall. In areas where this layer was disrupted, a small amount of colloidal gold were observed within the pectic layer of the cell wall. This exterior layer was not stained for polysaccharides with alkaline bismuth (Fig. 54).

To study which components of the cell wall are

important in cell wall porosity, enzyme digestions were performed. Treatment of roots with 10 mg/ml cellulase or protease had no effect on the porosity of the cell wall (Fig. 51, 53). In contrast, treatment of roots with pectinase concentrations of 10 mg/ml and less produced extensive changes in cell wall ultrastructure and porosity (Fig. 53). The pectic cell wall layer became less coherent and less dense. Colloidal gold probes were found throughout the cell wall. The root cells were completely disrupted by pectinase treatment. This could be observed by diminished fluoroscein diacetate staining, increased Evan's Blue staining (data not shown), and by the drastic alteration in ultrastructure. This disruption occurred whether or not the roots were pretreated with plasmolyzing medium.

A range of concentrations of pectinase were tested for its ability to change porosity, from 10 ug/ml to 10 000 ug/ml (10 mg/ml), see Table 5. The effect of the enzyme varied between cell types. For example, in roots treated with 50 ug/ml pectinase, in the elongation zone there was gold particles in the cell wall; in mature cells there was no gold in the cell wall. Even within one cell

type, the response to pectinase treatment was variable. After treatment with 100 ug/ml pectinase, the gold was always seen in the pectic layer of elongating cells but the gold did not always penetrate the cellulosic layer (Fig. 55). The size of the colloidal gold particles in the cell wall after pectinase treatment was measured using the Kontron IPS. The gold particles that had penetrated furthest into the wall were measured for each treatment. According to linear regression analysis, a significant increase in the pore size is observed with increasing concentrations of pectinase (Fig. 59).

The effect of the calcium chelator EGTA was similar to the effect of low concentrations of pectinase treatment: the pectic layer became diffuse, the porosity of the wall in this layer increased, and the gold did not penetrate the cellulosic layer (Fig. 56) . The root cells had distended endoplasmic reticulum after EGTA treatment, but in general were less disrupted than the pectinase treated.

The external surface of the root in the conventional preparations was delineated by the non-polysaccharide cuticle layer and some fine

wisps of polysaccharide (Fig. 55). In samples prepared using cryotechniques, the mucilage on the surface of the root looks very different. Whole frozen hydrated roots were viewed under the SEM with a cold stage (Fig. 57); the relationship between the surface of the root hairs and its environment was observed (Fig. 58). The extensive network of fibrils radiating from the cell wall (Fig. 58) was also present in freeze substituted material (see chapter 5).

In summary, the cell wall of Lobelia erinus consists of several layers of varying composition and porosity. The exterior of the cell wall is connected to the surrounding medium by a network of fibrils, as observed on frozen samples under the SEM. The most exterior layer of the cell wall proper is a non-polysaccharide layer which restricts access of gold particles but not lanthanum. This exterior layer covers the pectic layer which is easily disrupted by low concentrations of pectinase enzyme or EGTA, but not cellulase or protease. Beneath the pectic layer is the cellulose layer which forms another barrier layer, stopping colloidal gold particles from reaching the cell if they penetrate the pectic

layer. This cellulosic layer is only disrupted by high pectinase concentrations. The most internal layer is the plasma membrane surface coat (see chapter 2).

Table 5

Effect of pectinase treatment on cell wall porosity

[pectinase] ug/ml	colloidal gold cell wall porosity probe
10	gold does not enter wall except where breaks in cuticle layer occur
25	gold enters pectic layer completely, excluded from cellulosic layer in some cases
50	gold enters pectic layer completely, excluded from cellulosic layer in some cases
100	gold crosses pectic layer, enters cellulosic layer in most cases
1000	gold crosses pectic layer, crosses cellulosic layer completely

Figs. 51-53: Influence of wall components on cell wall porosity. All sections, no post stain.

Fig. 51: 10 mg/ml cellulase treatment, followed by 12 hours in 3-5 nm colloidal gold solution. Gold penetration of wall extremely limited. Note some penetration at break in cuticle layer (arrow).

52: 0.1 mg/ml pectinase treatment, followed by 12 hours in 3-5 nm colloidal gold solution. Gold crosses pectic layer of cell wall, and to lesser extent crosses cellulosic layer to penetrate to cell lumen.

Fig. 53: 10 mg/ml protease treatment followed by 12 hours in 3-5 nm colloidal gold solution. Results similar to no enzyme controls.

pl=pectic layer, cl=cellulosic layer, cy=cytoplasm, arrowhead indicates colloidal gold particles, arrow indicates exterior cuticle layer.

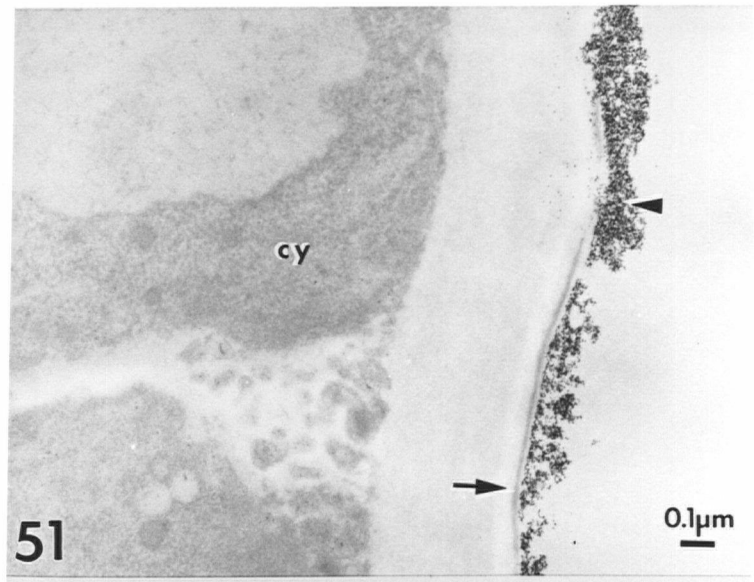

51

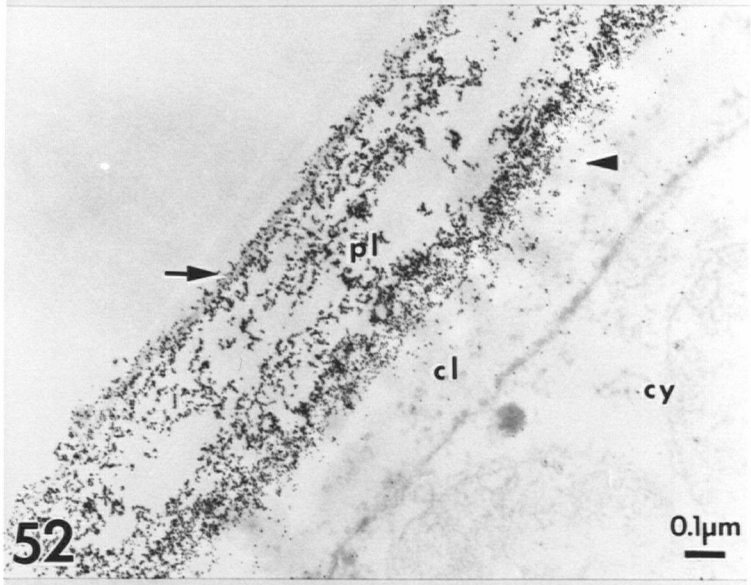

52

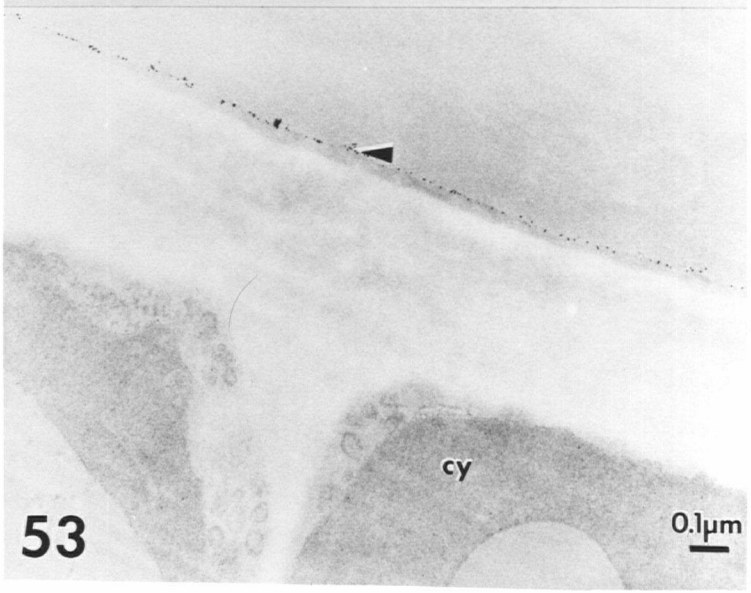

53

Figs. 54-56: Cell wall ultrastructure.

Fig. 54: cell wall stained with alkaline bismuth for polysaccharides. Cuticle layer does not react. Root treated with 10 ug/ml pectinase, followed by 12 hours in 3-5 nm colloidal gold solution. Gold does not enter wall where exterior layer intact.

Fig. 55: cell wall layers after digestion with 1.0 mg/ml pectinase, followed by 12 hours in 3-5 nm colloidal gold solution. Gold is seen in pectic layer but not in cellulosic layer. Cytoplasm of cells disrupted. Poststained with uranyl acetate/ lead citrate.

Fig. 56: 5 mM EGTA treatment followed by 12 hours in 3-5 nm colloidal gold. Gold enters pectic, but not cellulosic layers of cell wall. ER lumen distended. Poststained with uranyl acetate/ lead citrate.

pl=pectic layer, cl=cellulosic layer, er=endoplasmic reticulum, arrowhead indicates colloidal gold particles, arrow indicates cuticle cell wall layer.

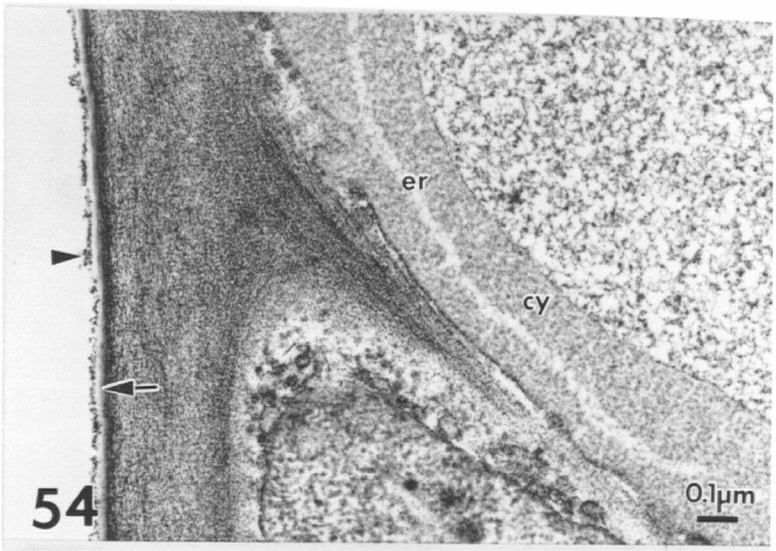
er
cy
54
0.1µm

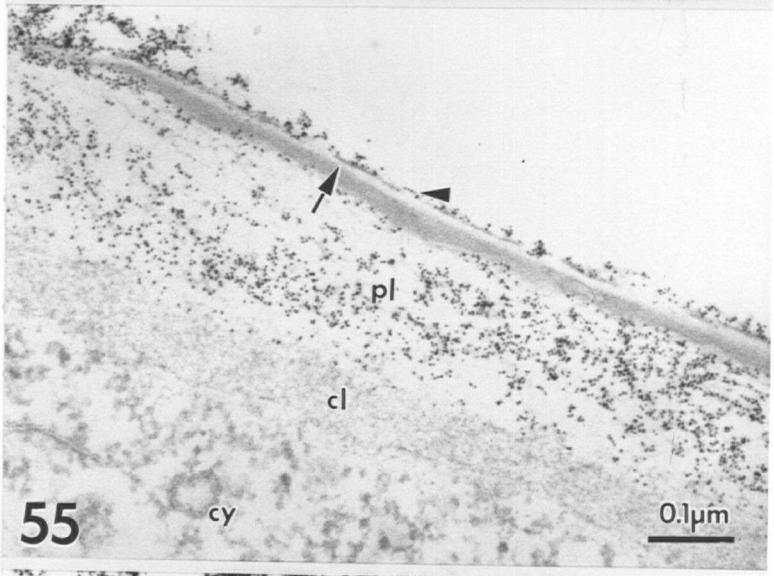
pl
cl
55
cy
0.1µm

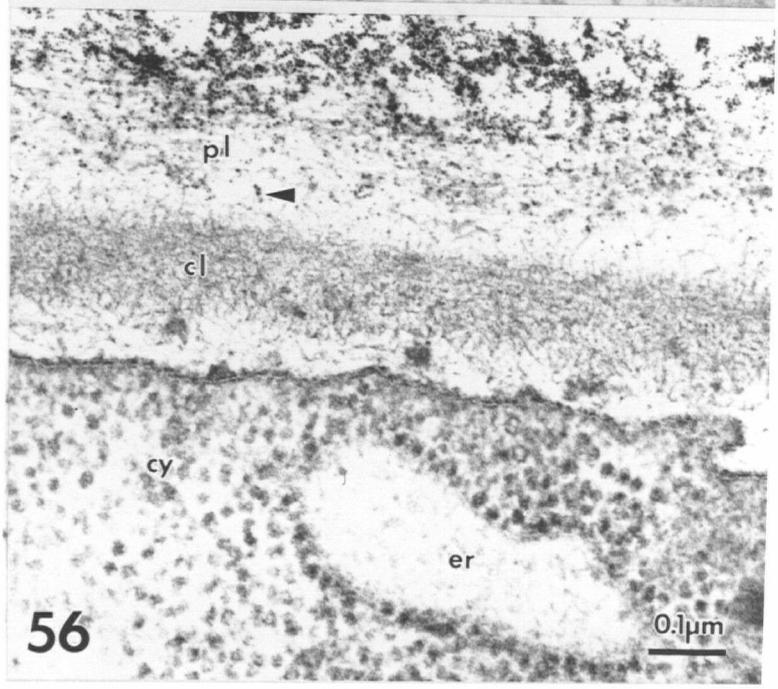
pl
cl
cy
er
56
0.1µm

Figs. 57-58: frozen hydrated samples of Lobelia erinus, viewed on cold stage of SEM.

Fig. 57: Whole frozen hydrated root, showing ice surrounding root hairs; root tip epidermal surface slightly freeze-dried. Mature epidermal cells can be seen where ice has sublimed away.

Fig. 58: Root hairs embedded in ice. Fibrils radiating out from surface of root.

rt=root tip, rh=root hair, me=mature epidermal cells.

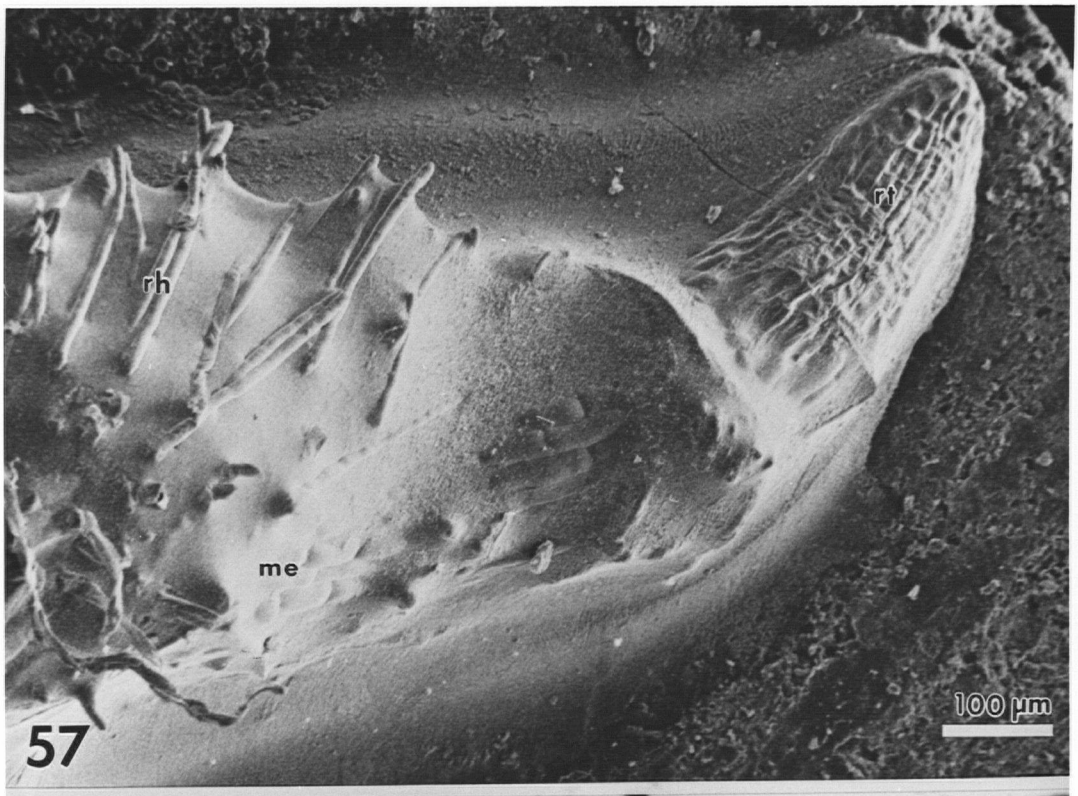

57

58

Fig. 59: Effect of pectinase on cell wall porosity.

Treatment with varying concentrations of pectinase allowed different sizes of colloidal gold probe to enter cell wall.

effect of pectinase on wall porosity

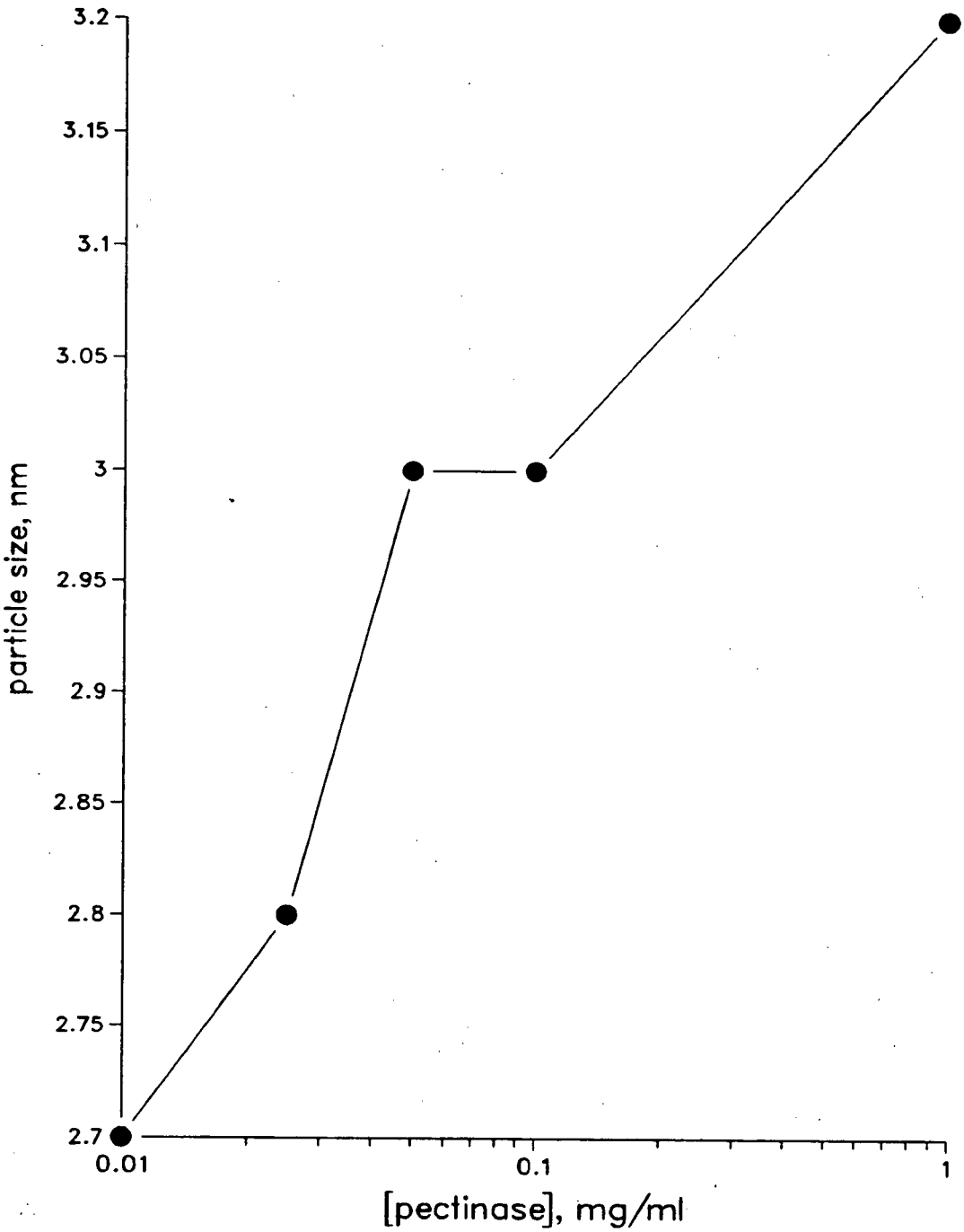

The extracellular medium for a higher plant cell consists of the cell wall components and the molecules capable of diffusing across the cell wall. Based on the pore size of 1-2 nm in intact cells and 2-3 nm in pectinase treated cells, predications can be made about what types of molecules may be encountered by the elongating Lobelia erinus root cells. Molecules such as ions and simple sugars would diffuse freely through the wall, penetrating throughout the apoplast as lanthanum does. In contrast, large proteins and particles, excluded from the cell wall, would not come in direct contact with the plant cell surface. This is an important consideration for assays of endocytosis and antibody studies on intact higher plant tissues.

It is difficult to reconcile a homogenous wall with porosity of 1-3 nm with processes like Agrobacterium infection, movement of oligosaccharide fragments, and changes in shape and size. The heterogenous composition of the cell wall provides a range of substrates for microbial enzymes such as pectinase, protease and cellulase (Collmer and Keen 1986). It seems likely that in the soil the condition, porosity, and

ultrastructure of the epidermal cell walls would be influenced by the nearby differentiated cells, soil bacteria, and mycorhizzae. In addition, the abrasion of the root surface by soil particles during growth could alter porosity in microenvironments around the root tip. It is useful to relate conditions that occur in soil with the *in vitro* experiments on cell wall porosity. The new approach of this study was to relate porosity to the conditions which may occur in soil such as the presence of microbial enzymes. This approach included the use of (i) intact tissues, i.e. not cultured cells (Baron-Epel *et al*. 1988) and (ii) intact cell wall, i.e. not cell wall fragments (Tepfer and Taylor 1981a).

The varied cell wall porosities of differentiated cell types (elongating and vacuolate; elongating and root cap) observed earlier in this study is analogous to the differences in wall porosity observed earlier by Carpita *et al*. (1979) in elongating cells and root hairs of *Raphanus sativus*. Similarly, distinctly different wall porosities have been reported in the bromeliad *Brocchinia reducta*, where lanthanum penetrated the cell wall of the trichome and

surrounding mesophyll cells but not the wall of the epidermal cells (Owen et al. 1988). These differences between cell types further reflect the heterogenous nature of the cell wall.

The mucilage layer covering the cell wall proper of the epidermal cells and root hairs does not present a porosity barrier to the probes tested here. There are two distinctive types of root mucilage: root cap mucilage and epidermal mucilage (Miki et al. 1980, Ray et al. 1988). It is generally very difficult to preserve this cell wall layer in TEM preparations (Chaboud and Rougier 1986, Foster 1982). Using cryotechniques the mucilage can be seen radiating from the root surface. The functions of this type of mucilage are believed to be ion exchange and conditioning of the soil to allow root to push through the soil during growth (Ray et al. 1988). The direct contact between these "rhizoplane fibrils" and soil particles may allow direct transfer of cations from the soil particle to the root (Leppard and Ramamoorthy 1975).

In the elongating Lobelia erinus cells, the entire cell wall is covered by a thin, nonpolysaccharide layer of cuticle. A similar

structure, "a definite cuticle-like membrane...near the surface of the gel" was reported in field grown plants such as clover and wheat (Foster 1982). The presence of a cuticle in roots has been noted in several cell types (Scott et al. 1958, Chaboud and Rougier 1986). The cuticle may act as barrier to entry to the root cell wall: in many cases, colloidal gold only penetrated the cell wall at breaks in the cuticle. Breaks in the cuticle may occur where the root is in contact with soil particles (Foster 1982).

The cuticle lies over the gel of the outer pectic cell wall layer. The porosity of the pectic layer was altered by treatment with pectinase and EGTA, but not cellulase and protease. Alteration in cell wall porosity by pectinase treatment was also reported recently in suspension cultured Glycine max cells, using a fluorescence microscopy assay (Baron-Epel et al. 1988). However protease, cellulase, and EGTA did not change porosity in those cells. The EGTA disruption in this study was limited to the pectic cell wall layer; the porosity of the cellulosic layer did not change.

The pectic layer is rich in carboxyl groups, which can be crosslinked by calcium bridges (Tepfer

and Taylor 1981b). This ionic bonding seems to contribute to maintaining a tightly crosslinked matrix, because disruption of the bridges with EGTA led to increased pore diameter. Based on the fluorescence studies of Baron-Epel et al. (1988) and the pectinase colloidal gold assays presented here, it appears that pectin is important in maintaining cell wall porosity. The gel forming properties of pectins could be essential to creating this molecular network. An aqueous gel can be considered the sum of three parts:

1. junction zones where polymers join
2. interjunction segments where the polymers are mobile, although less mobile than in free solution
3. water enclosed by this network (Jarvis 1984).

In the cell wall the junction would be formed by blocks of unbranched galacturonans, cross linked by calcium; the interjunction would be blocks of esterified galacturonans which are unable to bind calcium (ibid). If the interjunction zones are considered pores, their walls would be less highly charged than the junction zones. The pore size could vary by removal of calcium from the junction

zones by EGTA.

The position of the pectic layer on the outer cell wall makes it the first line of defense against pathogens (Collmer and Keen 1986). Fragments of the cell wall, oligosaccharins, act as signalling molecules when plants are attacked by some pathogens, and pectic fractions are amongst the most active oligosaccharins (Darvill et al. 1985, Ryan 1987). It was striking in this study how even low concentration of pectinase led to cell death; similar phytotoxic effects following pectinase treatment have been reported (Basham and Bateman 1975, Hahne and Lorz 1988).

It has been suggested on theoretical grounds that a protein network of extensin may mediate cell wall porosity (Cooper et al. 1987). Treatment of roots with protease did not change the porosity in these experiments, which suggests proteins are not an important factor in porosity. Extensins have been localized throughout the cell wall with the exception of the middle lamella (Stafstrom and Staehelin 1988). The middle lamella between cells is continuous with the outer pectic layer of the epidermal cells. The level of substrate may have been too low in the outer epidermal cell wall layer

to change the porosity significantly.

The cellulose rich region of the cell wall is interior to the pectic layer as well, which may be why the cellulase treatment does not influence porosity. The cellulosic layer surrounding the protoplast acted as a barrier to the passage of colloidal gold probes, although it was disrupted by higher concentration of pectinase. This suggests that pectins form part of the network surrounding the cellulose microfibrils, in addition to the xyloglucans (Hayashi et al. 1987, Moore and Staehelin 1988).

In conclusion, cutin and pectin are the most important components in cell wall porosity in intact Lobelia erinus roots, when compared to cellulose and proteins. The pore size of the cell wall would strictly limit the molecules that may interact with the root cell, but this porosity is plastic depending on exposure to factors which modify pectin.

Chapter 5:

A RE-EXAMINATION OF ENDOCYTOSIS USING ULTRA RAPID FREEZING AND FREEZE SUBSTITUTION

INTRODUCTION

Endocytosis occurs on a timescale of milliseconds over distances of micrometers. Transmission electron microscopy (TEM) must be used to study these subcellular structures, but the conventional preparative techniques used in TEM are poorly suited for dynamic events. The size scale of endocytosis requires TEM, but the time scale of endocytosis makes conventional fixation techniques inappropriate. An alternative to conventional techniques is fixation by ultrarapid freezing and freeze substitution.

There are limitations associated with conventional TEM fixation techniques (Gilkey and Staehelin 1986, Menco 1986, Sitte et al. 1987, Knoll et al. 1987). The most serious of these limitations for endocytosis is the slowness of the fixative penetration and cross reaction which may lead to vesicle and organelle rearrangements during fixation. The chemicals used in fixation must diffuse into the cells before cross linking reactions may begin; this time period may be several seconds to minutes (Mersey and McCully 1978, Bajer and Mole-Bajer 1969). In addition, not all molecules are crosslinked by any one fixative,

e.g. lipids are poorly fixed by aldehydes but react well with osmium tetraoxide (Hayat 1981). This is relevant in the study of endocytosis because the time lag between fixation of the membrane proteins with aldehyde and the fixation of membrane lipids with osmium may be as long as 1 to 2 hours. During this time period, lipases may still be active and membrane blebbing can occur (Wetzel and Scow 1980, Hasty and Hays 1978). Aldehyde fixation is accompanied by release and redistribution of ions such as H^+ and Ca^{2+} which may produce artifacts (Hall and Gupta 1984, Zierold and Steinbrecht 1987).

These problems can be avoided by ultrarapid freezing, which immobilizes molecules and organelles by solidifying the solvent surrounding them. The time for fixation changes from seconds to milliseconds: for example, a tissue is frozen to a depth of 10 um within 0.5 milliseconds (Jones 1984). Ultrarapid freezing techniques are based on the properties of water, one of the most neglected of the cell constituents. Water plays integral structural (hydration shells) and functional (solvent and reactant) roles in cells.

When water freezes, it is a two step process: first the nucleation of embryo ice crystals occurs, then the ice crystals expand and grow. In biological material, nucleation of ice crystals is "homogenous nucleation" because nuclei are clusters of pure water; in "heterogenous nucleation", foreign particles or surfaces act as nuclei around which crystals grow (Mazur 1970, Robards and Sleytr 1985).

The size of the ice crystals formed depends primarily on the rate of cooling, but sample geometry and solute concentration are also important (Plattner and Bachmann 1982). The quality of ultrarapid freezing is determined by these "crystallization kinetics...nucleation frequency and crystal growth rate" (Bachmann and Mayer 1987). If the rate of cooling is too slow, large ice crystals (several microns in diameter) are formed. These crystals have a characteristic lattice structure of hexagonal units, thus this common form of frozen water is called hexagonal ice (Robards and Sleytr 1985). Hexagonal ice significantly disrupts ultrastructure due to the large size of its crystals. Slow cooling can also result in the segregation of solution or cytoplasm

crystals of pure water that exclude solutes. This segregation of solutes into an "eutectic" phase with different freezing properties has been a consideration in freeze fracture experiments for many years (Hudson et al. 1979).

The ultimate goal of cryofixation is the solidification of water without the formation of ice crystals: the amorphous solid called vitreous ice. True vitrification only occurs under rigorous conditions of rapid freezing (cooling rate $>10^6$ $^{\circ}K$/sec) and very small sample volume (Sitte et al. 1987, Dubochet and McDowell 1981, Dubochet et al. 1982). Vitrified ice is found only in the top few microns of ultrarapidly frozen tissue blocks; true vitrification through the depth of uncryoprotected tissue is not possible (Dubochet et al. 1987).

The practical goal of cryofixation is to achieve a fast rate of cooling to minimize the size of the resulting ice crystals (Plattner and Bachmann 1982, Gilkey and Staehelin 1986). "Ideal fixation and specimen preparation require that constituents of the system keep their position within a range that is smaller than the resolution of the observation method" (Bachmann and Mayer 1987). The freezing rate must be in the range of

$>10^4$ ^oK/sec to have crystals no bigger than the limit of resolution of the TEM (Sitte et al. 1987).

For tissues, this fast rate of cooling can be achieved by bringing the sample into contact with a highly polished metal surface (copper or silver) which is held at liquid nitrogen (or liquid helium) temperature. Only the surface contacting the copper block and the underlying 10-40 um are ultrarapidly cooled. Beyond this depth the effect of the low thermal conductivity of ice overcomes the effect of the high thermal conductivity of the copper block (Plattner and Bachmann 1982).

This technique was pioneered by Van Harreveld and coworkers (Van Harreveld and Crowell 1964, Van Harreveld et al. 1974). It has been important, when used with deep etch platinum carbon replicas, in studies of neurotransmitter exocytosis and subsequent endocytosis at neuromuscular junctions (Heuser et al. 1979, Miller and Heuser 1984), and coated pit budding in fibroblasts (Heuser and Evans 1980, Heuser 1989). Copper block freezing has been used with freeze substitution to preserve delicate structures, for example silk moth antennae (Steinbrecht 1980) and ciliary patterns on Paramecium (Barlow and Sleigh 1979).

Previously most plant tissues were frozen by plunging into liquid cryogen such as Freon, or propane (Hereward and Northcote 1972, Fisher 1975, Browning and Gunning 1977, McCully and Canny 1985, Lancelle et al. 1986). Other methods of ultrarapid freezing such as propane jet-freezing and high pressure freezing have been applied to cultured higher plant cell suspensions and intact tissues (Fernandez and Staehelin 1985, Staehelin and Chapman 1987, Craig and Staehelin 1988). There have been few applications of the copper block method of ultrarapid freezing for plant material, except for suspensions of unicellular algae or chloroplasts (Kugrens and Lee 1987, Nishizawa and Mori 1989).

Ultrarapidly frozen material can be slowly dehydrated and fixed by freeze substitution. The samples are immersed in substitution medium such as acetone or methanol with osmium tetraoxide for 2 days and maintained at -80 $^{\circ}$ C. During this time, the solvent dissolves the ice, i.e. the water in the sample is removed (Steinbrecht and Muller 1987). The temperature is slowly allowed to rise, and osmium fixation stabilizes the cellular structures.

The copper block ultra rapid freezing method was used in the present study because it is spatially well suited for epidermal cells, and temporally well suited for endocytosis. With these new tools of ultrarapid freezing and freeze substitution, the process of endocytosis in elongating root cells of Lobelia erinus can be reevaluated. When the extracellular medium is labelled with lanthanum, endocytosis can be accurately traced as label is internalized and transported through intracellular compartments. The ultrarapid freezing/ freeze substitution study of secretion (see chapter 2) showed excellent preservation of organelles such as Golgi and PCR. The objective of this study is to re-examine endocytosis in situ, within the new context of the ultrarapidly frozen endomembrane system, unperturbed by chemical fixation.

METHODS AND MATERIALS

Lobelia erinus seedlings were germinated on filter paper moistened with distilled deionized water for 7 days. Seedlings were immersed in either 5 mM lanthanum nitrate or in distilled deionized water for 1 hour at room temperature, as described in chapter 1. In the last 5 minutes of the incubation period, samples were removed from the incubating solution, mounted on soft foam pads for copper block freezing, and maintained in a humid environment.

Two commercially available ultrarapid freezing devices were used in this study: Reichert- Jung MM-80 at the Electron Microscopy Facility at UBC or RMC MF7000 at the RMC cryotechniques course in the Electron Microscopy Laboratory at UCBerkeley.

Using the RMC setup, seedlings were mounted on an aluminum planchette which was backed with soft foam attached to a steel disk. When the copper block reached liquid nitrogen temperature, the disk was mounted on a magnet attached to the plunging arm of the apparatus. Immediately the sample was released to slam into the copper block; an electromagnet locked the sample against the block upon impact to prevent rebounce artefact. The

seedlings were removed from the aluminum planchette under liquid nitrogen by scraping the planchette with a razor blade. As the well frozen surface could be damaged, the samples were mounted on filter paper in subsequent experiments. After release from the planchettes, the samples were transferred to small plastic containers and processed for freeze substitution.

The protocol using the Reichert-Jung KF-80 varied slightly: the seedlings were mounted on filter paper, stuck to parafilm, glued to the soft foam pad which is backed by a steel planchette. When the copper block reached liquid nitrogen temperature, excess water was blotted off the filter paper and the planchette was stuck on the magnet of the MM80 arm. The sample was slammed against the polished copper surface, then kept at liquid nitrogen temperature. The parafilm next to the filter paper becomes brittle at this temperature, allowing easy separation of the samples from the foam. The filter paper containing the sample was then processed for freeze substitution in a Reichert-Jung CS Auto.

Freeze substitution was carried out at -80^{o} C for 48-56 hours, followed by a gradual rise in

temperature of 10° C/hour to a final temperature of 0° C. The substitution medium was 1 % OsO_4 in absolute acetone. When the RMC equipment was used, the temperatures during substitution were approximate. When the Reichert-Jung equipment was used, these values were controlled precisely. The results for the two setups were identical. At the end of the freeze substitution procedure, the substitution medium was removed and replaced several times with absolute acetone. The acetone then acted as the solvent for infiltration in Spurr's resin.

Silver sections were cut on a Reichert-Jung Ultracut E using a diamond knife. Section were picked up on formvar coated grids and viewed without poststaining or after 25 minutes in a saturated solution of uranyl acetate in 70 % methanol. All grids were viewed and photographed at 60 kV on a Zeiss 10C TEM.

RESULTS

When Lobelia erinus root tips are ultrarapidly frozen by contacting a copper block at -196 ^{o} C, a gradient of ice crystal sizes was formed (Fig. 60) as expected in an uncryoprotected sample. Near the epidermal cell surface, material may be vitrified or the ice crystals formed were extremely small due to the rapid rate of cooling. The preservation of ultrastructure in these regions was excellent. In contrast, at the basal portion of the epidermal cells, clear holes representing cytoplasmic damages by hexagonal ice crystals were in evidence.

Root cap cells covered the exterior surface of the root in the zone of elongation. In some cases, the root cap cells had collapsed due to excessive impact before freezing. The two types of cells, epidermal and root cap, had different freezing properties. The epidermal cells often demonstrated well preserved apical cytoplasm adjacent to the less well frozen basal portion of the root cap.

In the well preserved portions of the elongating epidermal cells, the pathways of endocytosis were labelled using lanthanum as an marker. Roots that had been incubated in lanthanum

nitrate before freezing showed electron dense deposits in the apoplast and within some membrane bound organelles. These deposits were identical in electron density as those found in experiments using conventional fixation techniques. The apoplastic labelling in the ultrarapidly frozen material was sparse. This may be due to loss of apoplastic lanthanum during epoxy resin infiltration; the resin took longer to infiltrate into ultrarapidly frozen material than conventionally prepared material.

Within the ultrarapidly frozen cells, the lanthanum labelling pattern was consistent with earlier experiments, i.e. vesicles and multivesicular bodies contained lanthanum deposits. The superior preservation of other organelles, such as the partially coated reticulum and dictyosomes, revealed that these endomembrane components are also labelled with lanthanum.

Lanthanum labelled vesicles were observed in the cortical cytoplasm (Figs. 61-63). The vesicle diameters were similar to those observed in conventional techniques, i.e. about 100 nm. There were few coated vesicles near the plasma membrane of the apical surface of well frozen epidermal

cells. Cortical microtubules were found in the vicinity of the labelled vesicles (Fig. 63).

The cortical cytoplasm of ultrarapidly frozen material often contained partially coated reticulum (PCR) (Fig. 67), the network of coated and smooth tubules and vesicles described by Pesacreta and Lucas (1985). This structure was difficult to distinguish in conventional preparations. After ultrarapid freezing and freeze substitution, the PCR was distinct, separate from the trans Golgi network (see chapter 2) and consisted of small tubular or vesicular portions as well as dilated vacuoles (not shown) about the same size as multivesicular bodies. The PCR was labelled with lanthanum, suggesting this organelle receives membrane material and vesicle contents from the plasma membrane following endocytosis.

Another endomembrane component that was clearly labelled after lanthanum treatment and ultrarapid freezing was the multivesicular body (Figs. 64-67). The lanthanum was clustered over the intraluminal vesicles of the multivesicular body. Lanthanum labelled vesicles were adjacent to the multivesicular body: these appear to be budding from or fusing with this organelle (Figs. 64-65).

In many cases, the multivesicular body was positioned adjacent to a dictyosome (Figs. 65, 68). This association was much more common in ultrarapidly frozen material than in conventionally fixed material.

The Golgi of the elongating epidermal cells as revealed by ultrarapid freezing and freeze substitution contains well preserved central polar dictyosome stack , an extensive peripheral network of small, regular vesicles and the trans Golgi network containing larger vesicles (Figs. 68-70, see also chapter 2). Lanthanum label appeared in dictyosome associated vesicles but not in the cisternae of the dictyosome. It is interesting that, in general, the subset of vesicles labelled with lanthanum appear to constitute a different population from the vesicles which were stained for polysaccharides using alkaline bismuth. Lanthanum labelled vesicles were smaller (60-100 nm) and located around the periphery of the dictyosome, while the polysaccharide containing vesicles were larger (100-150 nm) and located in the trans Golgi network (see chapter 2). In some cases, larger vesicles had lanthanum deposits (Fig. 70) but these were relatively infrequent. Labelled vesicles were

associated with the dictyosome in about 50 % of the dictyosomes in ultrarapidly frozen material, as opposed to about 10 % of the dictyosomes in conventionally prepared material.

In summary, lanthanum was used as an assay for endocytosis, followed by ultrarapid freezing and freeze substitution to conserve the vesicle and organelle distributions in the elongating epidermal root cells. The results confirmed earlier, conventional TEM experiments (see chapter 1) showing lanthanum labels cortical vesicles and multivesicular bodies. In addition, superior preservation of endomembranes using cryotechniques, showed lanthanum labelled the partially coated reticulum and dictyosome associated vesicles.

Fig. 60: Gradient of freezing. Cross section of elongating epidermal root cells, perpendicular to surface that contacted liquid nitrogen cooled copper mirror (surface indicated by open arrow heads). The cytoplasm of the epidermal cell near the root surface shows little or no ice crystal damage (asterix). In the basal portion of the cell, ice crystals have formed, displacing cytoplasm and chromatin. After freeze substitution clear spaces indicate where ice crystals had formed.

Figs. 61-63: lanthanum labelled vesicles.
Fig. 61: High magnification of cortical cytoplasm of cell shown in Fig. 60; lanthanum labelled vesicle in cortical cytoplasm.

Fig. 62: lanthanum labelled vesicle deeper in the cytoplasm

Fig. 63: Plasma membrane associated lanthanum labelled vesicles, near cortical microtubules

all closed arrows indicates lanthanum deposits. pm=plasma membrane, rc=root cap cell, cw=cell wall, er=endoplasmic reticulum, m=mitochondion, Nu=nucleus, mt=microtubule

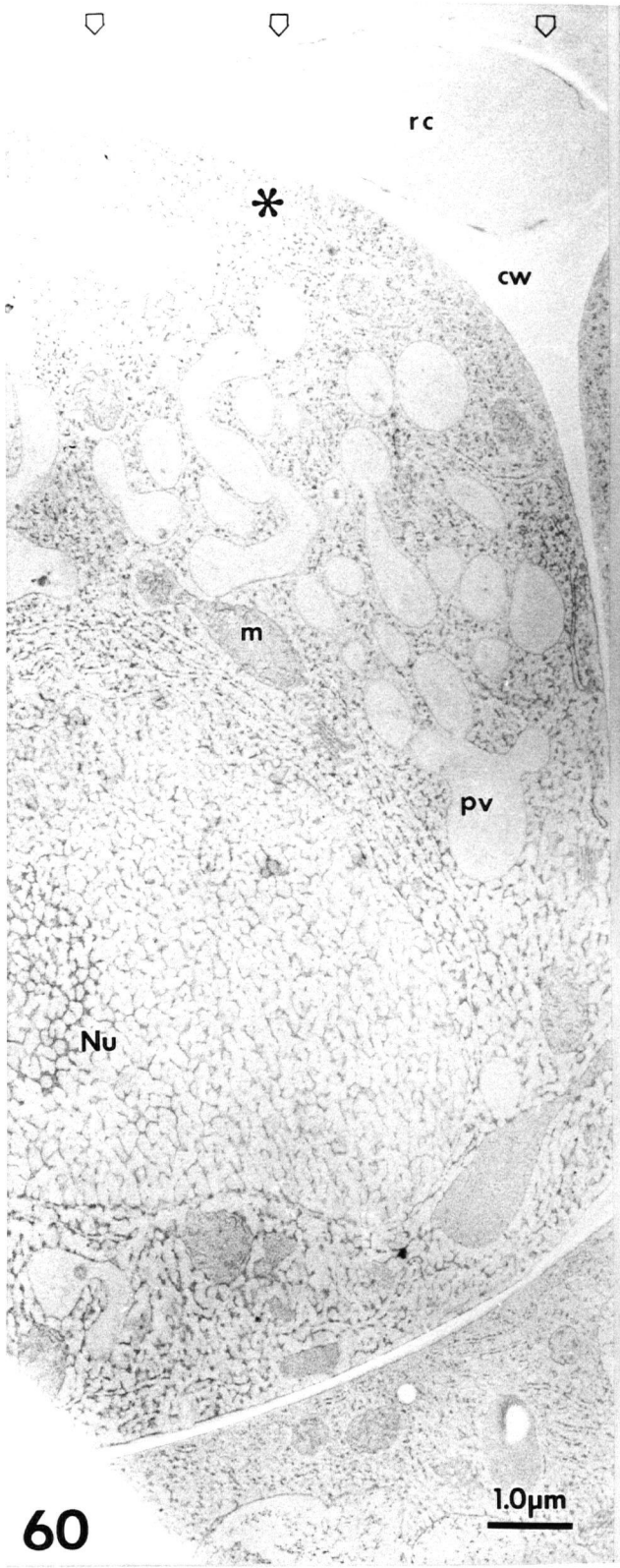

60

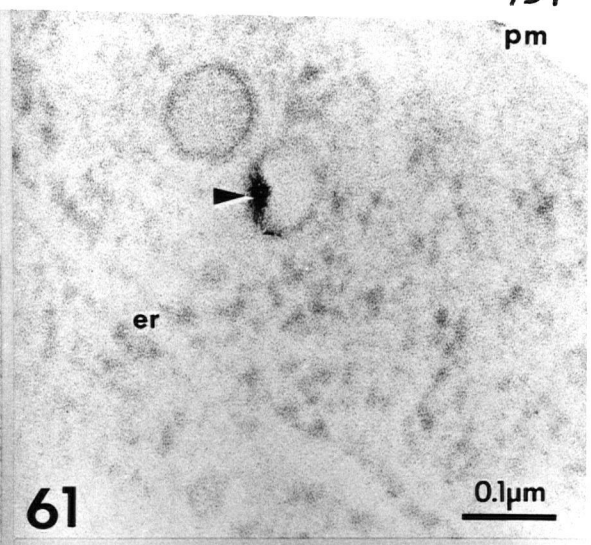

61

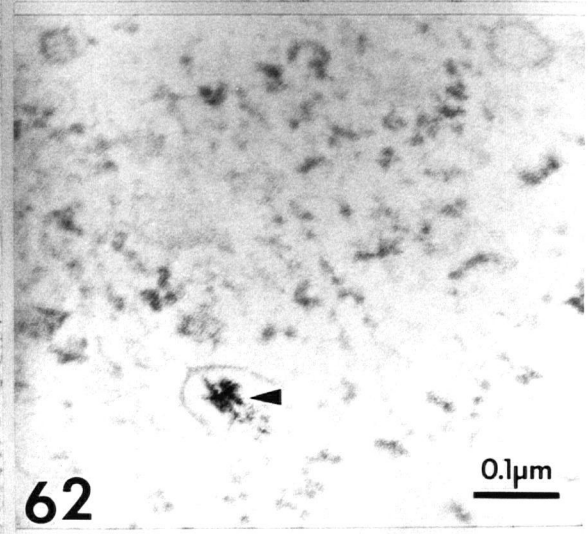

62

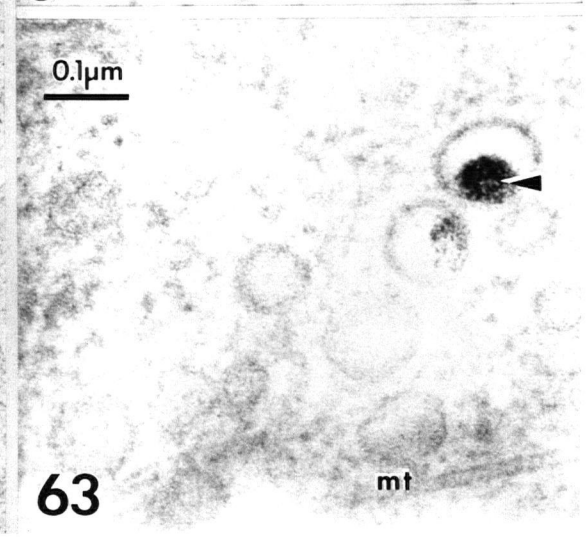

63

Figs. 64-66: Multivesicular bodies labelled with lanthanum.

Fig. 64: multivesicular body with vesicles fusing or budding. Intraluminal vesicles labelled with lanthanum. Sections not poststained.

Fig. 65: dictyosome adjacent to multivesicular body; these organelles are often associated. Sections stained with uranyl acetate/lead citrate.

Fig. 66: multivesicular body in cortical cytoplasm. Sections not poststained.

Fig. 67: Partially coated reticulum labelled with lanthanum. Note provacuole fusion.

pm=plasma membrane, mvb=multivesicular body, v=vesicle, d=dictyosome, m=mitochondrion, pcr=partially coated reticulum, pv=provacuole.

all arrowheads indicate lanthanum deposits

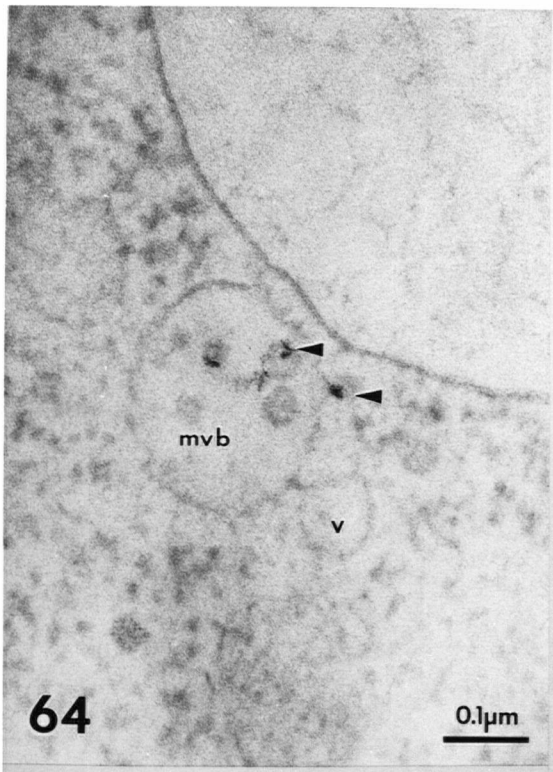
mvb
v
64
0.1µm

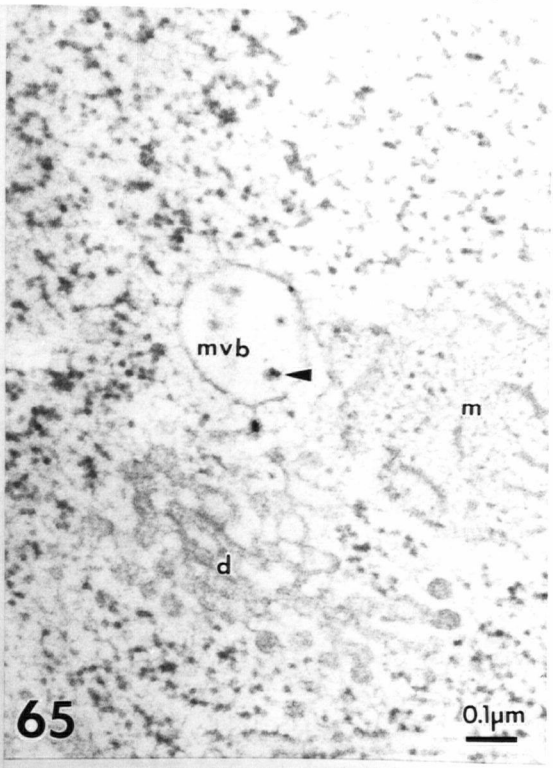
mvb
m
d
65
0.1µm

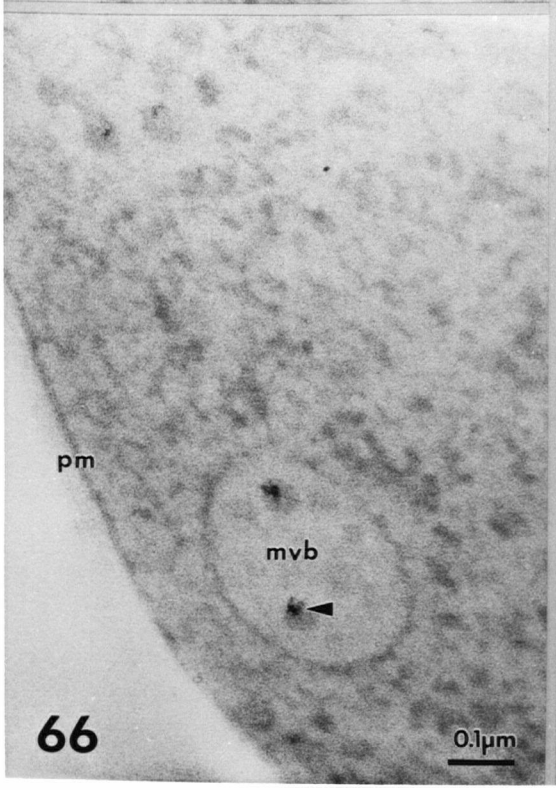
pm
mvb
66
0.1µm

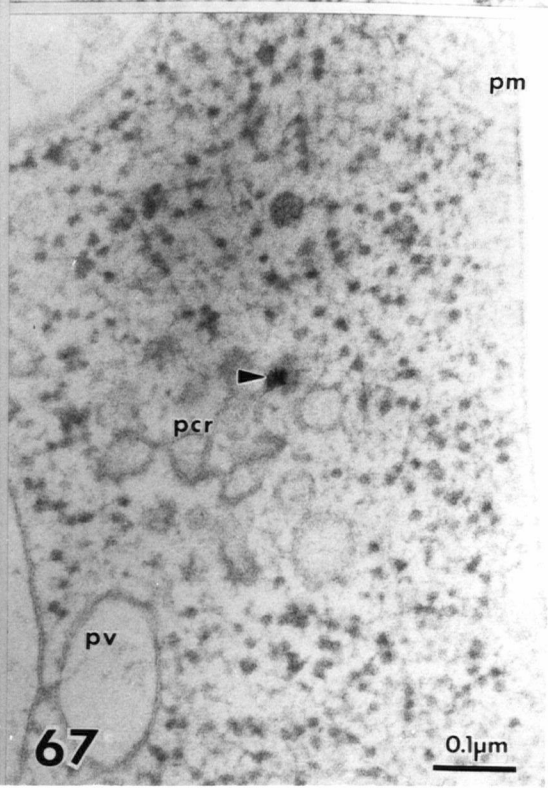
pm
pcr
pv
67
0.1µm

Figs. 68-70: Golgi with peripheral lanthanum labelled vesicles.

Fig. 68: Dictyosome and multivesicular body labelled with lanthanum. Vesicles near dictyosome are smaller size class than trans Golgi network vesicles. Multivesicular body intraluminal vesicles labelled.

Fig. 68: Higher magnification view of a dictyosome stack with nearby endoplasmic reticulum. Note small lanthanum labelled vesicle near dictyosome.

Fig. 69: Longitudinal section through dictyosome peripheral network. Lanthanum labels small peripheral vesicles as well as margin of larger vesicle type.

pm=plasma membrane, mvb=multivesicular body, d=dictyosome, er=endoplasmic reticulum,

all arrowheads indicate lanthanum deposits

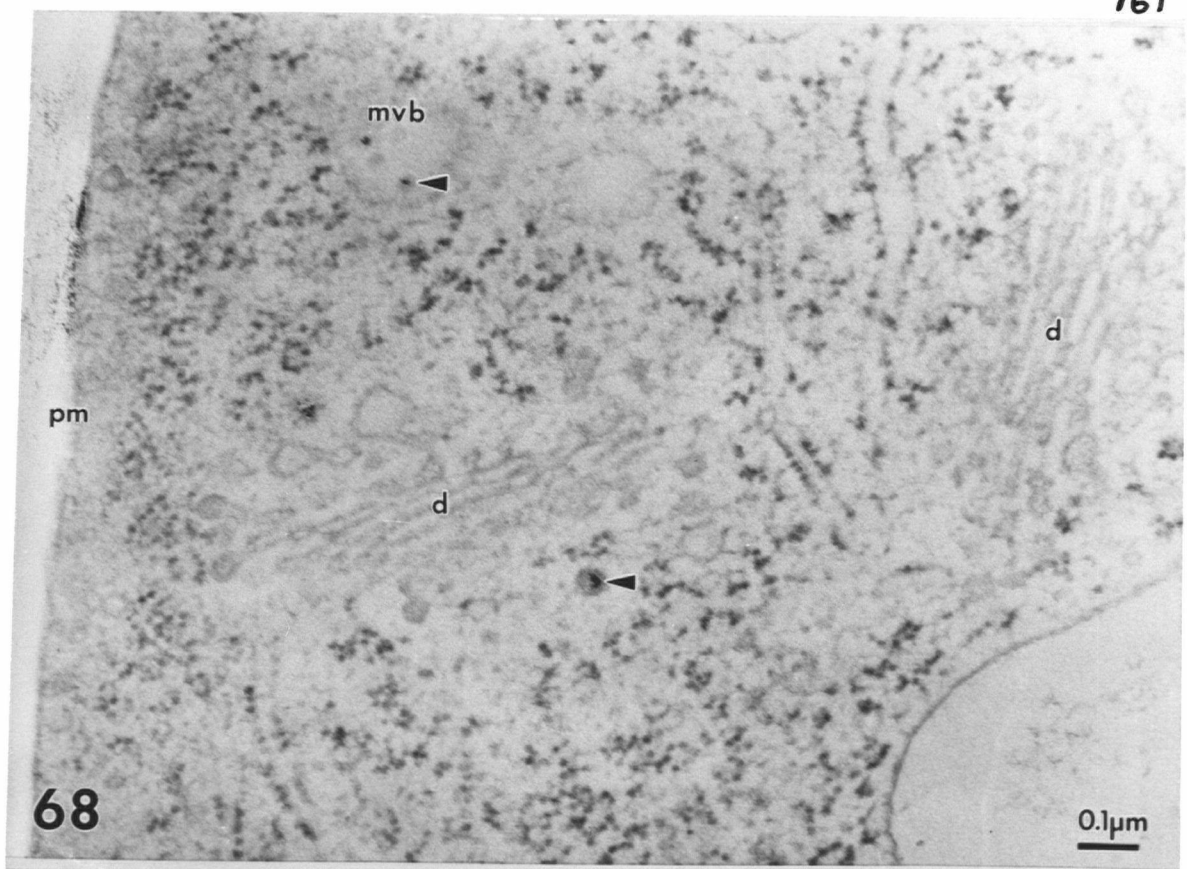
mvb
d
pm
d
68
0.1µm

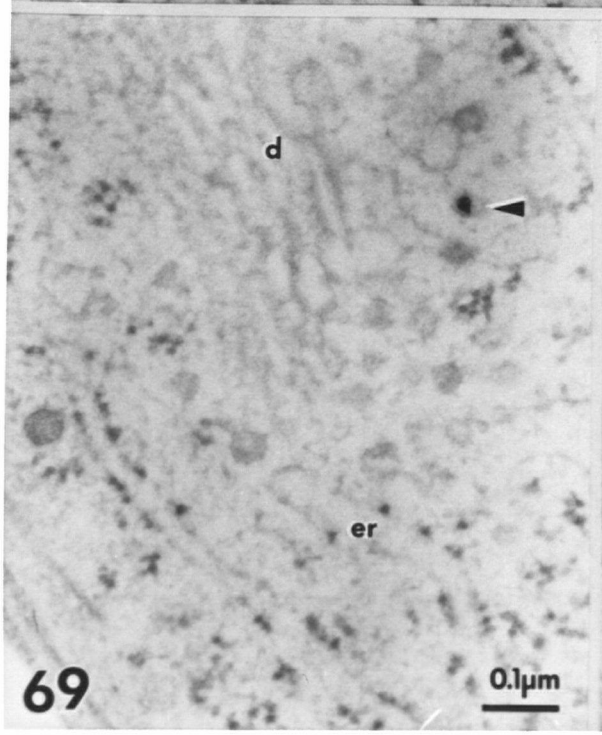
d
er
69
0.1µm

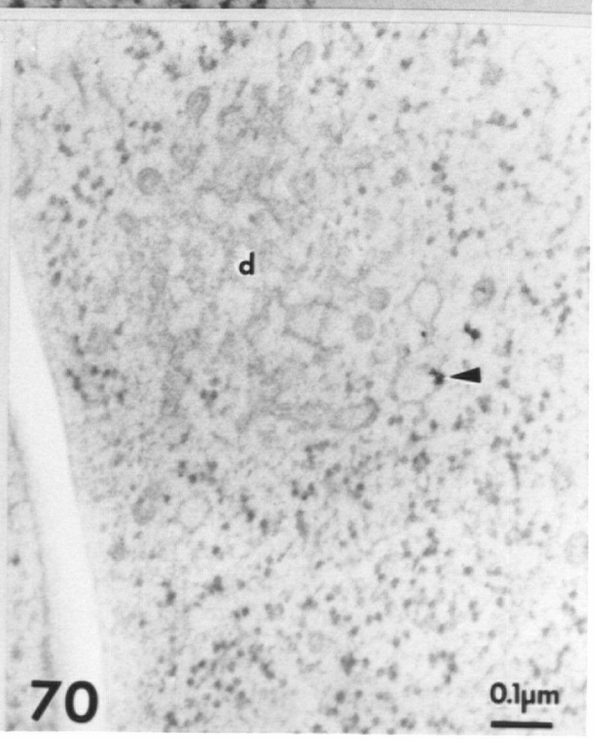
d
70
0.1µm

DISCUSSION

The results of this ultrarapid freezing study agree well with previous studies of endocytosis using conventional techniques (chapter 1, Joachim and Robinson 1984, Tanchak et al. 1984, Hubner et al. 1985, Tanchak and Fowke 1987). The lanthanum assay, when combined with ultrarapid freezing and freeze substitution, shows membrane and/ or contents are delivered to the partially coated reticulum, multivesicular body, and Golgi. Cryo techniques have never been used to study endocytosis in higher plants and a branching, less vesiculated endomembrane system is revealed. The presence of lanthanum labelled vesicles in ultrarapidly frozen cells suggests endocytotic vesicles do exist in higher plant cells and are not an artifact of chemical fixation.

Crucial to the study of endocytosis is the ability to define the nature of the vesicles related to the endomembrane system, i.e. one must be able to distinguish between endocytotic vesicles and other transport vesicles such as secretory vesicles. The population of endocytotic vesicles in this study were defined by the presence of lanthanum label. Ultrarapid freezing technique

allows for the further distinction between endocytotic and secretory vesicles through more accurate morphology and their distinct association with different parts of the Golgi. Endocytotic vesicles were associated with the periphery of the dictyosome and the secretory vesicles were associated with the trans Golgi.

When the results of this endocytosis study are considered with the results of the secretion study on the same cell type (chapter 2), it can be suggested that there are heterogenous vesicle populations in the cytoplasm. Vesicle heterogeneity should be considered when morphometric studies of secretion are carried out. Previous morphometric studies have assumed that all vesicles in the cortical cytoplasm are secretory (Cunningham and Hall 1986, Quaite et al. 1983, Kristen and Lockhausen 1983, Phillips et al. 1988). This endocytosis study shows a population of vesicles moving from the plasma membrane to multivesicular body and dictyosome which are distinct from the secretory vesicles.

The presence of this population of vesicles can be interpreted as evidence of vesicular membrane recycling in Lobelia erinus root secretory

cells. The endocytotic vesicles labelled with lanthanum could be carrying away excess membrane added by exocytosis of cell wall components. A population of vesicles whose primary function is moving bulk membrane material from the plasma membrane back to the endomembranes of the granulocrine secretory cell has been predicted on theoretical grounds (Raven 1987, Robinson 1985, Steer 1985).

The properties of the endocytotic vesicles observed in this study are consistent with a role in membrane recycling. The small radius of the vesicles (100 nm) means a large surface area/volume ratio which is an efficient mechanism for packing membrane material (see discussion chapter 2). Considerations of turgor as a restraining force on membrane internalization have suggested the work necessary to internalize a vesicle depends in part on the volume of the vesicle. "It follows that the uptake of fewer, large, coated vesicles against turgor may be thermodynamically impossible in contrast to the uptake of many small ones" (Gradmann and Robinson 1989). These authors assume all recycling vesicles would be coated but the argument holds for uncoated small vesicles as well.

In addition to a small radius, another important property of the endocytotic vesicles are

their location in the cortical cytoplasm when cells are ultrarapidly frozen. Lanthanum labelled vesicles were seen amongst the cortical microtubules next to the plasma membrane, as in conventional TEM preparations of elongating roots (see chapter 1). They are also found deeper in the cytoplasm; this is significant because vesicle profiles near the plasma membrane may just represent the neck of a plasma membrane infolding (Pastan and Willingham 1983). If lanthanum labelled vesicles are more than 1-2 um from the plasma membrane, the probability that the vesicle is separate from the plasma membrane is higher.

In the conventional study of endocytosis, long necked structures on the plasma membrane were observed (chapter 1) which were not observed in this ultrarapid freezing study. These structures were originally described in an ultrarapid freezing study by Staehelin and Chapman (1987) so these results are unexpected. In some cases vesicles fusing with the plasma membrane did have a flattened (oval) appearance, but further work is required in this area.

After ultrarapid freezing, the well preserved sections of the epidermal cell had few coated

vesicles. The coated membranes may not have been detected because most sampling was done on sections without poststain. The use of unstained sections means the majority of the electron density comes from osmium (membranes) and lanthanum (label for endocytosis), which is useful for looking at total endocytosis. Unfortunately, it is not conducive to detecting the protein coat on the cytoplasmic surface of 100 nm lanthanum labelled coated vesicles.

In this study, ultrarapid freezing provides a view of the endomembrane system with extensive branching of reticula, for example the partially coated reticulum, endoplasmic reticulum, and trans Golgi network. These branching structures are not as extensive in cells prepared with conventional methods (see chapters 1 and 2). One reason for this could be that conventional techniques use glutaraldehyde which has been shown to induce vesiculation of the endoplasmic reticulum (Mersey and McCully 1978). In other higher plant systems prepared using ultra rapid freezing techniques, a "continuous extensive network" of endoplasmic reticulum has been reported (Craig and Staehelin 1988, Fernandez and Staehelin 1985). The present

study used a different method of ultrarapid freezing (copper block rather than propane jet or high pressure freezing) but the results obtained support the concept of delicate, reticulate endomembrane compartments.

A similar induced vesiculation of the partially coated reticulum by glutaraldehyde could explain the absence of this structure in the earlier study of endocytosis using conventional TEM techniques (see chapter 1). The lanthanum labelled partially coated reticulum was found in the cortical cytoplasm, which is consistent with the theory that the PCR is an early endosome (chapter 2, Pesacreta and Lucas 1985, Tanchak et al. 1988). The PCR morphology, like the multivesicular body morphology, has been described in animal cells as a type of endosome (Miller et al. 1986).

The multivesicular body was one of the centers of vesicle budding and fusing observed in this study. According to the lanthanum assay for endocytosis, this organelle receives membrane and/or contents of vesicles derived from the plasma membrane. In animals, endosomes have complex functions such as uncoupling and sorting of receptors and ligands, and membrane recycling to

the plasma membrane in cells with high endocytosis such as macrophages (Schmid et al. 1988, de Chastellier et al. 1987). The pathways of receptors and ligands have not been elucidated in higher plants, but the delivery of vesicles to the multivesicular body seen in this study is consistent with a role in membrane turnover.

The multivesicular endosome has been considered a "late" endosome, i.e. located in the perinuclear region of the animal cell and destined for fusion with a primary lysosome (Miller et al. 1986, Griffiths et al. 1988). In this study, the location of the multivesicular body in the cortical cytoplasm suggests this organelle does not undergo an analogous migration to the cell interior. This may be a reflection of the differences in the organization of the Golgi in plants and animals. In animals the Golgi complex is in the perinuclear zone while in the higher plant cells the dictyosomes are scattered throughout the cytoplasm.

The intraluminal vesicles of the multivesicular body were often labelled with lanthanum in this study. This may indicate that these structures have different charge or lipid

composition than the limiting membrane of the multivesicular body. It is difficult to tell if these intraluminal structures are vesicles or tubules in three dimensions. The formation of tubules was considered a mechanism for extruding aqueous matrix and forming membrane enriched domains of the endosome in animal cells (Rome 1985, Geuze et al. 1984). It would be interesting to look at the acidity of the plant multivesicular body; in animal endosomes the slightly acid pH is believed to be important in separating the receptors from their ligands (Helenius et al. 1983, Anderson and Orci 1988).

The rate of ultrarapid freezing determines that the sampling is a small slice of time: the organelles in the well preserved surface zone are stopped within 1-2 milliseconds (Jones 1984). Although the TEM requires thin sectioned material and therefore still only provides a static image, this immobilization of the cytoplasm by ultrarapid freezing provides a precise static image.

In conclusion, ultrarapid freezing techniques have confirmed the existence of endocytosis in intact root tissue of Lobelia erinus. A distinct population of vesicles was labelled with lanthanum.

The size and location of these vesicles makes them good candidates for carrying excess plasma membrane added during cell wall secretion. The intracellular labelling of PCR and multivesicular bodies add support to the theories that these structures can be considered endosomes, and that these structures are also important in the flow of membrane through the plant cell.

GENERAL CONCLUSIONS

The results of the conventional TEM and ultrarapid freezing studies suggest endocytosis does occur in elongating roots of Lobelia erinus. When the number of endocytotic vesicles per cell was measured, the greatest amount of endocytosis was found in elongating cells. The greater amount of endocytosis observed in cells which are actively secreting, compared to non-secretory cells, can be interpreted as evidence of vesicular membrane recycling.

The vesicles in the cytoplasm displayed heterogeneity with respect to polysaccharide content, size, organelle associations, and ability to take up lanthanum. It was demonstrated that a population of small vesicles involved in endocytosis are distinct from the larger, polysaccharide containing secretory vesicles.

The membrane internalized by endocytosis becomes incorporated into multivesicular bodies and partially coated reticulum. Using a functional definition of an endosome as an organelle which receives membrane from the plasma membrane via endocytosis, and considering the morphological similarities to animal systems, these organelles

can be considered plant endosomes. Membrane recycling from the plasma membrane to the Golgi could be occurring via these intermediate organelles.

Preliminary experiments suggest microtubules play a role in vesicle movement during endocytosis in elongating Lobelia root cells. After disruption of microtubules with colchicine, there were signs that endocytosis had been perturbed, e.g. fewer lanthanum labelled vesicles and less label in the multivesicular bodies.

The cell wall porosity of the elongating cells of Lobelia erinus was dependent on the integrity of the pectin component of the cell wall. The pore size increased dramatically upon treatment with low concentrations of pectinase. The sensitivity to disruption probably means that the 1-2 nm pore size observed in intact laboratory grown roots represents a minimum that would rarely, if ever, occur in the soil where the root is exposed to microbial enzymes and abrasion.

In conclusion, endocytosis can be considered an important part of the homeostatic mechanism for controlling plasma membrane surface area in the elongating primary root cells of Lobelia erinus.

The organelles of the endomembrane system that were shown to be involved in endocytosis are outlined in Fig. 71. This revised model emphasizes the importance of endosomes in membrane flow, as well as the reticular nature of the endomembrane system and the heterogenous composition of vesicles in the cytoplasm. These experiments demonstrated the first step in this membrane recycling model, i.e. movement of vesicles from plasma membrane to endosome (Fig. 71). The second step in membrane recycling, i.e. endosome to Golgi, is proposed to be vesicle mediated as well, although further work is required in this area.

The endomembrane system of higher plants has been described in terms of ER, Golgi, and secretory vesicles. In the future, the presence of endosomes and endocytotic vesicles should also recognized as an integral part of the endomembrane system.

Fig. 71: Revised model of membrane flow in Lobelia erinus endomembrane system. Endocytosis of vesicles to endosomes shown by small arrowheads, based on lanthanum labelling experiments. Proposed pathway of membrane recycling from endosomes to Golgi shown by circles. Secretion of cell wall components shown with larger arrowheads. stipple=lanthanum, squares=secretory product, G=Golgi, c=cis, t=trans, er=endoplasmic reticulum, sv=secretory vesicle, cv=coated vesicle, mvb=multivesicular body, pcr=partially coated reticulum, mt=microtubules, pm=plasma membrane.

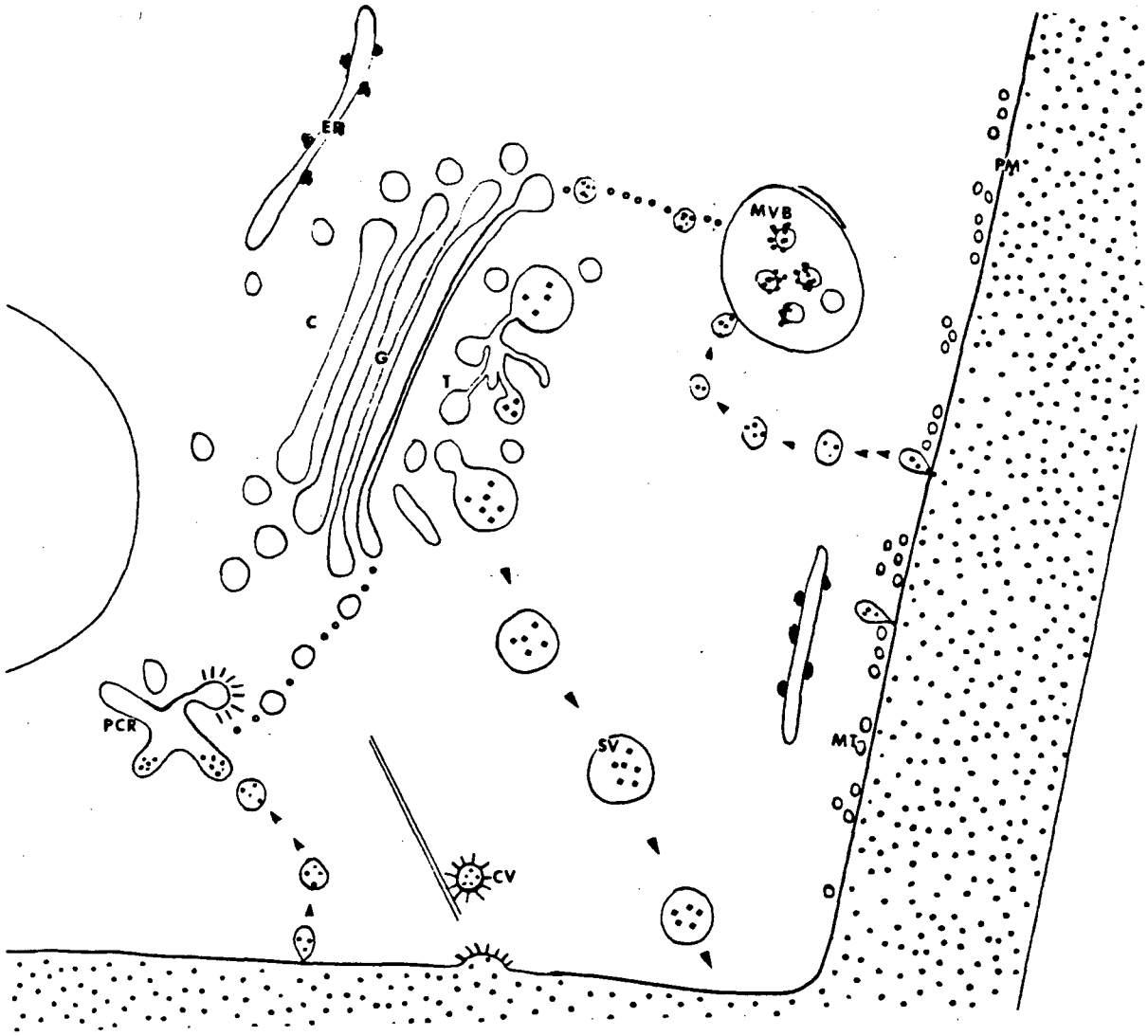

APPENDIX 1: CALCULATIONS OF AMOUNT OF PM ADDED TO CELL SURFACE DURING WALL SECRETION; COMPARISON WITH CELL SURFACE OBSERVED SUGGESTS MEMBRANE RECYCLING.

If V = volume of the cell wall excluding end walls then

V= 4 x length x width x wall thickness

for meristematic cells V = 4 x 20 x 20 x 0.15 = 240 um^3

for vacuolate cells V = 4 x 80 x 20 x 0.40 = 2560 um^3

Total volume of wall added during elongation =

2560 - 240 = 2320 um^3

20% of volume consists of cellulose which is added by plasma membrane bound enzymes rather than secreted, so volume of wall matrix secreted is

2320 - 0.2 (2320) = 1856 um^3

Each cell contributes half the wall thickness, so the volume of wall matrix synthesized by each cell is

1856 x 0.5 = 928 um^3

Assuming secretion via spherical Golgi derived vesicles of 100 nm diameter (radius = 50 nm = 0.05 um) (Quaite et al. 1983), and assuming the volume of matrix in the secretory vesicles and the cell wall are the same, the volume of one secretory vesicle can be calculated:

$V = 4/3 \times pi \times r^3$

$V = 4/3 \times pi \times 0.05^3 = 0.000523\ um^3$/vesicle

The number of vesicles required to produce the cell wall observed is

$928\ um^3 / 0.000523\ um^3 = \underline{1,773,361}$ vesicles per cell

The surface area (A) of one vesicle

$A = 4 \times pi \times r^2$

$A = 4 \times 3.14 \times 0.05^2\ um = 0.031\ um^2$

The total surface area predicted (A_p) to be added by the vesicles during elongation is:

$A_p = 1,773,361 \times 0.031\ um^2 = 54,974\ um^2$

This can be compared to the surface area observed in the mature cell (A_o):

$A_o = 4 \times 20 \times 80 = 6400\ um^2$

$A_p / A_o = 54,974 / 6400$

Therefore the surface area of plasma membrane which is expected to be added by vesicles during elongation is about 8.5 times the surface area of the plasma membrane observed in the mature cell.

Appendix 2: CYTOCHEMICAL TECHNIQUES FOR LOCALIZATION OF POLYSACCHARIDES.

periodate silver methenamine	Roland (1978), Thiery (1967), Ryser (1979)
ruthenium red en bloc	Roland (1970), Hayat (1981)
alcian blue en bloc	Trachtenberg and Fahn (1981), Hayat (1981)
pectinase-colloidal gold on epon sections	Vian et al. (1983) Bendayan (1984)
alkaline bismuth	Shinji et al.(1976) Park et al. (1987)

BIBLIOGRAPHY

Anderson RGW, Orci L (1988) A view of acidic intracellular compartments. J Cell Biol 106: 539-543

Auriac M-C, Tort M (1985) Ultrastructural evidence for a direct transport from apoplast to vacuoles in the storage cells of Japanese artichoke. Physiol Veg 23: 301-307

Bachmann L, Mayer E (1987) Physics of water and ice:implications for cryofixation. in: Cryotechniques in biological electron microscopy. Steinbrecht RA, Zierold K, editors. Springer-Verlag pp 3-34

Bajer A, Mole-Bajer J (1969) Formation of the spindle fibers, kinetochore orientation, and behaviour of the nuclear envelope during mitosis in endosperm. Fine structural and in vitro studies. Chromosoma 27: 479-484

Baker DA, Hall JL (1973) Pinocytosis, ATPase and ion uptake by plant cells. New Phytol 72: 1281-1291

Balch WE, Dunphy WG, Braell WA, Rothman JE (1984) Sequential intermediates in the pathway of intercompartmental transport in a cell free system. Cell 39: 525-536

Barlow DI, Sleigh MA (1979) Freeze substitution for preservation of ciliated surfaces for scanning electron microscopy. J Microsc 115: 81-95

Baron-Epel O, Gharyal PK, Schindler M (1988) Pectins as mediators of wall porosity in soybean cells. Planta 175: 389-395

Basham HG, Bateman DF (1975) Killing of plant cells by pectic enzymes: the lack of direct injurious interaction between pectic enzymes or their soluble reaction products and plant cells. Phytopathology 65: 141-153

Bendayan M (1984) Enzyme-gold electron microscopic cytochemistry: a new affinity approach for the ultrastructural localization of macromolecules. J EM Tech 1: 349-372

Besterman JM, Airhart JA, Woodworth RC, Low RB (1981) Exocytosis of pinocytosed fluid in cultured cells: kinetic evidence for rapid turnover and compartmentation. J Cell Biol 91: 716-727

Besterman JM (1985) Endocytosis-Exocytosis coupling in: Developments in Cell Biology I, secretory processes. Dean RT, Stahl P, eds. Butterworths, London. pp 58-73

Boston RS, Miller TJ, Mertz JE, Burgess RR (1982) In vitro synthesis and processing of wheat amylase. Plant Physiol 69: 150-154

Bowles DJ, Northcote DH (1972) The sites of synthesis and transport of extracellular polysaccharides in the root tissue of maize. Biochem J. 130: 1133-1145

Bowles DJ, Northcote DH (1974) The amounts and rates of export of polysaccharides found with the membrane system of maize root cells. Biochem J. 142: 139-144

Bowles DJ, Northcote DH (1976) The size and distribution of polysaccharides during their synthesis within the membrane system of maize root cells. Planta 128: 101-106

Bradfute DE, Chapman-Andresen C, Jensen WA (1964) Concerning morphological evidence for pinocytosis in higher plants. Exp Cell Res 36:207-210

Brady ST, Lasek RJ, Allen RD (1982) Fast axonal transport in extruded axoplasm from squid giant axon. Science 218: 1129-1131

Brossard-Chriqui D, Iskander S (1982) Ultrastructural changes of cytomembranes during the first hours of the in vitro culture of Datura innoxia Mill. leaf explants. Relations to sucrose uptake. Protoplasma 112: 217-225

Brown MS, Anderson RGW, Goldstein JL (1983) Recycling receptors:the round trip itinerary of migrant membrane proteins. Cell 32: 663-667

Brown RM (1969) Observations on the relationship of the Golgi apparatus to wall formation in the marine Chrysophycean alga, Pleurochrysis scherffellii Pringshein. J Cell Biol 41: 109-123

Browning AJ, Gunning BES (1977) An ultrastructural and cytochemical study of the wall-membrane apparatus of transfer cells using freeze substitution. Protoplasma 93: 7-26

Buckout TJ (1984) Characterization of Ca^{2+} transport in purified endoplasmic reticulum membrane vesicles from Lepidium sativa roots. Plant Physiol 76: 962-967

Buvat R (1963) Electron microscopy of plant protoplasm. Int Rev Cytol 14: 41-148

Carpita N, Sabularse D, Montezinos D, Delmer DP (1979) Determination of the pore size of cell walls of living plant cells. Science 205: 1144-1147

Cassab GI, Varner JE (1988) Cell wall proteins. Ann Rev Plant Physiol Plant Mol Biol 39: 321-353

Chaboud A, Rougier M (1986) Ultrastructural study of the maize epidermal root surface. I. Preservation and extent of the mucilage layer. Protoplasma 130: 73-79

Chrispeels MJ (1976) Biosynthesis, intracellular transport, and secretion of extracellular macromolecules. Ann Rev Plant Physiol 27: 19-38

Chrispeels MJ (1980) The endoplasmic reticulum. in: The Biochemistry of plants, 1. Tolbert NE, editor. pp 390-410

Collmer A, Keen NT (1986) The role of pectic enzymes in plant pathogenesis. Ann Rev Phytopathol 24: 381-409

Cooper JB, Chen JA, van Holst G-J, Varner JE (1987) Hydroxyproline-rich glycoproteins of plant cell walls. TIBS 12: 24-27

Cox G, Vesk M, Juniper B (1986) High voltage electron microscopy of cytoskeletal structures in whole plant cells. Nord J Bot 6: 641-649

Cram WJ (1980) Pinocytosis in plants. New Phytologist 84: 1-17

Craig S, Staehelin LA (1988) High pressure freezing of intact plant tissues. Evaluation of characterization of novel features of the endoplasmic reticulum and associated endomembranes. Eur J Cell Biol 46: 80-93

Crowdy SH, Tanton TW (1970) Water pathways in higher plants. I. Free space in wheat leaves. J Exp Bot 21: 102-111

Cunningham ME, Hall JL (1986) The effect of calcium antagonists and inhibitors of secretory processes on auxin induced elongation and fine structure of Pisum sativum stem segments. Protoplasma 133: 149-159

Darvill AG, Albersheim P, McNeil M, Lau JM, York WS, Stevenson TT, Thomas J, Doares S, Gollin DJ, Chelf P, Davis K (1985) Structure and function of plant cell wall polysaccharides. J Cell Sci Suppl 2: 203-317

Dauwalder M, Whaley WG (1982) Membrane assembly and secretion in higher plants. J Ultrastruc Res 78: 302-320

Dawson PJ, Hulme JS, Lloyd CW (1985) Monoclonal antibody to intermediate filament antigen cross reacts with higher plant cells. J Cell Biol 100: 1793-1798

deChastellier C, Land T, Ryter A, Thilo L (1987) Exchange kinetics and composition of endocytic membrane in terms of plasma membrane constituents: a morphometric study in macrophages. Eur J Cell Biol 44: 112-123

deDuve C (1963) Lysosomes. CIBA Foundation Symposium. DeRuck AVS, Cameron MB, editors. Churchill. London. p 126

Depta H, Andreae M, Blaschek W, Robinson DG (1987) Glucan synthase II activity in a coated vesicle fraction from zucchini hypocotyls. Eur J Cell Biol 45: 219-223

Dixon WT, Northcote DH (1985) Plant cell secretory processes. In: Developments in Cell Biology I, secretory processes. Dean RT, Stahl P, editors. Butterworths, London. pp 77-98

Djordjevic MA, Gabriel DW, Rolfe BG (1987) Rhizobium: the refined parasite. Ann Rev Phytopathol 25: 145-168

Doohan ME, Palevitz BA (1980) Microtubules and coated vesicles in guard-cell protoplasts of Allium cepa L. Planta 149: 389-401

Dorel C, Voelker TA, Herman EM, Chrispeels MJ (1989) Transport of proteins to the plant vacuole is not by bulk flow through the secretory system, and requires

positive sorting information. J Cell Biology 108: 327-337

Drew MC, Seear J, McLaren AD (1970) Entry of basic macromolecules into barley roots. Am J Bot 57: 837-843

Dubochet J, McDowall AW (1981) Vitrification of pure water for electron microscopy. J Microsc 124: RP3-4

Dubochet J, Chang J-J, Freeman R, Lepault J, McDowall AW (1982) Electron microscopy of frozen water and aqueous suspensions. J Microsc 128: 219-237

Dubochet J, Adrain M, Chang J-J, Lepault J, McDowall AW (1987) Cryoelectron microscopy of vitrified specimens. in: Cryotechniques in biological electron microscopy. Steinbrecht RA, Zierold K editors. Springer-Verlag. pp 114-131

Emons AMC, Traas JA (1986) Coated pits and coated vesicles on the plasma membrane of plant cells. Eur J Cell Biol 41: 57-64

Falconer MM, Seagull RW (1985) Immunofluorescent and calcofluor white staining of developing tracheary elements in Zinnia elegans L. suspension cultures. Protoplasma 125: 190-198

Farquhar MG (1981) Membrane recycling in secretory cells: implications for traffic of products and specialized membranes within the Golgi complex. Methods in Cell Biol 23: 400-427

Farquhar MG (1985) Progress in unraveling pathways of Golgi traffic. Ann Rev Cell Biol 1: 447-488

Farquhar MG, Palade GE (1981) The Golgi apparatus (complex) from artifact to center stage. J Cell Biol 91: 775-1035

Fernandez DE, Staehelin LA (1985) Structural organization of ultrarapidly frozen barley aleurone cells actively involved in protein secretion. Planta 165: 455-468

Fincher GB and Stone BA (1981) Metabolism of noncellulosic polysaccharides. In: Tanner W, Loewus FA, eds. Encycl Plant Physiol 13B: 68-132

Fisher DB (1975) Structure of functional soybean sieve elements. Plant Physiol 56: 555-569

Fisher KA (1982) Preparation of planar membrane monolayers for spectroscopy and electron microscopy. Methods Enzymol 88: 230-235

Fowke LR, Setterfield G (1969) Multivesicular structures and cell wall growth. Can J Bot 47: 1873-1877

Foster RC (1982) The fine structure of epidermal cell wall mucilages of roots. New Phytol 91: 727-740

Friend DS (1969) Cytochemical staining of the multivesicular body and Golgi vesicles. J Cell Biol 41: 269-279

Fry SC (1986) Cross-linking of matrix polymers in the growing cell walls of angiosperms. Ann Rev Plant Physiol 37: 165-186

Geuze HJ, Slot JW, Strous GJAM, Lodish HF and Schwartz AL (1983) Intracellular site of asialoglycoprotein receptor-ligand uncoupling: double label immunoelectron microscopy during receptor mediated endocytosis. Cell 32: 277-287

Geuze HJ, Slot JW, Strous GJAM, Peppard J, Von Figurea K, Hasilik A, Schwartz AL (1984) Intracellular receptor sorting during endocytosis: comparative immunoelectron microscopy of multiple receptors in rat liver. Cell 37: 195-204

Gibbons IR (1988) Dynein ATPases as microtubule motors. J Biol Chem 263: 15837-15840

Gilkey JC, Staehelin LA (1986) Advances in ultrarapid freezing for the preservation of cellular ultrastructure. J EM Tech 3: 177-210

Goldstein JL, Brown MS, Anderson RGW, Russell DW, Schneider WJ (1985) Receptor mediated endocytosis: concepts emerging from the LDL receptor system. Ann Rev Cell Biol 1: 1-39

Gradmann D, Robinson DG (1989) Does turgor prevent endocytosis in plant cells? Plant Cell Environ 12: 151-154

Graham RC and Karnovsky MJ (1966) The early stages

of absorption of injected Horseradish peroxidase in the proximal tubules of mouse kidney: Ultrastructural cytochemistry by a new technique. J Histochem Cytochem 14: 291-302

Griffing LR, Fowke LC (1985) Cytochemical localization of peroxidase in soybean suspension culture cells and protoplasts: intracellular vacuole differentiation and presence of peroxidase in coated vesicles and multivesicular bodies. Protoplasma 128: 22-30

Griffing LR, Ray PR (1985) Involvement of monovalent cations in Golgi secretion by plant cells. Eur J Cell Biol 36: 24-31

Griffing LR, Mersey BG, Fowke LR (1986) Cell fractionation analysis of glucan synthase I and II distribution and polysaccharide secretion in soybean protoplasts: Evidence for the involvement of coated vesicles in wall biogenesis. Planta 167: 175-182

Griffiths G, Pfeiffer S, Simons K, Matlin K (1985) Exit of newly synthesized membrane proteins from the trans cisterna of the Golgi complex to the plasma membrane. J Cell Biol 101: 949-964

Griffiths G, Simon K (1986) The trans Golgi network: sorting at the exit site of the Golgi complex. Science 234: 438-442

Griffiths G, Fuller SD, Back R, Hollinshead M, Pfeiffer S, Simons K (1989) The dynamic nature of the Golgi complex. J Cell Biol 108: 277-297

Hahne G, Lorz H (1988) Release of phytotoxic factors from plant cell walls during protoplast isolation. J Plant Physiol 132: 345-350

Hall TA, Gupta BL (1984) The application of EDXS to the biological sciences. J Microsc 136: 193-208

Harding K, Cocking EC (1986) The interaction between E. coli spheroplasts and plant protoplasts: a proposed procedure to deliver foreign genes into plant cells. Protoplasma 130: 153-161

Harris N (1986) Organization of the endomembrane system. Ann Rev Plant Phys 37: 73-92

Harris N, Oparka KJ (1983) Connections between dictyosomes, ER and GERL in cotyledons of mung

beans. Protoplasma 114: 93-102

Hasty DL, Hays ED (1978) Freeze fracture studies of the developing cell surface II. Particle free blisters on glutaraldehyde fixed corneal fibroblasts are artifacts. J Cell Biol 78: 756-768
177

Hayashi T, Marsden MPF, Delmer DP (1987) Pea xyloglucan and cellulose. V. Xyloglucan-cellulose interactions in vitro and in vivo. Plant Physiol 83: 384-389

Hayat MA (1981) Principles and techniques of electron microscopy: biological applications, 2nd edition, International Publishing

Heath IB (1974) A unified hypothesis for the role of membrane bound enzyme complexes and microtubules in plant cell wall synthesis. J Theor Biol 48: 445-449

Helenius A, Mellman I, Wall D, Hubbard A (1983) Endosomes. TIBS 10: 245-250

Hepler PK (1985) The plant cytoskeleton. in: Botanical Microscopy. Robards AW, editor. pp 233-262

Hepler PK, Newcomb EH (1967) Fine structure of cell plate formation in the apical meristem of Phaseolus roots J Ultrastruc Res 19: 498-513

Hereward FV, Northcote DH (1972) A simple freeze substitution method for the study of ultrastructurre of plant tissues. Exp Cell Res 70: 73-80

Heuser JE (1989) Effects of cytoplasmic acidification on clathrin lattice morphology. J Cell Biol 108: 401-411

Heuser JE, Reese TS, Dennis MJ, Jan Y, Evans L (1979) Synaptic vesicle exocytosis captured by quick freezing and correlated with quantal neurotransmitter release. J Cell Biol 81: 275-300

Heuser JE, Evans L (1980) Three dimensional visualization of coated vesicle formation in fibroblasts. J Cell Biol 84: 560-583

Hillmer S, Depta H, Robinson DG (1986) Confirmation of endocytosis in higher plant protoplasts using lectin-gold complexes. Eur. J Cell Biol 41: 142-149

Hillmer S, Freundt H, Robinson DG (1988) The partially coated reticulum and its relationship to the Golgi apparatus in higher plant cells. Eur J Cell Biol 47:206-212

Hirokawa N, Pfister KK, Yorifuji H, Wagner MC, Brady 178 ST, Bloom GS (1989) Submolecular domains of bovine brain kinesin identified by electron microscopy and monoclonal antibody decoration. Cell 56: 867-878

Hubner R, Depta H, Robinson DG (1985) Endocytosis in maize root cap cells: evidence obtained using heavy metal salts. Protoplasma 129: 214-222

Hudson CS, Rash JE, Graham WF (1979) Introduction to sample preparation for freeze fracture. in: Freeze fracture:methods, artifacts, and interpretations. Rash JE, Hudson CS editors. Raven Press. pp. 1-10

Jarvis MC (1984) Structure and properties of pectin gels in plant cell walls. Plant Cell Environment 7: 153-164

Joachim S, Robinson DG (1984) Endocytosis of cationic ferritin by bean leaf protoplasts. Eur J Cell Biol 34: 212-216

Jones GJ (1984) On estimating freezing times during tissue rapid freezing. J Microsc 136: 349-360

Keegstra K, Talmadge KW, Bauer WD, Albersheim P (1973) The structure of plant cell walls. III. A model of the walls of suspension cultured sycamore cells based on the interconnections of the macromolecular components. Plant Physiol 51: 188-196

Keith CH, di Paola M, Maxfield FR, Shelanski ML (1983) Microinjection of Ca^{++}-Calmodulin causes a localized depolymerization of microtubules. J Cell Biol 97: 1918-1924

Knoll G, Verkleij AJ, Plattner H (1987) Cryofixation of dynamic processes in cells and organelles. in: Cryotechniques in biological electron microscopy. Steinbrecht RA, Zierold K editors. Springer-Verlag. pp. 258-271

Kobayashi H, Fukuda H, Shibaoka H (1988) Interrelation between the spatial disposition of actin filaments and microtubules during the

differentiation of tracheary elements in cultured Zinnia cells. Protoplasma 143: 29-37

Kolset SO, Tolleshaug H, Berg T (1979) The effects of colchicine and cytochalasin B on uptake and degradation of asialoglycoproteins in isolated rat hepatocytes. Exp Cell Res 122: 159-167

Kornfeld R, Kornfeld S (1985) Assembly of asparagine linked oligosaccharides. Ann Rev Biochem 54: 631-664

Kristen U, Lockhausen J (1983) Estimation of Golgi membrane flow rates in ovary glands of Aptenia cordifolia using cytochalasin B. Eur J Cell Biol 2: 262-267

Kugrens P, Lee RL (1987) An ultrastructural survey of cryptomonad periplasts using quick freezing freeze fracture techniques. J Phycol 23: 365-376

Lancelle SA, Callaham DA, Hepler PA (1986) A method for rapid freeze fixation of plant cells. Protoplasma 131: 153-165

Ledbetter MC, Porter KC (1963) A "microtubule" in plant cell fine structure. J Cell Biol 19: 239-250

Leonard RT, Hodges TK (1980) The plasma membrane. in: The Biochemistry of Plants, 1. Tolbert NE, editor. pp 163-181

Leppard GG, Ramamoorthy S (1975) The aggregation of wheat rhizoplane fibrils and the accumulation of soil bound cations. Can J Bot 53: 1729-1735

Lloyd CW, Seagull RW (1985) A new spring for plant cell biology: microtubules as dynamic helices. TIBS 10: 476-478

MacRobbie EAC (1970) Quantized fluxes of chloride to the vacuole of Nitella translucens. J Exp Bot 21: 335-344

MacRobbie EAC (1982) Chloride transport in stomatal guard cells. Phil Trans R Soc Lond B 299: 469-481

McCully ME, Canny MJ (1985) The stabilization of labile configurations of plant cytoplasm by freeze substitution. J Microsc 139: 27-33

McCurdy DW, Sammut M, Gunning BES (1988) Immunofluorescent visualization of arrays of transverse cortical actin microfilaments in wheat root tip cells. Protoplasma 147: 204-206

McNeil M, Darvill AG, Fry SC, Albersheim P (1984) Structure and function of the primary cell walls of plants. Ann Rev Biochem 53: 625-663

Mahlberg P, Olsen K, Walkinshaw C (1971) Origin and development of plasma membrane derived invaginations in Vinca rosea L. Am J Bot 58: 407-416

Martin RB, Richardson FS (1979) Lanthanides as probes for calcium in biological systems. Quart Rev Biophys 12: 181-209

Mayo MA, Cocking EC (1969) Pinocytic uptake of polystyrene latex particles by isolated tomato fruit protoplasts. Protoplasma 68: 223-330

Mazur P (1970) Cryobiology: the freezing of biological systems. Science 168: 939-949

Menco BPM (1986) A survey of ultrarapid cryofixation methods with particular emphasis on applications to freeze-fracturing, freeze-etching, and freeze substitution. J EM Tech 4: 177-240

Mersey B, McCully ME (1978) Monitering the course of fixation in plant cells. J Microsc 139: 27-33

Miki NK, Clarke KJ, McCully ME (1980) A histological and histochemical comparison of the mucilages on the root tips of several grasses. Can J Bot 58: 2581-2591

Miller K, Beardmore J, Kanety H, Schlessinger J, Hopkins CR (1986) Localization of epidermal growth factor (EGF) receptor within the endosome of EGF-stimulated epidermoid carcinoma (A431) cells. J Cell Biol 102: 500-509

Miller TM, Heuser JE (1984) Endocytosis of synaptic vesicle membrane at the frog neuromuscular junction. J Cell Biol 98: 685-698

Mollenhauer HH (1971) Fragmentation of mature dictyosome cisternae. J Cell Biol 49: 212-214

Mollenhauer HH, Morre DJ (1976) Cytochalasin B but not colchicine inhibits migration of secretory vesicles in root tips of maize. Protoplasma 87: 39-48

Montague MJ, Ray PM (1977) Phospholipid synthesizing enzymes associated with Golgi dictyosomes from pea tissue. Plant Physiol 59: 225-230

Moore, R (1986) Cytochemical localization of calcium in cap cells of primary roots of Zea mays L. J. Exp. Bot. 37: 73-79. 181

Moore PJ, Staehelin LA (1988) Immunogold localization of the cell wall matrix polysaccharides rhamnogalacturonan I and xyloglucan during cell expansion and cytokinesis in Trifolium pratense L. implications for secretory pathways. Planta 174: 433-445

Morejohn LC, Fosket DE (1986) Tubulins from plants, fungi and protists. in: Cell and molecular biology of the cytoskeleton. Shay JW, editor. Plenum Press pp 257-330

Morre DJ (1970) In vivo incorporation of radioactive metabolites by the Golgi apparatus and other cell fractions of onion stem. Plant Physiol 45: 791-799

Morre DJ (1975) Membrane biogenesis. Ann Rev Plant Phys 26: 441-481

Morre DJ, Mollenhauer HH (1974) The endomembrane concept: a functional integration of endoplasmic reticulum and Golgi apparatus. in:Dynamic aspects of plant ultrastructure. Robards AW, editor. pp 84- 137

Morre DJ, Mollenhauer HH (1976) Transition elements between endoplasmic reticulum and Golgi apparatus in plant cells. Cytobiologie 13: 297-306

Morre DJ, Mollenhauer HH (1980) The Golgi apparatus. in: The Biochemistry of Plants, 1. Tolbert NE, editor. pp 438-483

Morre DJ, Mollenhauer HH (1983) Dictyosome polarity and membrane differentiation in outer cap cells of the maize root tip. Eur J Cell Biol 29: 126-132

Nassery H, Jones RL (1976) Salt induced pinocytosis in barley and bean. J Exp Bot 27: 358-367

Nishizawa N, Mori S (1977) Invagination of plasma lemma: its role in the absorption of macromolecules in rice roots. Plant Cell Physiol 18: 767-782

Nishizawa N, Mori S (1978) Endocytosis (heterophagy) in plant cells: involvement of ER and ER-derived vesicles. Plant Cell Physiol 19: 717-730

Nishizawa N, Mori S (1984) Dessication induced heterophagy in corn root cells. J Elec Microsc 33: 230-235

Nishizawa N, Mori S (1989) Ultrastructure of the thylakoid membrane in tomato leaf chloroplast revealed by liquid helium rapid freezing and substitution fixation method. Plant Cell Physiol 30: 1-7

Northcote DH, Lewis DR (1968) Freeze etched surfaces of membranes and organelles in the cells of pea root tips. J Cell Sci 3: 199-206

Novikoff AB (1964) GERL, its form and function in neurons of rat spinal ganglia. Biol Bull 127: 358

O'Neil RM, LaClaire JW II (1988) Endocytosis and membrane dynamics during wound response of the green alga Boergesenia. Cytobios 53: 113-125

Orci L, Glick BS, Rothman JE (1986) A new type of coated vesicle carrier that appears not to contain clathrin: its possible role in protein transport within the Golgi stack. Cell 40: 171-184

Orci L, Maehotra V, Amherdt M, Serafini T, Rothman JE (1989) Dissection of a single round of vesicular transport: sequential intermediates for intercisternal movement in the Golgi stack. Cell 56: 357-368

Owen TP, Benzing DH, Thomson WW (1988) Apoplastic and ultrastructural characterizations of the trichomes from the carnivorous bromeliad Brocchinia reducta. Can J Bot 66: 941-948

Paschel BM, Shpetner HS, Vallee RB (1987) Map1C is a microtubule activated ATPase which translocates microtubules in vitro and has dynein like properties. J Cell Biol 105: 1273-1282

Palevitz BA (1987) Actin in the preprophase band of Allium cepa. J Cell Biol 104: 1515-1519

Park P, Ohno T, Kato-Kikuchi H, Miki H (1987) Alkaline bismuth stain as a tracer for Golgi vesicles of plant cells. Stain Technology 62: 251-256

Parthasarathy MV (1985) F-actin architecture in coleoptile epidermal cells. Eur J Cell Biol 39: 1-12

Pasten I, Willingham MC (1983) Receptor mediated endocytosis: coated pits, receptosomes, and the Golgi. TIBS 10: 250-255

Pavelka M (1987) Functional Morphology of the Golgi apparatus. Advances in Anatomy, Embryology, and Cell Biology 106 Springer-Verlog

Pesacreta TC, Lucas WJ (1985) Presence of a partially coated reticulum in angiosperms. Protoplasma 125: 173-184

Phillips GD, Preshaw C, Steer MW (1988) Dictyosome vesicle production and plasma membrane turnover in auxin stimulated outer epidermal cells of coleoptile segments from Avena sativa (L.). Protoplasma 145: 59-65

Pickett-Heaps JD (1966) Incorporation of radioactivity into wheat xylem walls. Planta 71: 1-14

Pickett-Heaps JD (1967) The effects of colchicine on the ultrastructure of dividing plant cells, xylem wall differentiation and distribution of cytoplasmic microtubules. Devel Biol 15: 206-236

Picton JM, Steer MW (1981) Determination of secretory vesicle production rates by dictyosomes of Tradescantia using cytochalasin D. J Cell Sci 63: 303-310

Picton JM, Steer MW (1985) The effects of ruthenium red, lanthanum, fluoroscein isothiocyanate, and trifluoperazine on vesicle transport, vesicle fusion, and tip extension in pollen tubes. Planta 163: 20-26

Plattner H, Bachmann L (1982) Cryofixation: a tool in biological ultrastructural research. Int Rev Cytol 79: 237-304

Powell AJ, Peace GW, Slabas AR, Lloyd CW (1982) The detergent resistant cytoskeleton of higher plant protoplasts contains nucleus associated fibrillar bundles in addition to microtubules. J Cell Sci 56: 319-335

Preston RD (1974) The physical biology of plant cell walls. Chapman and Hall, publishers.

Quaite E, Parker RE, Steer MW (1983) Plant cell extension: structural implications for the origin of the plasma membrane. Plant Cell Environment 6: 429-432

Raven JA (1987) The role of vacuoles. New Phytol 106: 357-422 (Appendix II: Energetics of membrane recycling during cell wall synthesis)

Ray TC, Callow JA, Kenndey JF (1988) Composition of root mucilage polysaccharides from Lepidium sativum. J Exp Bot 39: 1249-1261

Record Rd, Griffing LR (1988) Convergence of the endocytic and lysosomal pathways in soybean protoplasts. Planta 176: 425-432

Revel JP, Karnovsky MJ (1967) Hexagonal array of subunits in intercellular junctions of the mouse heart and liver. J Cell Biol 33: C7-C12

Robards AW, Sleytr UB (1985) Low temperature methods in biological electron microscopy. in: Practical methods in electron microscopy series, 10. Glauert AM editor, Elsevier.

Roberts IN, Lloyd CW, Roberts K (1985) Ethylene induced microtubule reorientations: mediation by helical arrays. Planta 164: 439-447

Robinson DG, Grimm I, Sachs H (1976) Colchicine and microfibril orientation. Protoplasma 89: 375-380

Robinson DG (1980) Dictyosome-ER associations in higher plant cells? a serial section analysis. Eur J Cell Biol 23: 22-36

Robinson DG (1984) Membranes and secretion in higher plants. Ann Proc Phytochem Soc Eur 24: 147-161

Robinson DG (1985) Plant membranes: endo- and plasma membranes of plant cells. Cell Biology, a series monograph. series editor Bittar EE.

Robinson DG, Eisenger WR, Ray PM (1976) Dynamics of the golgi system in cell wall matrix polysaccharide synthesis and secretion by pea cells. Ber Deutsch Bot Ges Bd 86: 147-161

Robinson DG, Kristen U (1982) Membrane flow via the Golgi apparatus of higher plant cells. Int Rev Cytol 77: 89-127

Robinson DG, Depta H (1988) Coated vesicles. Ann Rev Plant Physiol Plant Mol Biol 39: 53-99

Rochester CP, Kjellbom P, Larsson C (1987) Lipid composition of plasma membrane from barley leaves and roots, spinach leaves and cauliflower inflorescences. Physiologia Plantarum 71: 257-263

Roland J-C (1978) General preparation and staining of thin sections. in: Electron microscopy and cytochemistry of plant cells. Hall JL, editor. Elsevier pp 1-63

Roland J-C, Vian B (1971) Reactivite du plasmalemme vegetal etude cytochimique. Protoplasma 73: 121-137

Romagnoli P, Herzog V (1987) Reinternalization of secretory proteins during membrane recycling in rat pancreatic acinar cells. Eur J Cell Biol 44: 167-175

Rome LH (1985) Curling receptors. TIBS 10: 151

Romanenko AS, Kovtun GY, Salyaev RK (1986) Pinocytotic uptake of uranyl ions by radish root cells: probable mechanisms of pinocytosis. Ann Bot 57: 1-10

Rothman JE, Miller RL, Urbani LJ (1984) Intercompartmental transport in the Golgi is a dissociative process: facile transfer of membrane protein between 2 Golgi populations. J Cell Biol 9: 260-271

Rozema J, Riphagen I, Sminia T (1977) A light and electron microscope study of the structure and

function of the salt gland of Glaux maritima. New Phytol 79: 665-671

Ryan CA (1987) Oligosaccharide signalling in plants. Ann Rev Cell Biol 3: 295-317

Ryser U (1979) Cotton fibre differentiation: occurrence and distribution of coated and smooth vesicles during primary and secondary wall formation. Protoplasma 98: 223-239

Sakaguchi S, Hogetsu T, Hara N (1988) Arrangement of cortical microtubules in the shoot apex of Vinca major L. Planta 175: 403-411

Saxton MJ, Breidenbach RW (1988) Receptor mediated endocytosis in plants is energetically possible. Plant Physiol 86: 993-995

Schmid SL, Fuchs R, Male P, Mellman I (1988) Two distinct subpopulations of endosomes involved in membrane recycling and transport to lysosomes. Cell 52: 73-83

Schnapp BJ, Vale RD, Sheetz MP, Reese TS (1985) Single microtubules from squid axoplasm support bidirectional movement of organelles. Cell 40: 455-462

Scott FM, Hamner KC, Baker E, Bowler E (1958) Electron microscope studies of the epidermis of Allium cepa. Am J Bot 45: 449-461

Seagull RW (1983) The role of the cytoskeleton during oriented microfibril deposition. I. Elucidation of the possible interaction between microtubules and cellulose synthase complexes. J Ultrastruc Res 83: 168-175

Seagull RW, Falconer MM, Weerdenburg CA (1987) Microfilaments: dynamic arrays in higher plant cells. J Cell Biol 104: 995-1004

Setterfield G, Bayley ST (1957) Studies on the mechanism of deposition and extension of primary cell walls. Can J Bot 35: 435-444

Shannon TM, Henry Y, Picton JM, Steer M (1982) Polarity in higher plant dictyosomes. Protoplasma 112: 189-195

Shannon TM, Steer MW (1984) The root cap as a test system for the evaluation of Golgi inhibitors. J Exp Bot 35: 1697-1707

Shannon TM, Picton JM, Steer MW (1984) The inhibition of dictyosome vesicle formation in higher plant cells by cytochalasin D. Eur J Cell Biol 33: 144-147

Sheetz MP, Vale R, Schnapp B, Schroer T, Reese T (1986) Vesicle movements and microtubule based motors. J Cell Sci Suppl 5: 181-188

Shinji E, Shinji Y, Mizuhira V (1976) Histochemical study of Dermatophyta under an electron microscope-Trichophyton mentagrophytes cell wall. Acta Histochem Cytochem 9: 292-305

Slot JW, Geuze HJ (1985) A new method of preparing probes for multiple label cytochemistry. Eur J Cell Biol 38: 87-93

Simmonds T, Setterfield G, Brown DL (1983) Organization of microtubules in dividing and elongating cells of Vicia hajastana Grossh. in suspension cultures. Eur J Cell Biol 32: 59-66

Sitte H, Edelmann L, Neumann K (1987) Cryofixation without pretreatment at ambient pressure. in: Cryotechniques in biological electron microscopy, Steinbrecht RA, Zierold Z editors. Springer-Verlag. pp 87-113

Staehelin LA, Kiermayer O (1970) Membrane differentiation in the Golgi complex of Micrasterias denticulata Breb. visualized by freeze etching. J Cell Sci 7: 787-792

Staehelin LA, Chapman RL (1987) Secretion and membrane recycling in plant cells: novel intermediary structures visualized in ultrarapidly frozen sycamore and carrot suspension cells. Planta 171: 43-57

Steer MW (1985) Vesicle Dynamics. In: Botanical Microscopy. Robards AW, editor. Oxford Scientific Publications pp 129-155

Steinbrecht RA (1980) Cryofixation without cryoprotectants. Freeze substitution and freeze etching of an insect olfactory receptor. Tissue Cell 12: 73-100

Steinbrecht RA, Muller M (1987) Freeze substitution and freeze drying. in:Cryotechniques in biological electron microscopy. Steinbrecht RA, Zierold Z editors. Springer-Verlag. pp 149-168.

Steinman RM, Mellman IS, Muller WA, Cohn ZA (1983) Endocytosis and the recycling of plasma membrane. J Cell Biol 96: 1-26.

Storrie B, Pool RR, Sachdeva M, Maurey KM, Oliver C (1984) Evidence for both prelysosomal and lysosomal intermediates in endocytic pathways. J Cell Biol 98: 108-115

Strafstrom JP, Staehelin LA (1988) Antibody localization of extensin in cell walls of carrot storage roots. Planta 174: 321-332

Suzuki M, Takebe I, Kajita S, Honda Y, Matsui C (1977) Endocytosis of polystyrene spheres by tobacco leaf protoplasts. Exp Cell Res 105: 127-135

Tanchak MA, Griffing LR, Mersey BG, Fowke LC (1984) Endocytosis of cationized ferritin by coated vesicles of soybean protoplasts. Planta 162: 481-486

Tanchak MA, Fowke LC (1987) The morphology of multivesicular bodies in soybean protoplasts and their role in endocytosis. Protoplasma 138: 173-182

Tanchak MA, Rennie PJ, Fowke LC (1988) Ultrastructure of the partially coated reticulum and dictyosomes during endocytosis by soybean protoplasts. Planta 175: 433-441

Taylor ARD, Hall JL (1979) An ultrastructural comparison of lanthanum and silicotungstic acid/chromic acid as plasma membrane stains of isolated protoplasts. Plant Sci. Letters 14: 139-144

Tepfer M, Taylor IEP (1981a) The permeability of plant cell walls as measured by gel filtration chromatography. Science 213: 761-763

Tepfer M, Taylor IEP (1981b) The interaction of divalent cations with pectic substances and their influence on acid-induced cell wall loosening. Can J Bot 59: 1522-1525

Thiery J-P (1967) Mise en evidence des

polysaccharides sur coupes fines en microscopie electronique. J Microsc 6: 987-1018

Tooze FJ, Tooze SA (1986) Clathrin coated vesicular transport of secretory proteins during the formation of ACTH containing secretory granules in AtT20 cells. J Cell Biol 103: 839-850

Trachtenberg S, Fahn S (1981) The mucilage cells of Opuntis ficus-indica (L.) Mill. Bot Gaz 142: 206-213

Ulrich JM, McLaren AD (1965) The absorption and translocation of C^{14} labelled proteins in young tomato plants. Am J Bot 52: 120-126

Vale RD, Reese TS, Sheetz MP (1985) Identification of a novel force generating protein, kinesin, involved in microtubule based motility. Cell 42: 39-50

Vale RD (1987) Intracellular transport using microtubule based motors. Ann Rev Cell Biol 3: 347-378

Van der Valk P, Rennie PJ, Connolly JA, Fowke LC (1980) Distribution of cortical microtubules in tobacco protoplasts. An immunofluorescence microscopic and ultrastructural study. Protoplasma 105: 27-43

Van Deurs B, Sandvig K, Peeersen OW, Olsnes S, Simons K (1988) Estimation of the amount of internalized ricin that reaches the trans Golgi network. J Cell Biol 106: 253-267

Van Harreveld A, Crowell J (1964) Electron microscopy after rapid freezing on a metal surface and substitution fixation. Anat Rec 149: 381-386

Van Harreveld A, Trubatch J, Steiner J (1974) Rapid freezing and electron microscopy for the arrest of physiological processes. J Microsc 100: 189-198

Van Steveninck RFM, Van Steveninck ME, Chescoe D (1976) Intracellular binding of lanthanum in root tips of barley (Hordeum vulgare). Protoplasma 90: 89-97

Vaughn MA, Vaughn KC (1987) Effects of microfilament disrupters on microfilament distribution and morphology in maize root cells. Histochemistry 87: 129-137

Varner JE, Liang-Shiou Lin (1989) Plant cell wall architecture. Cell 56: 231-239

Vian B, Reis D (1972) Apports de l'utilization de resines hydrosoluble a l'etude des polysaccharides dans le cellule vegetale. C R Acad Sci Paris 274: 1663-1666

Vian B, Brillouet J-M, Satiat-Jeunemaitre B (1983) Ultrastructural visualization of xylans in cell walls of hardwood by means of xylanase-gold complex. Biol. Cell 49: 179-182

Von Heijne G (1985) Structural and thermodynamic aspects of the transfer of proteins into and across membranes. Curr Topics in Membranes and Transport 2: 151-174

Walter P, Blobel G (1982) Signal recognition particle contains a 7 S RNA essential for protein translocation across the endoplasmic reticulum. Nature 299: 691-698

Walter P, Gilmore R, Blobel G (1984) Protein translocation across the endoplasmic reticulum. Cell 38: 5-8

Wetzel MG, Scow RO (1980) Morphological studies of lipolysis and lipid transport in heart of suckling rat. J Cell Biol 87: 197a

Whaley WG, Mollenhauer HH (1966) The golgi apparatus and cell plate formation-a postulate. J Cell Biol 17: 217-225

Wheeler H, Baker BL, Hanchey P (1972) Pinocytosis in root cap cells exposed to uranyl salts. Am J Bot 59: 858-868

Wick SW, Seagull RW, Osborn M, Weber K, Gunning BES (1981) Immunofluorescence microscopy of organized microtubule arrays in structurally stabilized meristematic plant cells. J Cell Biol 89: 685-690

Wickner WT, Lodish HF (1985) Multiple mechanisms of protein insertion into and across membranes. Science 230: 400-407

Wieland FT, Gleason ML, Serafine TA, Rothman JE (1987) The rate of bulk flow from the endoplasmic reticulum to the cell surface. Cell 50: 289-300

Yamaguchi Y, Nagai R (1981) Motile apparatus in Vallisneria leaf cells I. Organization of microfilaments. J Cell Sci 48: 193-205

Yang JT, Laymon RA, Goldstein LSB (1989) A three domain structure of kinesin heavy chain revealed by DNA sequence and microtubule binding analyses. Cell 56: 879-889

Zierold K, Steinbrecht RA (1987) Cryofixation of diffusible elements in cells and tissues for electron probe microanalysis. in: Cryotechniques in biological electron microscopy. Steinbrecht RA, Zierold K editors. Springer-Verlag. pp 272-284